The Dissertation Committee for Yichen Lin Certifies that this is the approved version of the following dissertation:

ALTERED SPERMATOGENESIS OF DEATH LIGAND GENE DEFICIENT MICE AND THE INFLUENCE OF PHTHALATES IN GERM CELL APOPTOSIS AND ENHANCED TESTICULAR CANCER PROGRESSION

Committee:

John H. Richburg, Supervisor

Shawn B. Bratton

Edward M. Mills

Bob G. Sanders

Casey W. Wright

ALTERED SPERMATOGENESIS OF DEATH LIGAND GENE DEFICIENT MICE AND THE INFLUENCE OF PHTHALATES IN GERM CELL APOPTOSIS AND ENHANCED TESTICULAR CANCER PROGRESSION

by

Yichen Lin, B.S; M.S

Dissertation

Presented to the Faculty of the Graduate School of

The University of Texas at Austin

in Partial Fulfillment

of the Requirements

for the Degree of

Doctor of Philosophy

The University of Texas at Austin

May 2012

Dedication

I dedicate this dissertation to Dr. Pei-Li Yao
and my son George Deyuan Lin.
I also dedicate to my parents;
Mr. Ho-Jin Lin and Mrs. Ming-lung Do
who supported me throughout the process.

Acknowledgements

I would like to thanks my mentor, Dr. John H. Richburg for giving me an opportunity to work in his lab and for his guidance in becoming a great scientist. He encouraged and fully supported me to finish t the last year of my PhD study. This dissertation could not have been finished without his advising. Also, I would like to thank Dr. Shawn Bratton, Dr. Edward Mills, Dr. Bob Sanders, and Dr. Casey Wright for serving on my committee. They all have provided helpful suggestions during my graduate study.

I would also like to thank my fellow lab members for their help and friendship: Dr. Caitlin Murphy, Jessica Dwyer, James Harman, Angela Stermer, and Emily Lao. Special thanks go to Jessica Dwyer who worked with me over several years improve my English in both oral and writing in many papers, seminars, and dissertation; she is great teacher. Thanks to Emily Lao for helping me refine my presentation before my defense. I am also grateful to some members in Dr. Bratton's lab: Ting-Chun Yeh, Miao-Der (Sophie) Chen, Chu-Chiao "Crystal" Wu, and Kuei-Ting "Michelle" Yang, for their help and friendship. I also want to thank Ms. Joanne Click for helping me improve my English and correcting the grammatical errors in my dissertation. She has also supported and encouraged me during the challenges of life.

I would like to thank to Dr. Pei-Li Yao, who is the most important person to me for 14 years now. She has been providing me support and encouragement during my study in graduate school, in science, and in life. I could not have started or finished at University of Texas at Austin without her. Last, I would also like to thank to my parents, sister, and my son, Ho-Jin Lin, Ming-Lune Do, Feilica Lin, and George Deyuan Lin, who have continuously given me their support and encouragement.

ALTERED SPERMATOGENESIS OF DEATH LIGAND GENE DEFICIENT MICE AND THE INFLUENCE OF PHTHALATES IN GERM CELL APOPTOSIS AND ENHANCED TESTICULAR CANCER PROGRESSION

Yichen Lin, Ph.D.

The University of Texas at Austin, 2012

Supervisor: John H. Richburg

Testicular germ cell apoptosis is a process that begins in early development and continues in the adult testis. It is important during spermatogenesis for maintaining homeostasis of different types of germ cells. The number of sperm produced depends on the supportive capacity of surrounding Sertoli cells, which provide nutrition and an adaptive environment for growth and development of the germ cells. There are two major pathways that regulate germ cell apoptosis: extrinsic and intrinsic. We hypothesize that Sertoli cells use the extrinsic pathway to eliminate germ cells when exposed to phthalates, a common Sertoli cell toxicant.

Death ligands, which are involved in the extrinsic pathway, were used in this research to test this hypothesis. Here, we demonstrate that: 1) the loss of FasL and TRAIL protein expression results in decreased production of mature spermatids in the adult testis, likely as a result of alterations in germ cell homeostatsis during the first wave of spermatogenesis. 2) The high baseline incidence of germ cell apoptosis in peripubertal

FasL$^{-/-}$ and TRAIL$^{-/-}$ mice is correlated with increases in levels of TRAIL and FasL, respectively. 3) The decline in germ cell apoptosis observed after MEHP treatment in FasL$^{-/-}$ mice closely corresponds to the occurrence of increased levels of c-FLIP. 4) A more predominant role of FasL occurs in controlling the proper number of germ cells during the first wave of spermatogenesis in peri-pubertal mice. TRAIL is more critical for maintaining long-term homeostasis of the germ cell population in adult testis as well as in the reproductive function. 5) Several possible genes are involved in the altered spermatogenesis and development in the testis of gene-deficient mice. 6) Findings described in Chapter 6 indicate cellular mechanisms triggered by MEHP exposure that act to enhance tumor progression/metastasis in testicular embryonal carcinoma cells (NT2/D1).

Taken together, these novel findings provide important mechanistic insights into the functional roles of FasL in the testis at distinct developmental periods and further indicate that FasL itself is required for the regulation of c-FLIP levels in the testis. Additionally, exposure to environmental toxicants, such as the phthalates, can enhance testicular cancer metastasis and invasion.

Table of Contents

List of Tables

List of Figures

List of abbreviations

ABP	Androgen binding protein
APAF-1	Apoptotic protease activating factor-1
AT/RT	Teratoid/rhabdoid tumor
ANOVA	Analysis of variance
BTB	Blood-testis barrier
Caspase	Cysteniyl aspartate-specific protease
c-FLIP/CFLAR	Cellular FLICE inhibitor
DAB	Diaminobenzidine
DBP	Dibutyl phthalate
DD	Death domain
DED	Death effector domain
DEHP	Di-(2-ethylhexyl)phthalate
DISC	Death inducing signaling complex
DMEM	Dulbecco's modified Eagle's media
DMSO	Dimethyl sulfoxide
DR	Death Receptor
EDCs	Endocrine disruptin compounds
EDTA	Ethylenediamine tetra acetic acid

EGF	Epidermal growth factor
ELISA	Enzyme-linked immunosorbent assay
FADD	Fas associated death domain protein
FASL	Fas ligand
FDA	The Food and Drug Administration
FLICE	FADD-like interleukin 1-beta converting enzyme
FSH	Follicle stimulating hormone
GADPH	Glyceraldehydes-3-phosphate dehydrogenase
gld	Generalized lymphoproliferative disease
IAP	Inhibitor of apoptosis
LH	Luteinizing hormone
lpr	Lymphoproliferation spontaneous mutation
FSH	Follicle stimulate hormone
MEHP	Mono-(2-ethylhexyl)phthalate
MMP	Matrix metalloproteinase
MOMP	Mitochondrial outer membrane permeabilization
NO	Nitric oxide
PAS-H	Periodic acid-Schiffs-Hematoxylin
PBS	Phosphate buffered saline
PCR	Polymerase chain reaction

PGCs	Primordial germ cells
PND	Postnatal day
PVC	Poly vinyl chloride
PVDF	Poly vinylidene fluoride
ROS	Reactive oxygen species
RT-PCR	Reverse transcription polymerase chain reaction
SCO	Sertoli cell only syndrome
SDS	Sodium dodecyl sulphate
SSC	Spermatogonial stem cell
TDI	Toleralbe daily intake
TDS	Testicular dysgenesis syndrome
TI	Tolerable intake
TIMP	Tissue inhibitors of metalloproteinase
TNF	Tumor necrosis factor
TRAIL	TNF related apoptosis inducing ligand
TUNEL	Terminal deoxynucleotidyl transferase mediated
XIAP	X-lined IAP

Chapter 1: Introduction

1.1 Overview of the testes

Testes are important parts of the male reproductive organ. In the mammalian system, the paired testes are located in the scrotal sac below the main trunk of the organism. The primary functions of testes are the production of sperm and the release of sex hormones, such as testosterone. There are two major compartments in each testis: the seminiferous tubule and interstitial space (Figure 1-1). The interstitial space includes Leydig cells and macrophages cells that reside in the space between tubules (Figure 1-2). The prominent cells in this area are Leydig cells that serve primarily to secrete testosterone [1].

The functional unit in the testis is the seminiferous tubule [2] that provides the environment for the spermatogonia to continuously form spermatozoa, a repetitive, ongoing process for the male reproductive cycle that is known as spermatogenesis [3]. The seminiferous tubules are convoluted loops that both begin and end in the specialized region of the testis called the rété testis. The straight parts of the tubules lie mostly along the long axis of the testis. Walls of the seminiferous tubules are formed by the lymphatic endothelium, the peritubular myoid cells, and acellular elements [1]. The seminiferous tubules are composed of

Sertoli cells and germ cells. The Sertoli cells are irregular in shape and extend from the basal lamina; different types of germ cells are supported by the Sertoli cells. From the basal lamina to the lumen, germ cells at different stages of development are spermatogonia, spermatocytes, round spermatids, and elongated spermatids. A detailed description and explanation of the functions of Sertoli cells and germ cells are covered in sub- chapters of this study.

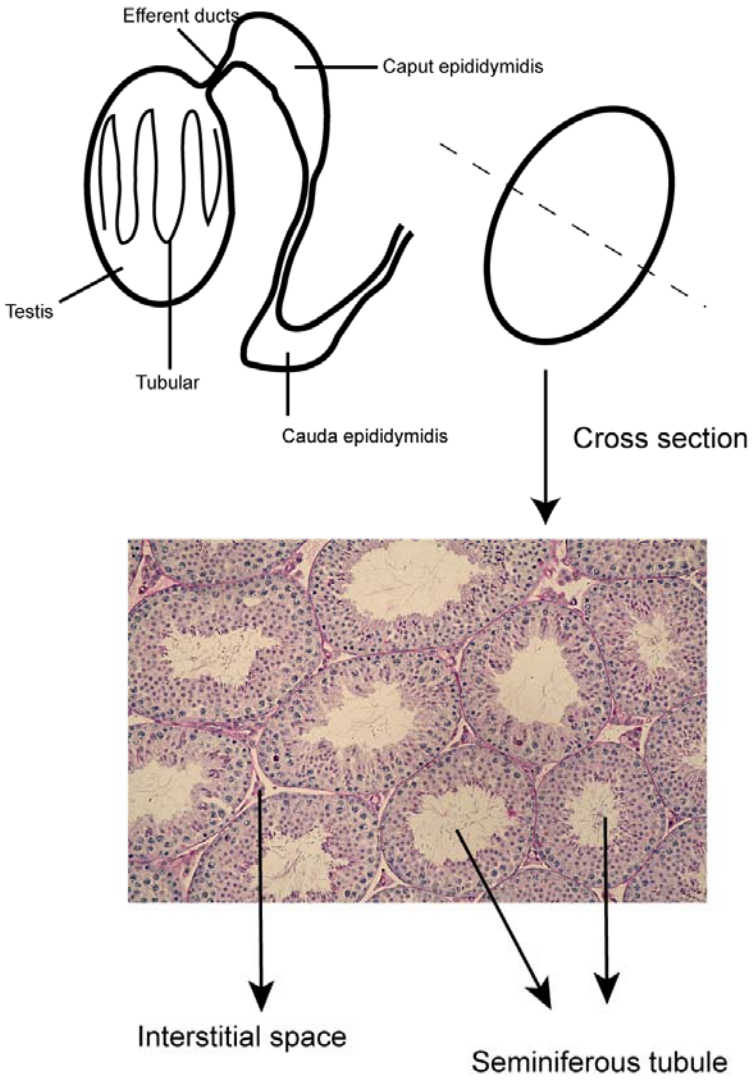

Figure 1.1 Morphology of the seminiferous tubule and interstitial space in mouse testis.

The morphology of the seminiferous tubule and the interstitial space are shown in a 5µm cross-session of paraffin-embedded mouse testis from a 44-day-old C57BL/6J mouse with Periodic acid-Schiffs-Hematoxylin (PAS-H) staining.

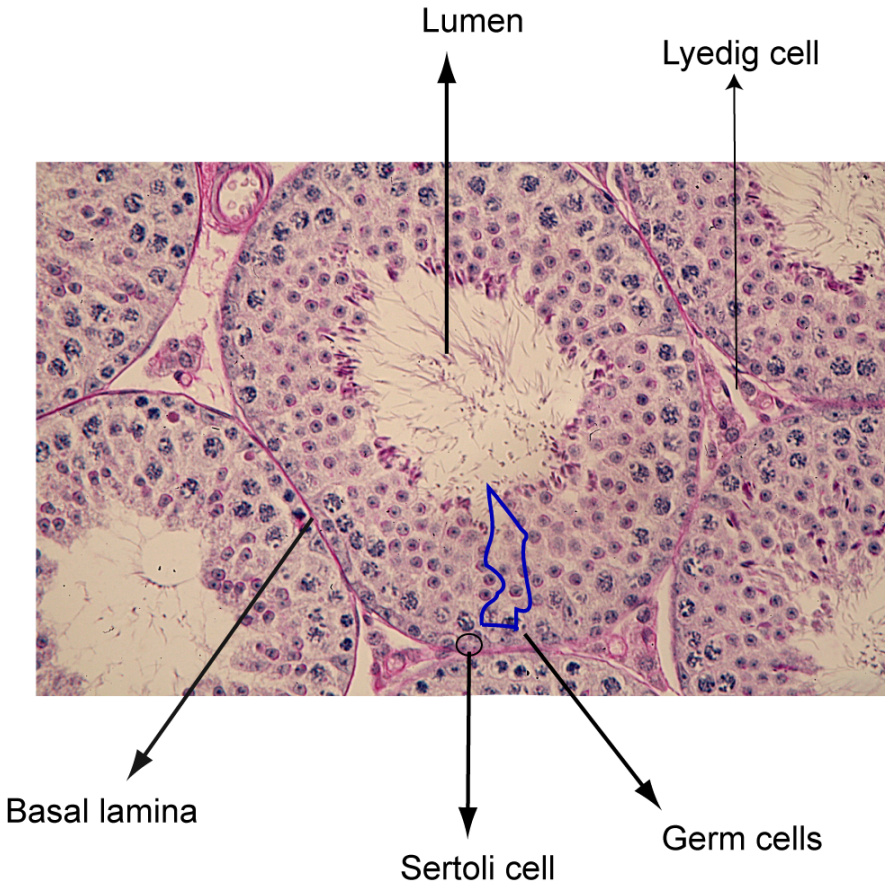

Figure 1.2 Section of seminiferous tubules in an adult mouse testis with PAS-H staining.

The seminiferous tubule contains Sertoli cells, germ cells, basal lamina, and lumen. Leydig cells exist within the interstitial space. The blue line delineates different types of germ cells, including spermatogonia, round spermatocytes, elongated spermatocytes, and spermatids.

1.1.1 The Structure and function of Sertoli cells

Enrico Sertoli discovered the Sertoli cell in 1860 when he was an 18-year-old student at the University of Pavia in Northern Italy [4]. He published his observations and this cell was later named “the cells of Sertoli” or “Sertoli cell.” The Sertoli cells are the main somatic cells in the seminiferous tubules. The size of Sertoli cells is from 75-100 μm, and the volume of Sertoli cells is about 2000-3000 μm^3 to 6000-7000 μm^3[1,5]. The cells extend from the basement membrane to of the lumen of the seminiferous tubules (Figure 1-3). The shape of Sertoli cells is columnar and the surface is irregular. Enrico Sertoli in his first publication used the term “mother cells” to suggest that the function of Sertoli cells is to support the development of germ cells [6,7]. Sertoli cells are important for spermatogenesis, the process of germ cell maturation. The major functions of Sertoli cells include: 1) providing supportive structure for spermatocytes and spermatids, 2) delivery of nutrients to the developing spermatozoa, and 3) mediating hormone effects [1,7].

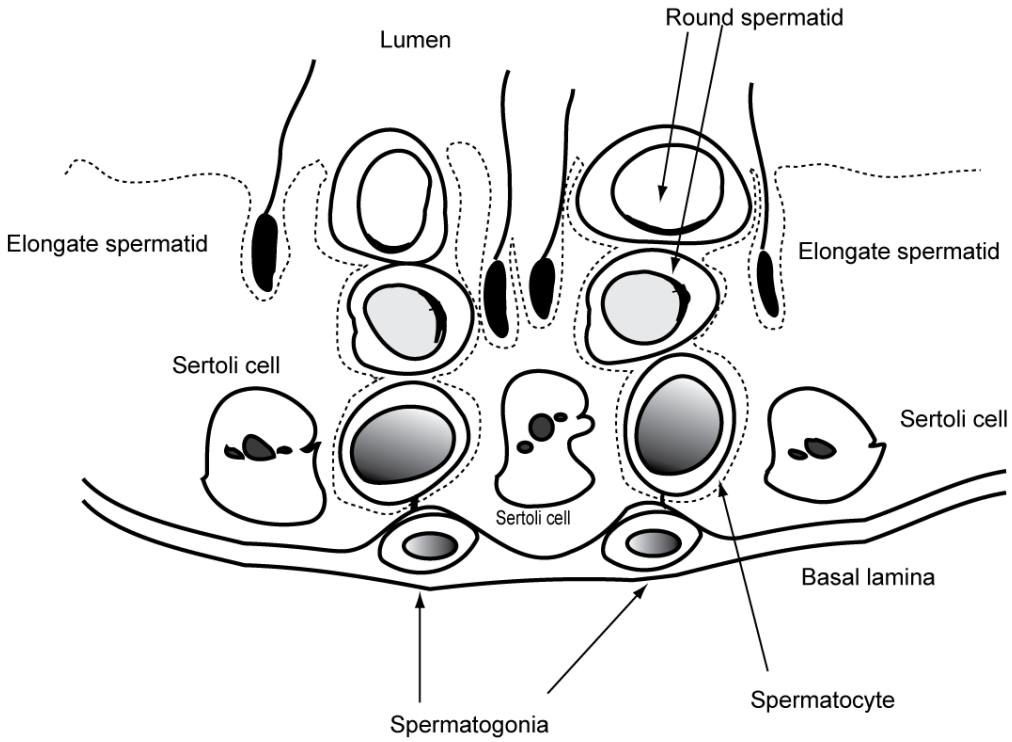

Figure 1.3 Diagram of a portion of a seminiferous tubule. The cytoplasm of Sertoli cells extends from the basement membrane to the lumen and is connected to different types of germ cells. Spermatogonia are surrounded by the basal lamina on one side and Sertoli cells on the other side. Round spermatocytes develop the acrosome around the nucleus and then become elongated and eventually form the tail structure. Elongated spermatids then become mature spermatozoa and are released into the lumen during spermiation.

1.1.2 Germ Cells and Spermatogenesis

Spermatogenesis is a process by which spermatozoa develop from stem cells [1]. Spermatogenesis can be envisioned as having three different phases: the proliferative phase (spermatogonia), the meiotic phase (spermatocytes), and the differentiation phase (spermatids) (Figure 1-4, 1-5) [1].

In the proliferative phase, the spermatogonia can undergo cell replication by mitosis to increase the number of cells for later meiosis and differentiation. There are three major types of spermatogonia: the spermatogonia stem cell (SSC), the proliferative spermatogonia, and the differentiating spermatogonia [1].

Two different spermatogonial development models have been proposed [8]. In the first model, suggested by Huckins and Oakberg, the A_{single} (A_s) spermatogonia refer to spermatogonia stem cells, which can renew themselves or divide to form the next A_{paried} (A_{pr}) spermatogonia. In their model, Apr spermatogonia can further divide to form $A_{aligned}$ (A_{al}) spermatogonia and then continue to differentiate into type A_1 spermatogonia. Further, A_2 to A_4 spermatogonia can continue to develop from A_1 spermatogonia, and then enter the next phase of intermediate (In) spermatogonia. Type B spermatogonia develop from In spermatogonia and continue the process of meiosis.

Another model, proposed by Clermont and Bustos-Obregon, suggests that A_s and A_{pr} are spermatogonia stem cells, called A_0. This phase of spermatogonia

is thought to maintain quiescence until the loss of proliferative spermatogonia stem cells causes the stimulation of a proliferation signal to A_0 that, in turn, starts the generation of proliferative spermatogonia stem cells [8]. In the first model uses A1 to A4 spermatogonia to represent the renewal of stem cells while the second model uses A_1 instead of A1 to A_4 to represent the same stages of stem cell renewal. Following the A_1 phase are phases A_2, A_3, and A_4, which can continue to develop into type B spermatogonia or can dedifferentiate to A_1 spermatogonia.

After the proliferative phase, the most mature spermatogonia become primary spermatocytes by the process of the meiotic phase. The type B spermatogonia will divide into preleptotene spermatocytes (PI), and the PI cells will then be the last cells in the cell cycle to have the S-(synthetic) phase. The morphology of type B spermatogonia and PI are only slightly different: the size of type B spermatogonia is about 30% smaller than PI spermatocytes, and type B spermatogonia has more chromatin than PI spermatocytes [1].

In the meiotic phase, the morphology of nuclear changes is the main characteristic that distinguishes different types of spermatocytes. In this phase, PI spermatocytes will lose nuclei chromatin and subsequently form chromatin thread in leptotene (L). The chromatin threads are condensed, but the chromosomes are not yet paired. The chromosomes pair in the zygotene (Z) cells, and the pairing apparatus, called the synaptonemal complex, can be observed only by electron

microscopy. When zygotene cells become pachytene (P) cells, the chromosomes are almost fully paired and genetic material starts to cross over or exchange. In this stage, the sex chromatic may be observed. The diplotene (Di) cells constitute the largest primary spermatocytes and germ cells and have the largest interchromosomal clear areas.

The meiosis phase starts with diplotene cells and via the metaphase, anaphase, and telophase the diplotene cells become secondary spermatocytes (2) that are considered to be meiosis I (M-I). The second meiosis (M-II) can quickly proceed and form spermatids. The meiosis I cells (metaphase I, anaphase I, and telophase I cells) are similar in size to the diplotene cells, but the meiosis II cells are smaller than the meiosis I.

The spermiogenic phase is important for the development of a flagellum, the development of an acrosome, the nuclear condensation, and the elimination of cytoplasm. This process of cell transformation changes occurs without cell division. When round spermatids are formed, germ cells stop to divide and undergo a dramatic differentiation in the nucleus and the cytoplasm to form elongated spermatids. In order to become spermatozoa, the nuclear condensation, the formation of acrosomes, the development of tails, the formation of mitochondrial spiral, and the elimination of extraneous cytoplasm. The spermatozoa will be released from Sertoli cells into the lumen and enter the epididymis for ejaculation [1].

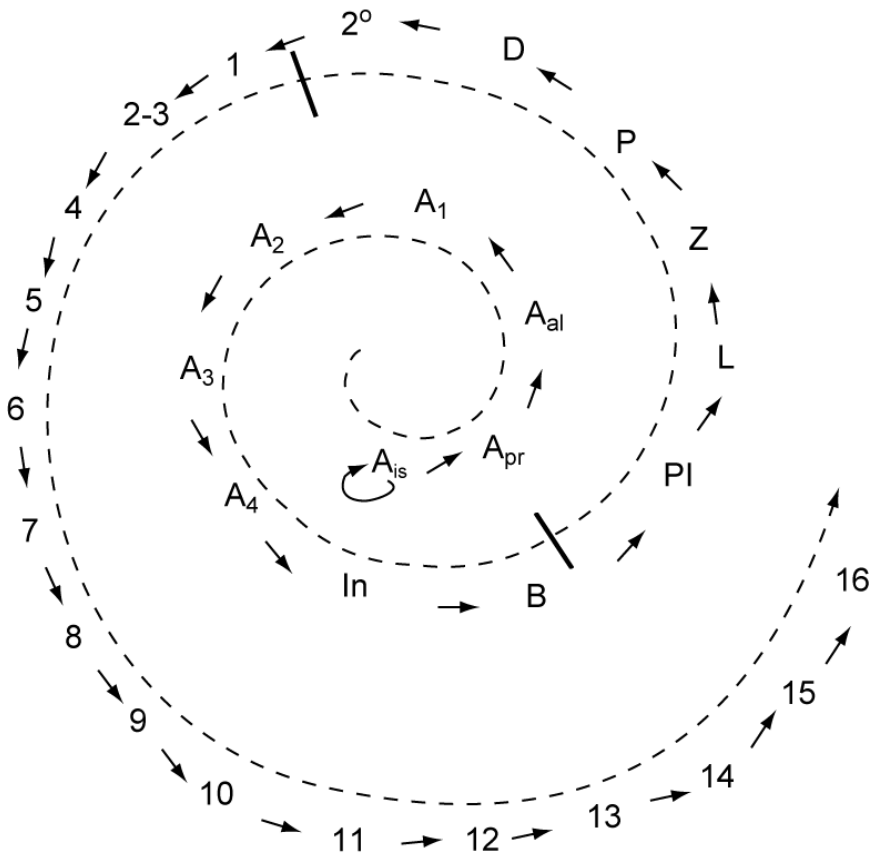

Figure 1.4 Diagram of mouse spermatogenesis.

This figure shows the process of spermatogenesis from stem cell to spermatozoa. A_{is} to B is the spermatogonia phase. PI to 2^{o} is the spermatocytes phase. 1 to 16 is the spermatids phase. A: Type A spermatogonia; A_{is}: $A_{isolated}$; A_{pr}: A_{paired}; Aal : $A_{aligned}$; B: Type B spermatogonia; In: Intermediate; PI: Preleptoten spermatocytes; L: Leptotene ; Z: Zygotene; P: Pachytene ;D:Diplotene; 2^{o}: Secondary spermatocytes.

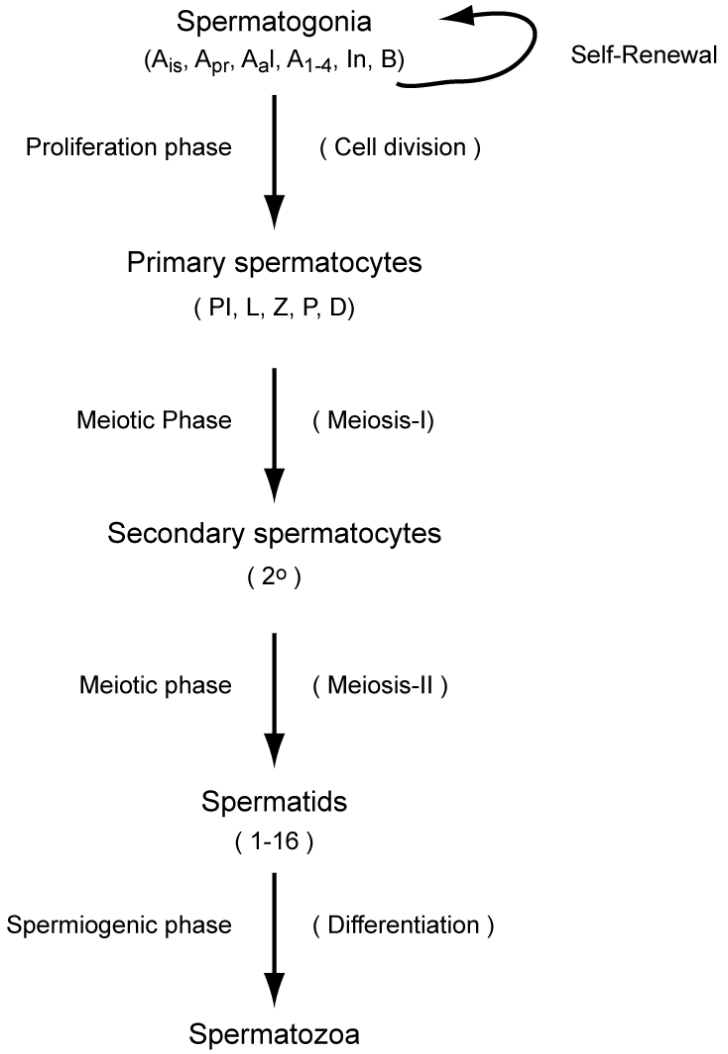

Figure 1.5 Diagram of spermatogenesis

Spermatogenesis is a process that starts from spermatogonia (stem cells) to form Spermatozoa. Spermatogonia stem cells have the ability of self-renew and maintain a basic level of population of stem cells. Some spermatogonia can continue morphological development to become primary spermatocytes, and then the primary spermatocytes can undergo a one-way development process to form secondary spermatocytes, spermatids, and spermatozoa.

1.2 Apoptosis

Apoptosis is a process of program cell death. By definition, it is a genetically directed process of cell self-destruction. The term apoptosis originated from the Greek word *apoptōsis*, which means a falling off. The first description of characteristics of apoptosis was published in the *British Journal of Cancer* in 1972 by Dr. Kerr, Wyllie, and Currie [9]. Those characteristics include morphological changes in cell type, such as membrane blebbing, cell shrinkage, nuclear fragmentation, and chromatin condensation. The apoptosis process involves two main signaling pathways: the extrinsic pathway (death receptor pathway) and the intrinsic pathway (mitochondrial pathway).

1.2.1 The intrinsic pathway

In the intrinsic or mitochondrial pathway, cytochrome *c* is stimulated to be released from the mitochondria in response to changes in the permeability of the outer membrane of the mitochondria, called mitochondrial outer membrane permeabilization (MOMP). The MOMP, in turn, induces the formation of the apoptosome complex following activation of a cascade of cysteinyl *asp*artate protein*ases* (caspases). This process can result in irreversible events in cell death. MOMP can be inhibited by the Bcl-2 family, which contains both anti-apoptotic

and pro-apoptotic proteins. Those proteins share some Bcl-2 homology domains (BH1~BH4). Bcl-2, Bcl-XL, Bcl-w, Bcl-B, Al, and Mcl1 belong to the anti-apoptotic proteins, which include three or four BH regions. The pro-apoptotic proteins are Bax, Bak, Bcl-xs, Bok, Bid, Bim, Bik, Noxa, Puma, Bcl-Gs, Blk, Bmf, and Hrk, which share only the BH3 domain.[10] Bax and Bak appear to be required for MOMP and are present in most cells in inactive forms but can be triggered by other proteins, such as the BH-3 only proteins [11,12,13]. Cytochrome c, which can be released following the MOMP occurrence, binds to monomeric apoptotic protease activating factor-1 (APAF-1) and induces a conformational change in APAF-1 to form the apoptosome. The apoptosome then binds to pro-caspase 9 to initiate the intrinsic pathway [14,15]. Auto-cleavage is triggered by the oligomerization of pro-caspase 9 on the apoptosome so that pro-caspase 9 can become active caspase 9, and active caspase 9 can continue to cleave the effector caspases, such as caspase 3 and caspase 7, eventually resulting in cell death (Figure 1-6). Caspase activity can be modulated by caspase-binding proteins of the inhibitor of the apoptosis proteins (IAPs) family, such as human X-lined IAP (XIAP) [16,17]. Moreover, caspase inhibitors can be antagonized by the pro-apoptotic proteins, such as SMAC/DIABLO) [18,19].

1.2.2 The extrinsic pathway

The extrinsic signaling pathway is best characterized by the action of the tumor necrosis factor (TNF) superfamily of protein ligands on their cognate receptors [20]. The intrinsic pathway is distinguished by the release of cytochrome *c* from the mitochondria [21,22,23]. Common to both of these signaling pathways is the activation of a family of caspases that results in characteristic structural, biochemical, and morphological changes associated with cellular apoptosis [24]. A conformational change is induced in the cell membrane when death ligands bind to the receptors on the cell surface, and other protein molecules join this process of cell death (Figure 1-6).

Fas ligand (FasL/CD95L/TNFSF6) and Fas receptor (Fas/CD95/TNFRSF6) are the best understood proteins of the tumor necrosis factor (TNF) superfamily of ligands and receptors [25]. Engagement of homotrimers of Fas by homotrimers of FasL recruits the adapter protein, Fas associated death domain protein (FADD), to bind to Fas [26]. FADD serves, through its C-terminal death domain (DD), to couple Fas receptors to the "initiator" enzyme pro-caspase-8 (also named FADD-like interleukin 1-beta converting enzyme, FLICE) through the mutual association of N-terminal death effector domains (DED) that exist in both FADD and pro-caspase-8. This complex of Fas, FADD and pro-caspase-8 is referred to as the death-inducing signaling complex (DISC) [27,28]. The close apposition of two

molecules of pro-caspase-8 allows for their further proteolytic processing which results in the formation of the active caspase-8 enzyme [29]. Active caspase-8 can then cleave other distinct "downstream" caspase enzyme family members, resulting in a caspase-cascade that cleaves substrates necessary for the instigation of apoptosis (Figure 1-7). The initiation of this caspase cascade at the DISC is regulated by the cellular FLICE inhibitor, c-FLIP (c-FLIP, CFLAR), which lacks proteolytic caspase activity [30,31,32]. In this way, c-FLIP prevents the recruitment and subsequent activation of caspase-8. Although this simplified description of death receptor-mediated signaling is widely accepted, there are many nuances to its regulation and even evidence of various non-apoptotic functions involved in the activation of Fas or by FasL itself [33] Nevertheless, the extent of the recruitment of either procaspase-8 or c-FLIP to the DISC is a common key determinant for the events keyed off by death receptor activation. When the DISC is formatted, pro-caspase-8/pro-caspase-10 (but pro-caspe-10 is not available in mice) can cleave and activate the initiator caspases without being blocked by c-FLIP. The initiator caspases then activate a second group of caspases, as known as effector caspases (pro-caspase 3 ,6, 7; the same effectors in the intrinsic pathway), by proteolytic cleavage at specific sites. Activated caspase-3 cleaves a variety of cellular substrates, such as DNA repair enzymes, cellular and nuclear structural proteins, and endonuclease inhibitors. Then cell death occurs.

Another member of the TNF family, tumor necrosis factor related apoptosis-inducing ligand (TRAIL/Apo2L/TNFSF10) [34], is also expressed in human and rodent testis [35,36,37]. TRAIL is a type II transmembrane protein that binds to two receptors in humans, DR4 (TRAIL-R1/TNFRSF10A) and DR5 (TRAIL-R2/ TNFRSF10B), whereas there is only one receptor in mice, called TRAIL-R (MK/mDR5), and it is equally homologous to both human death receptors. [38,39]. The interaction between TRAIL and DR5 triggers a signaling pathway similar to the Fas-FasL system by transmitting signals through DISC, the activation of caspase 8; subsequently, the effector caspases are activated (Figure 1-7) [40].

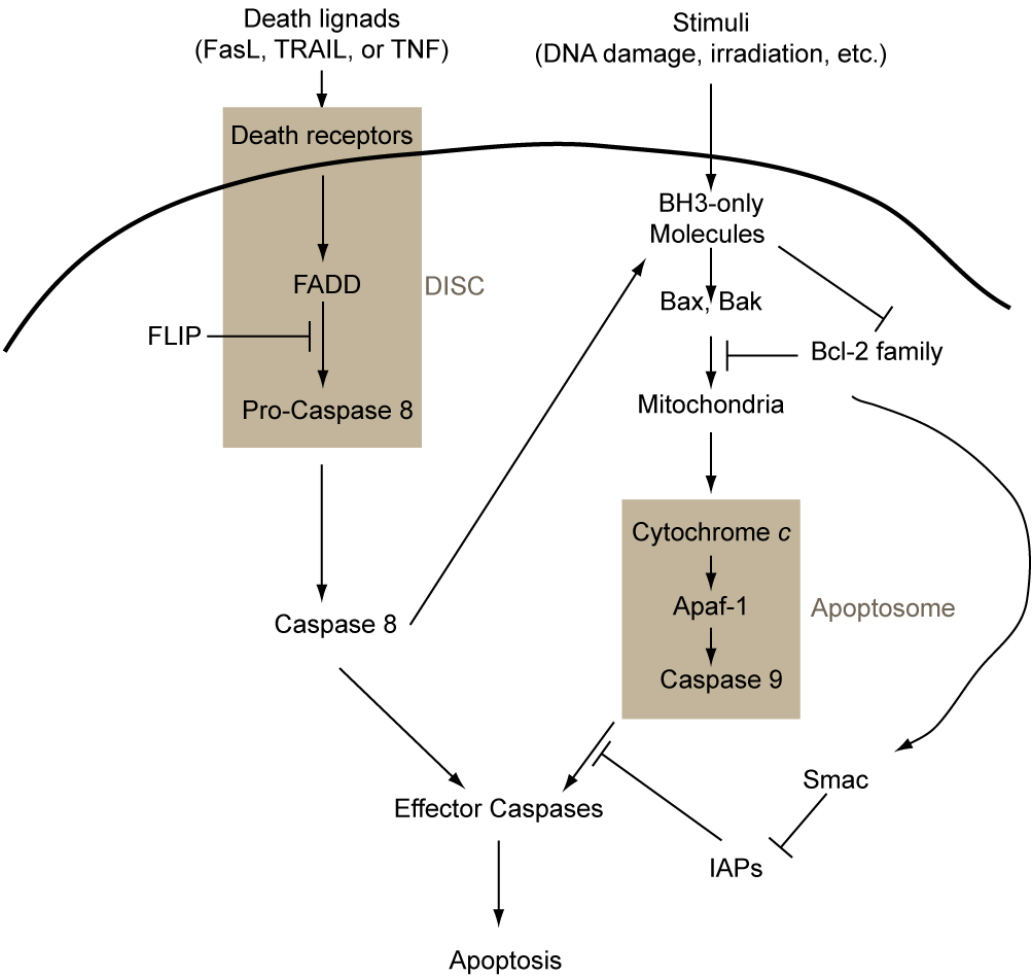

Figure 1.6 The scheme of apoptosis pathway

Intrinsic pathway: BH3 molecules release after cell stimulation (DNA damage, UV, etc), and release Bax/Bak from the Bcl-2 family. Bax/Bak can induce mitochondrial outer membrane permeabilization (MOMP) that can cause cytochrome c release from mitochondria, and further bind to APAF-1 to make conformation changes. Then this structure recruits caspse-9 to form an apoptosome, and it can activate the effector to process cell death. Apoptosome is also regulated by IAPs, which can be inhibited by Smac/DIABLO. The detail extrinsic pathway is described in Figure 1-7.

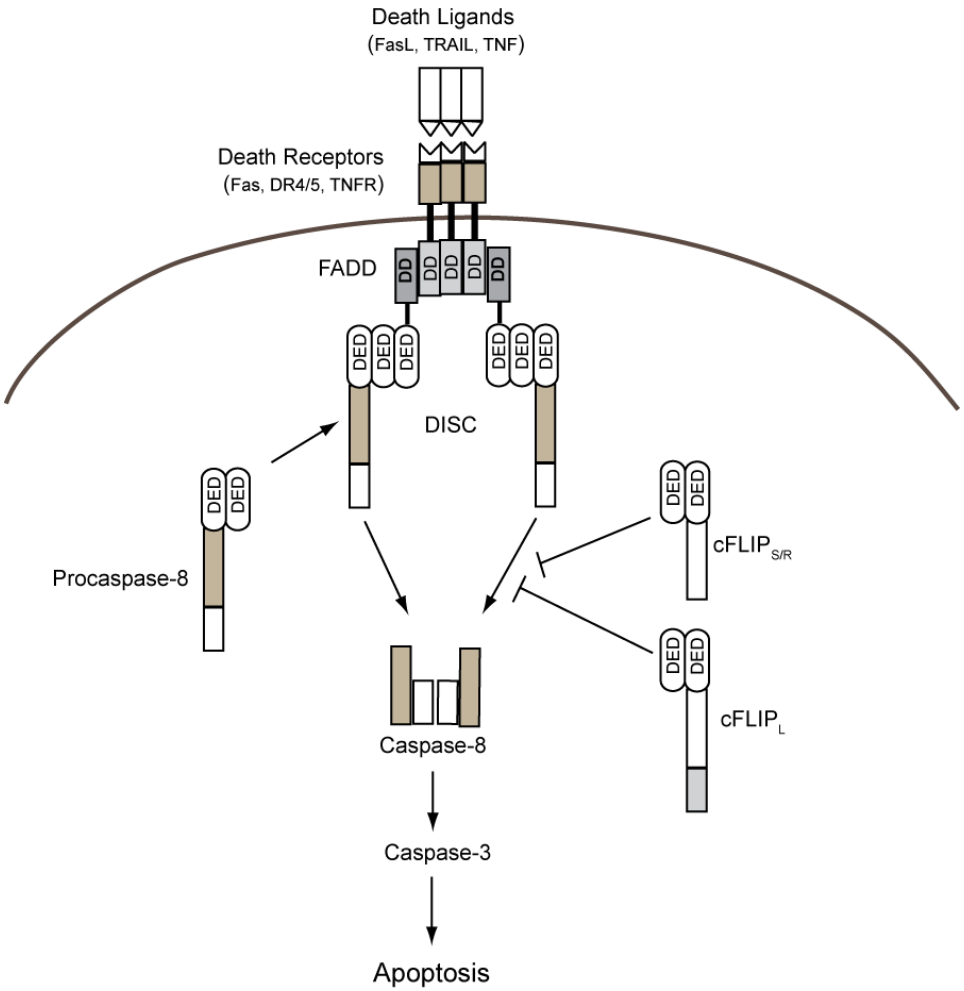

Figure 1.7 The extrinsic apoptosis pathway

FasL (TRAIL/TNF) and Fas (TRAIL-R/TNFR) belong to the TNF superfamily. First, FasL forms trimmers and then binds to Fas on the cell surface and becomes a cluster structure. This structure recruits FADD via recognition of the DD domain, and FADD then attracts the pro-caspase-8 through DED domain. The death-induced signaling complex (DISC) is then formed and pro-caspase-8 becomes activated caspase-8. Activated caspase-8 can further activate pro-caspase-3 to turn on cell death.

1.2.3 Testicular function of germ cell apoptosis

A low level of spontaneous germ cell apoptosis occurs in the testis of adult mammals under various physiological conditions. It is generally believed that apoptosis of germ cells serves as a mechanism to delete damaged cells as well as to limit the size of the germ cell population to match the supportive capacity of the Sertoli cells [41,42,43]. During the peripubertal period, a time when the first wave of spermatogenesis is nearing completion, a significantly higher rate of apoptosis is seen [1,44]. The mechanisms that control the "physiological" testicular germ cell apoptosis in both adult and peripubertal animals have not been clearly established. Many articles show that both intrinsic and extrinsic pathways may play important roles in the regulation of germ cell apoptosis [45].

1.2.3.1 Regulation of the intrinsic pathway during male germ cell development

When primordial germ cells (PGCs) migrate to the genital ridge from the base of the allantois in the embryonic stage, excess cells are generated to regulate apoptosis, and this process is controlled mainly by Bcl-xL and Bax [46]. A deficiency of Bax or an overexpression of Bcl-x and Bcl-2 can cause infertility in male transgenic mice by the over-accumulation of spermatogonia and spermatocytes in the first wave of spermatogenesis following the later death of

robotic germ cells [46,47,48]. Low levels of Bcl-xL show increased germ cell death similar to Bax over-expression while Bcl-2 deficient mice display normal spermatogenesis [49]. The loss of the Bcl-x function can be rescued by deletion of both copies of the Bax gene, resulting in a restoration of germ cell survival [46]. Therefore, a balance between anti-apoptotic and pro-apoptotic proteins is important in contributing to the normal development of spermatogenesis.

1.2.3.2 Regulation by extrinsic pathway during male germ cell development

It has been reported that up-regulation of the Fas receptor is associated with spermatocyte apoptosis during the first wave of spermatogenesis [50]. However, mice with point mutation of the Fas gene, referred to as homozygous for the lymphoproliferation spontaneous muataion (Fas^{lpr}), or with point mutation of the FasL gene, referred to as *g*eneralized *l*ymphoproliferative *d*isease (gld), are fertile with normal spermatogenesis [43]. It appears that the *lpr* mutation has either no effect or, due to tissue-specific regulation or a unique system, is present to restore proper levels of Fas. Both testis weight and spermatid heads increase in *gld* mice, but some incidence of germ cell apoptosis occurs [51]. Fas/FasL apoptosis system is involved in human hypospermatogenesis, such as maturation arrest (MA) and Sertoli cell only syndrome (SCO). The up-regulation of FasL is shown in the testis of patients with SCO and MA, which suggests that Fas/FasL may be

associated with hypospermatogenesis [52]. It has also been suggested that altered meiotic and postmeiotic germ cell maturation may be due to increased Fas expression to eliminate defective germ cells in humans [53]. However, the detailed mechanism of the extrinsic pathway associated with germ cell development remains unclear.

1.3 Toxicant injury model in the testis – Mono-(2-ethylhexyl) phthalate (MEHP) injury model

1.3.1 Phthalates

Phthalates are a group of synthetic chemicals, such as plasticizers, that are widely used in industry to give flexibility to polyvinyl chloride (PVC) products, such as plastic bags, food packaging, blood-storage containers, medical devices, and children's toys [54,55,56]. Phthalates not only exist in PVC products but also can be found in cosmetics, perfumes, and pesticides [55,57,58]. Phthalates are not chemically bound to PVC products and be released from products into indoor air, foodstuff, and other materials. Therefore, humans may be easily exposed to Phthalate compounds in living environments by direct contact or indirect contamination. Phthalates have known to cause respiratory tract diseases, such as allergy [55,59,60].

Phthalates have been broadly studied in animals following oral exposure; however, there is limited information about humans [61,62]. To date, the evaluation of environmental phthalate exposure to humans is unclear. Although most studies are based on animal models with a few reports on human [63], results show a positive correlation between phthalate exposure and reproductive disorders. Phthalates have known to induce toxicity responses in the liver, kidney,

thyroid gland and reductive organs (testis and Ovaries) based on acute and chronic treatment in rodents. In non-cancer effects studies, the data suggest that treatments with phthalates are sensitive to reproductive/developmental tracts with adverse effects [64]. Andrade and his colleagues reported the effects of DEHP on sexual development of male and female offspring in rodent models, and results show that changes in androgenic functioning are more sensitive endpoints and include a significant delay in the onset of puberty (preputial separation) at doses of 15 mg/kg/day and higher [65,66,67,68,69]. Another group of scientists studied the effects of DEHP on Leydig cell androgen and estradiol biosynthesis in male rats and found that significant decreases in serum testosterone and leutenizing hormone (LH) concentrations resulted from *in utero* exposure [70,71,72]. Additionally, decreases in semen quality and quantity may be associated with phthalate exposure in humans [73,74], and can impact perinatal testicular and genital development [75].

Most studies have focused on di(2-ehtylhexyl)phthalate (DEHP) because it is the most common phthalate used in plastic products, and most reproductive system research is based on the DEHP exposure model, such as cases described in the previous paragraph. In 2002, The Food and Drug Administration (FDA) published a risk assessment for DEHP by comparing tolerable intake (TI; calculated as 600-800 μg/kg/day parenteral and 40 μg/kg/day orally) to exposure dosage. However, the scientific Committee on Toxicity, Eco-toxicity and the

Environment of European Commission established a lower dose for tolerable daily intake (TDI) for DEHP 37 μg/kg/day and while the U.S. Environmental Protection Agency set an even lower reference dose at 20 μg/kg/day. In 2006, the National Toxicology Program reported the minimal concern dose for reproductive toxicity for DEHP to be even lower at 1-30 μg/kg/day. Due to the FDA's use of the classical risk assessment to evaluate the impact of DEHP, other researchers and agencies have expressed concern that the FDA may have under-evaluated the toxicity of DEHP, especially in endocrine disrupting compounds (EDCs).

DEHP is a diester of phthalic acid and the branched-chain 2-ethylhexanol and is easy to accumulate in fatty acid, such as adipocytes, due to its lipophilic property [76,77]. DEHP is hydrolyzed to mono-(2-ethylhexyl)phthalate (MEHP) and 2-ethylhexyanol (2-EH) by lipase and esterase in the intestines, pancreas, liver, kidney, and testes [56,78]. MEHP can further oxidize into different sub-metabolic products (mono-(5-carboxy-2-ethylpentyl)phthalate, mono-(2-ethyl-5-oxohexyl)phthalate, and mono-(2-ethyl-5-hydroxyhexyl)phthalate) by cytochrome p450, alcohol dehydrogenases, and aldehyde dehydrogenase. Therefore, the concentration of MEHP is required by the activity of these enzymes in the metabolic rate of DEHP [79].

1.3.2 Cellular response and testicular injury with MEHP exposure

MEHP, the primary metabolic product of DEHP, which can induce testicular toxicity, has been investigated in animals and humans [75,78,79,80]. Two studies have addressed this issue. The first study documented relatively good reproducibility of urinary phthalate monoester levels in two first-morning urine specimens collected for two consecutive days from 46 African-American women; day-to-day intra-class correlation coefficients ranged from 0.5 to 0.8 [81]. Recently, the temporal variability in urinary phthalate metabolite levels among 11 men who collected up to nine urine samples each during a three month period was evaluated [82]. The severe vacuolation of Sertoli cell cytoplasm and early sloughing of spermatids and spermatocytes can be observed in the testis in rodents after DEHP/MEHP exposure [79,83,84]. Further studies have demonstrated that the Sertoli cells are initial and primary targets that result in disruption of the balance, connection, and interaction between Sertoli cells and germ cells [84,85,86,87]. DEHP and MEHP can also inhibit Sertoli cell proliferation in neonatal rats resulting in a decrease in the number of Sertoli cells in the testis and alteration of the supportive capacity of Sertoli cells during spermatogenesis [88,89,90]. It has been reported that MEHP can reduce Follicle-stimulating hormone (FSH)-stimulated cAMP accumulation in Sertoli cells in rodents and can alter gene expression in Sertoli cells

[91,92,93,94]. In addition, MEHP can decrease the level of transferrin and androgen binding protein (ABP) in Sertoli cells and reduce fluid secretion in seminiferous tubules, which can impair germ cells development and differentiation [95,96]. Not only Sertoli cells are injured by MEHP exposure but also the function of steroidgenesis of Leydig cells are impaired following DEHP/MEHP treatment, which may impact the male reproductive system. The number and size of Leydig cells are decreased by DEHP exposure in young rats, resulting in a decrease in the level of testosterone [97]. High dose MEHP (250 μM) can directly inhibit the production of testosterone in primary rat Leydig cells, which may be regulated by steroidogenic acute regulatory (StAR) protein. However, even a low dose of MEHP (25-100 μM) can stimulate basal steroid synthesis in mouse Leydig tumor cells, suggesting that anti-steroidgenic effects of DEHP may prematurely initiate the onset of puberty and theoretically affect the hypothalamic-pituitary-gonadal axis by MEHP exposure [98].

1.3.3 Model of MEHP-induced germ cell apoptosis

Apoptosis naturally occurs during germ cell development in the testis and is involved in both the extrinsic and intrinsic apoptotic pathways. Germ cell apoptosis is important for controlling the appropriate number of germ cells so that each Sertoli cell can provide efficient nutrition and an adequate environment for

growth [42,99,100]. When germ cells are abnormal or have been injured by environmental toxicants, apoptosis is triggered to eliminate the abnormal cells [101]. We hypothesize that the Fas/FasL signaling may play a primary role to reduce damaged germ cells in response to MEHP exposure in the testis. The mechanism of MEHP may induce Sertoli cell injury and lead to an increase in the incidence of testicular germ cells apoptosis [43,51,102,103,104,105]. Although Sertoli cells express a basal level of FasL, the expression of FasL protein is increased when Sertoli cells are treated with MEHP. The ability of Sertoli cells to support a certain number of germ cells is reduced after injury by toxicants and more FasL can bind to Fas to form trimer superstructure so that cell death occurs via the classical extrinsic apoptotic pathway, described in session 1.2.2 (Figure 1-7). *Gld* mice, with a point mutation in C terminal of *FasL* gene, show a significant reduction in apoptosis after MEHP treatment, thus indicating that the Fas/FasL signaling system may participate in the apoptosis of toxicant-induced germ cells [51]. However, details about the mechanism of MEHP induced FasL expression in Sertoli cells remain unclear. If another death ligand TRAIL is involved in the toxicant induced model, that mechanism is also not well understood. Even though the effects of phthalates on human health are controversial due to variations in exposure time, dosage, and different animal models, it is important to unmask the issue of how phthalates may cause health problems in humans [60,73]. Therefore, it is important to understand the details of regulation of death ligands expression

after MEHP exposure, and how these processes relate to Sertoli cell injury and germ cell apoptosis.

1.4 Testicular cancer and testicular dysgenesis syndrome

Testicular cancer is most prevalent in young adult men ages 15-40 years (about 1~2% of all cancers in men) and is approximately 5 times more common in Caucasians than in other races [106,107,108]. Correlations of this disease has been reported to occur with other common testicular disorders that likely arise from shared mechanisms, such as poor semen quality and reduced sperm numbers, undescended testis, and hypospadias [109]. The incidence of these diseases has dramatically increased over the past 50 years, and it has been hypothesized that environmental influences, rather than genetic defects, account for this increase [109]. Together, cryptorchidism, hypospadias, subfertility, and testicular germ cell tumor are thought to comprise testicular dysgenesis syndrome (TDS) [109,110]. Therefore, a better understanding of the underlying mechanisms that lead to testicular cancer development and/or testicular tumor progression induced by environmental toxicants may offer insights into the etiology of other testicular diseases. Phthalates have been shown to induce hepatotoxicity and cause hepatocelluar tumorigenesis through several mechanisms [111,112,113], but little is known about the incidence of testicular cancer formation or the mechanism(s) that accounts for tumor promotion triggered by environmental stimuli. Recently, it has been shown that *in utero* dibutyl phthalate (DBP) exposure to rats exhibits similar pathologies to human TDS, such as cryptorchidism, hypospadias,

infertility, reduced spermatogenesis, and multinucleated gonocytes [114,115]. MEHP exposure also results in a decrease in testosterone levels and insulin-like factor 3 expression which are directly associated with clinical features of TDS [116,117].

1.5 Dissertation aims

Spermatogenesis is a process critical for germ cell division and morphologic development for the formation of spermatozoa. For a normal function of spermatogenesis it is important to understand how the Sertoli cells maintain a homeostasis environment for germ cell development. Germ cell apoptosis occurs during the period of testis development. First, we will discuss how apoptosis in a mouse model impacts spermatogenesis when there is a loss of a death ligand (FasL/TRAIL) (**Chapter3~5**). As introduced in previous sections, spermatogenesis may be disrupted by environmental toxicants, such as phthalates. Based on this idea, we will use the MEHP model to test whether total loss of a death ligand can provide better protection from toxicant treatments and how loss of a death ligand may influence the extrinsic pathway when one of the death ligands is absent (**Chapter 3~5**). In previous studies we showed that expression of c-Myc gene can be altered following MEHP exposure in the testes. Recent reports also discuss how environmental toxicants may cause or enhance the results of TDS in male reproduction. These findings have led us to hypothesize that MEHP may enhance the progression of testicular cancer, which is a TDS (**Chapter 6**).

The novel observation in this dissertation is that 1) The loss a death ligand can cause even more germ cell death in the testis, which infers that the death ligand may respond to environmental stress by eliminating abnormal germ cells.

The loss of a death ligand may also play another role during the first wave of spermatogenesis. 2) The apoptotic rate is decreased in FasL gene deficient mice with MEHP treatment and that reduction in the apoptosis of germ cells may be due to the loss of FasL in Sertoli cells that promotes the expression c-FLIP in germ cells. 3) We found that MEHP may have the ability to alter adhesion molecules and promote invasion and migration in testicular cancer cells. Therefore, this dissertation provides a more detailed understanding about how the death of ligands can influence germ cell apoptosis during normal development of testis as well as during treatment for environment toxicants. We also point out factors that many toxicologists may overlook when toxicants are not classified as carcinogens and those toxicants are, therefore, considered safe below certain exposure concentrations. For example, in instances where testicular cancer patients continue to be exposed to environmental toxicants, the development of the tumor may enhance progression over a shorter period of time.

Chapter 2 .Materials and Methods

2.1 *Animals*

All mice used in this study were maintained at the University of Texas Animal Resource Center. Mice were housed at a constant temperature (22±0.5°C) at 35-70% humidity with a 12L:12D photoperiod. Mice were given standard lab chow and water *ad libitum*. All procedures involving mice were performed in accordance with the guidelines of the University of Texas at Austin's Institutional Animal Care and Use Committee in compliance with guidelines established by the National Institutes of Health. Breeding pairs of wild-type C57BL/6J mice were purchased from The Jackson Laboratory (Bar Harbor, ME). Breeding pairs of FasL heterozygous mice ($FasL^{+/-}$), that are on a C57BL/6 background, were provided by Dr. Saoussen Karray, INSERM, Paris, FR [118]. FasL gene deficient mice ($FasL^{-/-}$) on a C57BL/6J background were generated by mating $FasL^{+/-}$ mice and their genotypes were confirmed by genomic PCR as described previously [118]. Breeding pairs of TRAIL gene deficient mice ($TRAIL^{-/-}$) were provided by Amgen Inc. (Thousand Oaks, CA; originally created by the laboratory of Dr. Lisa M. Sedger)[119]. In order to characterize the basic testicular phenotype, C57BL/6J, $FasL^{-/-}$, and $TRAIL^{-/-}$ mice were killed at PND 28 and PND 44 by CO_2

inhalation. The testes were rapidly removed and either frozen in liquid nitrogen and stored at -80°C for protein analysis, or immersion-fixed overnight in Bouin's solution (Polysciences, Inc., Warrington, PA), washed in 70% ethyl alcohol-Li_2CO_3 saturated solution and embedded in paraffin for histology analysis.

2.2 *Cell line*

The human testicular embryonal carcinoma cell line, NTERA-2 cl. D1 (NT2/D1), was purchased from American Type Culture Collection (ATCC, Manassas, VA), and cultured in Dulbecco's modified Eagle's media (DMEM, ATCC) supplemented with 10% fetal bovine serum and 1% penicillin-streptomycin (all Invitrogen, Carlsbad, CA) at 37°C with 5% CO_2.

2.3 *Total protein preparation for cell line and testis and western blot analysis*

Cultured cells were trypsinized with 0.25% trypsin-EDTA and centrifuged at 1200 rpm for 5 minutes at 4 ℃. Pellets were resuspended in homogenization buffer containing RIPA buffer (1% NP-40, 0.5% Sodium dexoycholate and 0.1% SDS in 1X PBS) with 100 μM Na_3Vo_4, 10μM E64 and protease inhibitor cocktail (Roche, Indianapolis, IN), and incubated on ice for 30 minutes. After

centrifugation at 14,000 rpm for 20 minuted 4 ℃, the supernatant containing total proteins was collected and stored at -80 ℃.

Testis were freshly collected from mice or stock samples from -80 ℃, and testis were transferred to homogenizer with 500 µl homogenization buffer on ice (3 ml RIPA buffer, 90 µl Aprotinin(0.3 mg/ml) ,30 µl Na_3Vo_4 (10 mg/ml), 15 µl PMSF (10mg/ml), 0.6 µl Leupertion (10mg/ml), and 3 ul E64. The testis were ground several times, and a small fraction were collected in the Eppendorf on ice for 30 minutes. The samples were centrifuged at 14,000 rpm for 20 minutes at 4 ℃, and the supernatant was collected and transferred to new Eppendorf tubes. This step was repeated several times until the lysate became clean. The supernatant was collected and stored at -80 ℃.

The concentration of total proteins was measured by the Lowery Method. The total proteins (30µg) were separated by gradient SDS page and transferred to PVDF membrane. Total cellular proteins were detected using primary antibodies against FasL (1:500, Santa Cruz Biotenchnology Inc., Santa Cruz, CA), TRAIL (1:250, Invitrogen), c-FLIP (1:1000, Enzo, NY), c-Myc, MMP-2, MMP-9 (1:1000, Abcam Inc., Cambridge, MA), α-tubulin , β-actin (1:500, Santa Cruz Biotenchnology Inc., Santa Cruz, CA) coupled with horseradish peroxidase-conjugated secondary antibodies (1:5000, Santa Cruz Biotechnology Inc. or

1:1000, Cell Signaling Inc, MA). The ECL chemiluminescent substrate (Amersham Bioscicence, Piscataway, NJ) was used as the detection reagent and α-tubulin or β-actin as the internal control for gel loading. Images of western blots were captured using a Kodak Gel Logic 100 Imaging system (Kodak, Rochester, New York). Densitometry for bands on western blots was determined by ImageJ software (National Institute of Mental Health, Bethesda, Maryland). All experiments were performed in triplicate and repeated at least three times.

2.4 *MEHP treatment*

MEHP exposure in peri-pubertal rodents has been reported to be a good model to test the interaction between Sertoli cells and germ cells by decreasing Sertoli cell support [103,120,121,122]. PND 28 $FasL^{-/-}$ and C57BL/6J mice were given a single dose of MEHP (1 g/kg, TCI America, Portland, OR) by oral gavage at a volume equal to 4 ml/kg, a standard procedure for investigating the consequences of MEHP-induced Sertoli cell injury [123]. Control animals received a similar volume of vehicle (corn oil). Both control and MEHP-treated mice were killed at 0, 6, 12 and 24 hours after MEHP exposure.

2.5 *Physiologic characterization of the testis*

The body and testis weights of mice at PND 28 and 44 were measured. The number of mice used by types: PND 28 C57BL/6J mice (n=26), $FasL^{-/-}$ mice (n=40), and $TRAIL^{-/-}$ mice (n=34); PND 44 C57BL/6J mice (n=8), $FasL^{-/-}$ mice (n=16), and $TRAIL^{-/-}$ mice (n=10).

2.6 *Testicular histopathology*

Cross-sections (5 μm) of paraffin-embedded testes were evaluated for morphological changes by using periodic acid-Schiffs-Hematoxylin (PAS-H) staining. Testis cross-sections were imaged using a Nikon E800 microscope and captured with a Canon 5D digital camera (Canon U.S.A. Inc., NY). The number of mice by type used for the evaluation of testicular morphology: PND 28 C57BL/6J mice (n=7), $FasL^{-/-}$ mice (n=8), and $TRAIL^{-/-}$ mice (n=4); PND 44 C57BL/6J mice (n=6), $FasL^{-/-}$ mice (n=6), and $TRAIL^{-/-}$ mice (n=3).

2.7 *Testicular spermatid head counts*

Testicular spermatid head counts were performed as previously described with slight modifications [51]. Briefly, testes from PND 44 mice were

homogenized in DMSO/saline solution containing 0.9% (w/v) NaCl and 10% (v/v) DMSO, and then homogenization-resistant spermatid heads were counted using a hemocytometer. The average number of spermatid heads was determined from 12 C57BL/6J mouse testes, 13 $FasL^{-/-}$ mouse testes, and 8 $TRAIL^{-/-}$ mouse testes. Each testis sample was counted three times. The daily sperm production per testis was calculated by using 4.84 days as the time divisor [124].

2.8 *Terminal deoxy-nucleotidyl transferase-mediated digoxigenin-dUTP nick end labeling (TUNEL) assay*

Apoptotic fragmentation of DNA in mouse paraffin-embedded testis cross sections was determined by TUNEL analysis using the ApopTag^{TM} kit (Chemicon, Temecula, CA). The apoptotic index (AI) was calculated as the percentage of essentially round seminiferous tubules in a cross-section that contained more than three TUNEL-positive germ cells. At least two testicular cross-sections per mouse were analyzed. The apoptotic index was determined from 6 C57BL/6J mice and 7 $FasL^{-/-}$ mice at PND 28 and 4 C57BL/6J mice and 5 $FasL^{-/-}$ mice at PND 44. The number of each group for MEHP-treated C57BL/6J mice: 0h (n=7), 1h (n=3), 3h (n=3), 6h (n=4), 12h (n=3) and 24h (n=3). The number of each group for MEHP-treated $FasL^{-/-}$ mice: 0h (n=8), 1h (n=4), 3h (n=6), 6h (n=4), 12h (n=4) and 24h (n=3).

2.9 *Immunohistochemistry*

Expression of cleaved caspase-9 in the germ cells was determined by immunohistochemstry. Cross-sections (5 μm) of paraffin-embedded testes from PND 28 C57BL/6J and $FasL^{-/-}$ mice were deparaffinized and rehydrated, and antigens were unmasked by heating in 10 mM sodium citrate solution. Sections were incubated with 3% H_2O_2 to block endogenous peroxidase activity and then incubated in blocking buffer containing 10% horse serum. The primary antibody used in this study was rabbit-anti-cleaved-caspase-9 (1:100, Cell Signaling, Danvers, MA). Sections were incubated in primary antibody at 4℃ overnight. Immuno-detection was performed by standard procedures using the VectaStain ABC kit (Vector Labs, Burlingame, CA) and DAB as the substrate (Vector Labs). At least two testicular cross-sections per mouse were analyzed. The number of each group for MEHP-treated C57BL/6J mice: 0h (n=3), 12h (n=3). The number of each group for MEHP-treated $FasL^{-/-}$ mice: 0h (n=4), 12h (n=3). All sections were observed using a Nikon E800 microscope. The percentage of cleaved caspase-9 positive germ cells was calculated as the number of positive germ cells/total germ cells x100.

2.10 *Immunofluorescence*

Expression and localization of c-FLIP in testis cross sections was determined by immunofluorescence detection of c-FLIP antibody (rabbit-anti-c-FLIP; 1:100, Cell Signaling). Cross-sections (5 μm) of paraffin-embedded testes from C57BL/6J and $FasL^{-/-}$ mice were deparaffinized, rehydrated, heated in 10 mM sodium citrate and incubated in blocking buffer containing 10% horse serum, followed by overnight incubation in primary antibodies at 4℃. Sections were then incubated in Alexa Fluor conjugated anti-rabbit antibody (1:500, Molecular Probes, Gaithersburg, MD) for 1 h and mounted in Vectashield Mounting Medium (Vector Labs). Fluorescent signals were detected using excitation/emission wavelength of 495 nm/521 nm. Images were captured by a Nikon E800 microscope captured with a Nikon Cool-SNAP digital camera, and processed using MetaMorph Imaging software (v. 4.1) (Downingtown, PA). Two testicular cross-sections per mouse were analyzed. The number of each group for MEHP-treated C57BL/6J mice: 0h (n=3), 12h (n=3). The number of each group for MEHP-treated $FasL^{-/-}$ mice: 0h (n=4), 12h (n=3).

2.11 *Gelatin zymography*

The MMP-2 and MMP-9 gelatinolytic activity in media derived from NT2/D1 cells was assayed by gelatin zymography with minor modifications [122]. Briefly, 12 h after the addition of MEHP (200 μM) to $2x10^6$ NT2/D1 cells, conditioned media were collected and directly applied to a 10% Zymogram gel (Invitrogen). After electrophoresis, the gels were washed twice for 15 min with 2.5% Triton X-100 in 50mM Tris-HCl (pH 7.5) to remove the SDS and restore enzyme activity and incubated in developing buffer (50 mM Tris-HCl, pH 7.5, 200 mM NaCl, 10 mM $CaCl_2$ and 0.02% sodium azide) overnight at 37˚C. The gels were then stained with 30% methanol/10% acetic acid containing 0.5% (w/v) Coomassie Brilliant blue R-250 for 30 min and destained in the same solution without dye. Clear bands shown on the blue background indicated enzyme activity.

2.12 *Measurement of soluble*

MMP-2 levels - NT2/D1 cells ($2x10^6$) were exposed to MEHP for various time periods. The culture media were collected and centrifuged to remove cellular debris. The supernatant was rapidly frozen at -80˚C until assayed for MMP-2 by

ELISA (R&D Systems, Inc.) following the manufacture's protocol. The cell number was counted to normalize the protein expression assayed by ELISA.

2.13 *Invasion assay*

The *in vitro* invasion assay was performed using transwell chambers with 8 μm pores in the polycarbonate filters (Costar, Cambridge, MA) as previously described [125]. Transwell membranes were coated with Matrigel diluted in serum-free media (1:3 dilution, BD Biosciences, San Diego, CA). Non-treated or MEHP-treated NT2/D1 cells ($1x10^5$) were seeded on Matrigel and incubated at 37˚C for 18 h. Membranes coated with Matrigel were wiped with Q-tips, fixed with methanol and stained with 20% Giemsa solution (sigma, St. Louis, MO). Cells attached to the lower surface of the filters were then counted under a light microscope (x200 magnification). Cells are photographed by Canon-5D digital camera attached to a light microscope.

2.14 *Migration assay*

Cell migration was estimated by a wound-healing test in NT2/D1 cells. Non-treated or MEHP-treated NT2/D1 cells ($5x10^5$) were seeded into 6-cm culture plates and grown to almost confluent cell monolayer. A pipette tip was

used to scratch cell monolayer to generate the cell-free zone in the middle of culture plates. Cell debris was removed by washing with PBS. Cells were then incubated at 37˚C for up to 36 h. The number of cells migrating into the cell-free zone was counted under a light microscope (x200 magnification). Cells were photographed by Canon-5D digital camera attached to a light microscope.

2.15 *Gelatinase inhibitor SB-3CT treatment in vitro*

It has been shown that SB-3CT is able to inhibit the activity of endogenous gentalinases, including MMP-2 [126]. NT2/D1 cells ($5x10^5$) were treated with 10 μM of SB-3CT (Chemicon, Temecula, CA) in the presence of MEHP (200 μM) for 12 h. Treated cells were then used for invasion and migration assays.

2.16 *Microarray and data analysis*

Microarray analysis was performed using Human and Mouse Whole Genome OneArray v.5 manufactured by Phalanx Biotech Group (Belmont, CA), carrying 29,187 human genome probes (26423 probes for mouse) and 1,088 experimental control probes (872 control probes for mouse). Total RNA from mouse testis treated with MEHP for 12 hours, and from NT2/D1 cells treated with MEHP for 0, 3 and 24 h was isolated using Qiagen RNeasy kit (Qiagen, Valencia,

CA). Array hybridization, image processing, signal intensity acquisition and data normalization were performed by Phalanx Biotech Service Group. Normalized values for each data point were averaged using three biological replicates. Significant expression differences were defined as a *p*-value <0.05 and genes with a value greater than 2-fold or 4-fold change were selected by Cluster Software (Stanford University and Massachusetts Institute of Technology). Selected genes were grouped according to their biological function and clustered using a hierarchical cluster method (TreeView, Stanford University and Massachusetts Institute of Technology).

2.17 *Semi-quantitative reverse transcription-polymerase chain reaction (RT-PCR)*

To confirm the results derived from the microarray analysis, 11 differentially expressed genes were randomly selected from the cluster analysis, and their mRNA levels were measured by semi-quantitative RT-PCR. First strand cDNA was prepared using 5 μg of total RNA with Superscript II reverse transcriptase and oligo-dT primer (all Invitrogen). The primers used to amplify differentially expressed genes are listed in Table 2.1 Glyceraldehyde-3-phosphate dehydrogenase (*GAPDH*) was quantified as an internal control. PCR reaction was performed by 28 cycles of 92°C for 30 sec, 54°C for 1 min and 72°C for 30 sec followed by 72°C for 5 min with 1 unit of *Taq* DNA polymerase. PCR products

were separated on 1.5% agarose gel and images were captured using a Kodak Gel Logic 100 Imaging system. Densitometry for bands on PCR products was determined by ImageJ software. The relative expression level of each gene was normalized by the value of GAPDH.

2.18 *Statistical analysis*

In this study, the minimum number of animals necessary to achieve statistical significance were used after performing statistical power analysis (α=0.05, β=0.05) to test if the power of sample size was sufficient [127,128]. Statistical results were presented as the individual means ± SEM. The data were subjected to a Student *t*-test or parametric one-way analysis of variance (ANOVA) and statistical significance using Fisher's protected least significant difference was considered to be achieved when $p \leq 0.05$.

Table 2.1 Nucleotide sequence of RT-PCR primers designed to generate MEHP-regulated genes

Gene name	Accession No.	Primer sequence (5'→3')
Neurotensin (NTS)	NM_006183.3	F: aagcacatgttccctcttgg
		R: aagccctgctgtgacagatt
Inhibitor of DNA binding 1 (ID1)	NM_002165.2	F: cggatctgagggagaacaag
		R: ctgagaagcaccaaacgtga
Vinculin (VCL)	NM_014000.2	F: ctttgctgctacaggggaag
		R: ggatatgggacgggaagttt
Gap junction protein alpha 1 (GJA1)	NM_000165.3	F: atgagcagtctgcctttcgt
		R: tctgcttcaagtgcatgtcc
LFNG O-fucosylpeptide 3-beta-N-acetylglucosaminyltransferase (LFNG)	NM_002304.2	F: cctgtgtcatagccccaagt R: ctccccactcagaagagctg
Interleukin 17 receptor D (IL17RD)	NM_017563.3	F: ctgtctctgccactgatgga
		R: ccaagatctgctttgcatga
Claudin 6 (CLDN6)	NM_021195.4	F: ttttgtttctgcctcctgct
		R: gcctccgcattagttccata
β1-Catenin (CTNNB1)	NM_001904.3	F: gaaacggctttcagttgagc
		R: ctggccatatccaccagagt
Methionyl-tRNA synthetase (MARS)	NM_004990.2	F: cctgcagtatcctgctgaca
		R: tccatcagcgcttgtatctg
Matrix metalloproteinase 2 (MMP2)	NM_004530.4	F: atgacagctgcaccactgag
		R: atttgttgcccaggaaagtg
Inhibitor of DNA binding 3 (DDIT3)	NM_001195053.1	F: gcgcatgaaggagaaagaac
Glyceraldehyde 3-phosphate dehydrogenase (GAPDH)	NM_002046.3	F: gagtcaacggatttggtcgt R: ttgattttggagggatctcg

F: Forward; R: Reverse

Chapter 3: FasL Gene–Deficient Mice Display a Limited Disruption in Spermatogenesis and Inhibition of Mono-(2-ethylhexyl) Phthalate–Induced Germ Cell Apoptosis

(The data presented in this chapter were published in ***Toxicology Science*** 2010; 114(2):335-345. The co-authors, Dr. Pei-Li Yao contributed to collect part of data and Dr. Richburg was sponsor for this research)

3.1. Introduction and Rationale

The mechanisms responsible for the control of physiological apoptosis of germ cells in the testis have not been clearly resolved, but the direct involvement of FasL/Fas signaling in triggering germ cell apoptosis has been described in rodents after exposure to the Sertoli cell toxicant mono-(2-ethylhexyl) phthalate (MEHP) [43,123]. The functional participation of FasL/Fas signaling in MEHP-induced germ cell apoptosis has been shown experimentally by challenging *gld* (*g*eneralized *l*ymphoproliferative *d*isease) mutant mice with MEHP [51]. The *gld* mice have a mutation that causes a single amino acid change in FasL, preventing it from binding to and activating its receptor Fas [129]. Although these mice are fertile and show similar basal germ cell apoptotic rates as wild-type mice, a significant reduction in the incidence of germ cell apoptosis has been seen in the *gld* mice in response to MEHP exposure as compared to the C57BL/6J wild-type

mice [51]. However, since the protection from MEHP-induced germ cell apoptosis was not complete, it is thought that the mutant form of FasL in *gld* mice may retain some of its activity.

In this chapter, to adequately test the hypothesis that FasL is required for the regulation of germ cell apoptosis during distinct peripubertal periods, we evaluated the testis of FasL gene deficient ($FasL^{-/-}$) mice during the first wave of spermatogenesis (PND 28, the peripubertal age) as well as the period directly after the completion of the first wave of spermatogenesis (PND 44, adulthood). In addition, the sensitivity of PND 28 $FasL^{-/-}$ mice to the testicular effects MEHP exposure was characterized.

3.2. RESULTS

3.2.1 *Assessment of testicular parameters in FasL$^{-/-}$ and C57BL/6J wild-type mice*

In order to initially characterize the testis of FasL$^{-/-}$ mice, the body weights, testis weights, and testicular spermatid head counts were measured in peripubertal (PND 28) and adult (PND 44) mice (Table 3.1). No significant differences in body weights or testis weights were evident between FasL$^{-/-}$ and C57BL/6J mice at PND 28 (Table 3.1). In adults (PND 44), the body weights of FasL$^{-/-}$ were significantly increased compared to the C57BL/6J mice (22.15±0.27 g and 19.5±0.54 g, respectively), while no differences were observed between their testis weights. The testis/body weight ratio in adult FasL$^{-/-}$ mice was not significantly decreased as compared to C57BL/6J mice (0.0035 and 0.0038, respectively). Measurements of spermatid head counts revealed that adult FasL$^{-/-}$ mice have significantly reduced mature spermatids (51±1.32%) as compared to C57BL/6J mice.

Table 3.1 Comparison of C57BL/6J wild-type and FasL$^{-/-}$ mice baseline testicular parameters [a]

Mouse strain	Body weight (g)		Testis weight (g)		Spermatid heads/g testis/day ($X10^6$)
	PND 28	PND 44	PND 28	PND 44	PND 44
C57BL/6J	14.53±0.40 (26)	19.50±0.54 (8)	0.0528±0.0026 (26)	0.0744±0.0024 (8)	40.24±0.68 (12)
FasL$^{-/-}$	15.00±0.58 (40)	22.15±0.28 (16)[b]	0.0489±0.0028 (40)	0.0794±0.0017 (16)	21.06±0.11 (13)[b]

[a] Data represent the mean ± SEM, and numbers of examined mice and testis in each strain are indicated in parentheses.

[b] $p<0.05$, by ANOVA followed by Fisher's protected least significant differences test.

3.2.2 *Abnormal testicular histopathology in young FasL$^{-/-}$ mice*

Evaluation of the histology of testicular cross sections from PND 28 FasL$^{-/-}$ mice revealed that 7 out of 10 FasL$^{-/-}$ mice had abnormal tubules and about 3% of the seminiferous tubules showed a significant loss of germ cells. However, only 1 out of 10 C57BL/6J mice showed some similar abnormal tubules. The most severely affected seminiferous tubules were populated by only Sertoli cells and few spermatogonia (Fig 3.1A-D). In contrast, the testes of adult PND 44 FasL$^{-/-}$ mice showed numerous germ cells and apparently normal histology (Fig 3.2A-D), despite the lower number of mature spermatids produced. These observations indicate that the seminiferous epithelium of adult FasL$^{-/-}$ mice is able to partially recover from the drastic germ cell loss seen in the peripubertal period.

3.2.3 *Increased basal apoptotic rate in germ cells in FasL$^{-/-}$ mice*

Contrary to our expectations, FasL$^{-/-}$ mice at both PND 28 (Fig 3.1E) and PND 44 (Fig 3.2E) showed dramatic increases in the basal numbers of TUNEL-positive germ cells as compared to C57BL/6J wild-type mice. The testis of FasL$^{-/-}$ mice showed a basal germ cell apoptotic index (AI) of 20.58 at PND 28, and 5.26 at PND 44. The testis of C57BL/6J mice had a relatively low germ cell AI at both PND 28 (5.16) and PND 44 (1.50).

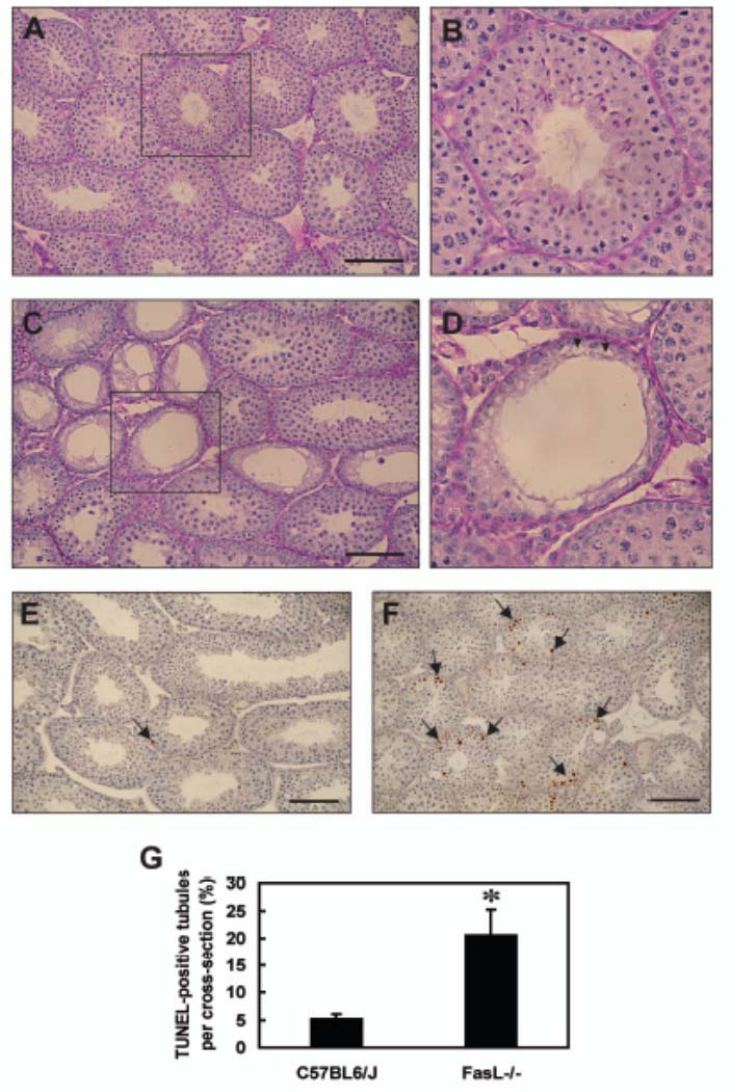

Fig 3.1 Testicular histopathology of PND 28 C57BL/6J and FasL gene-deficient (FasL$^{-/-}$) mice. Cross-sections (5 μm) of paraffin-embedded testis tissues were stained with periodic acid-Schiffs-Hematoxylin (PAS-H) staining (A-D) or TUNEL assay (E, F). A, B, E: C57BL/6J wild-type mice; C, D, F: FasL$^{-/-}$ mice; B, D: the magnification of one seminiferous tubule of A and C (boxed area). Arrow heads indicate Sertoli cell vacuolization. Arrows indicate TUNEL-positive germ cells (brown spots). The bar represents 100 μm. G: the germ cell apoptotic rate by TUNEL assay. PND 28 FasL$^{-/-}$ mice have a significantly increased incidence of TUNEL-positive germ cells (*<0.05, Student *t*-test)

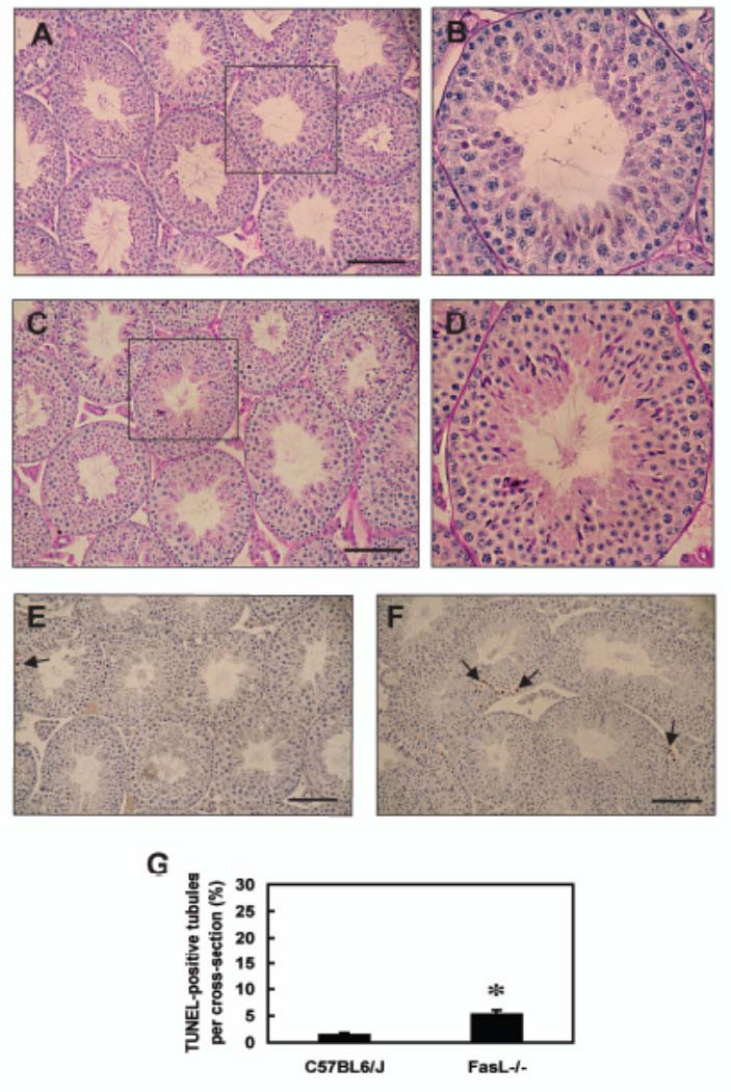

Fig 3.2 Testicular histopathology in PND 44 C57BL/6J and FasL$^{-/-}$ mice. Cross-sections (5 μm) of paraffin-embedded testis tissues from PND 44 mice were stained with PAS-H staining (A-D) and TUNEL assay (E, F). A, B, E: C57BL/6J mice; C, D, F: FasL$^{-/-}$ mice; B, D: the magnification of one seminiferous tubule of A and C (boxed area). Arrows indicate TUNEL-positive germ cells (brown spots). The bar represents 100 μm. G: the apoptotic rate in germ cells by TUNEL assay. PND 44 FasL$^{-/-}$ mice have a significantly increased incidence of TUNEL-positive germ cells (*<0.05, Student *t*-test).

3.2.4 *Germ cell apoptosis decreased in FasL$^{-/-}$ mice after MEHP exposure*

In order to evaluate the effect of MEHP on germ cell apoptosis, PND 28 FasL$^{-/-}$ and C57BL/6J mice were treated with 1 g/kg of MEHP for various time periods; a treatment paradigm that has been employed for the evaluation of death-receptor dependent germ cell apoptosis was used [76]. In C57BL/6J mice, increases in the number of apoptotic germ cells were apparent in a time-dependent manner after MEHP exposure (Fig 3.3); these findings were consistent with previous reports [51,122]. As described above, the basal AI in the testis of FasL$^{-/-}$ mice was 20±4.59, a level very near the maximal AI seen in MEHP treated C57BL/6J mice (Fig 3.1G). In response to MEHP exposure, this high basal AI FasL$^{-/-}$ mice was found to significantly decrease at 6 hours after exposure and remain at this decreased level at both the 12 and 24 hour time points (Fig 3.3). The maximal difference in the AI between the FasL$^{-/-}$ and C57BL/6J mice was observed at the 12 hour time point with ~50% difference (10.09 and 23.86, respectively).

3.2.5 *MEHP exposure does not result in an increase in the cleavage of caspase 9 in FasL$^{-/-}$ mice.*

In order to assess the participation of the intrinsic pathway in FasL$^{-/-}$ mice after MEHP exposure, we evaluated the level of cleaved caspase-9, the active form of this enzyme, in testicular cross-sections by immunohistochemistry. The level of cleaved caspase-9 decreased in C57BL/6J mice after MEHP treatment, but no significant differences were observed in FasL$^{-/-}$ mice (Fig. 3.4).

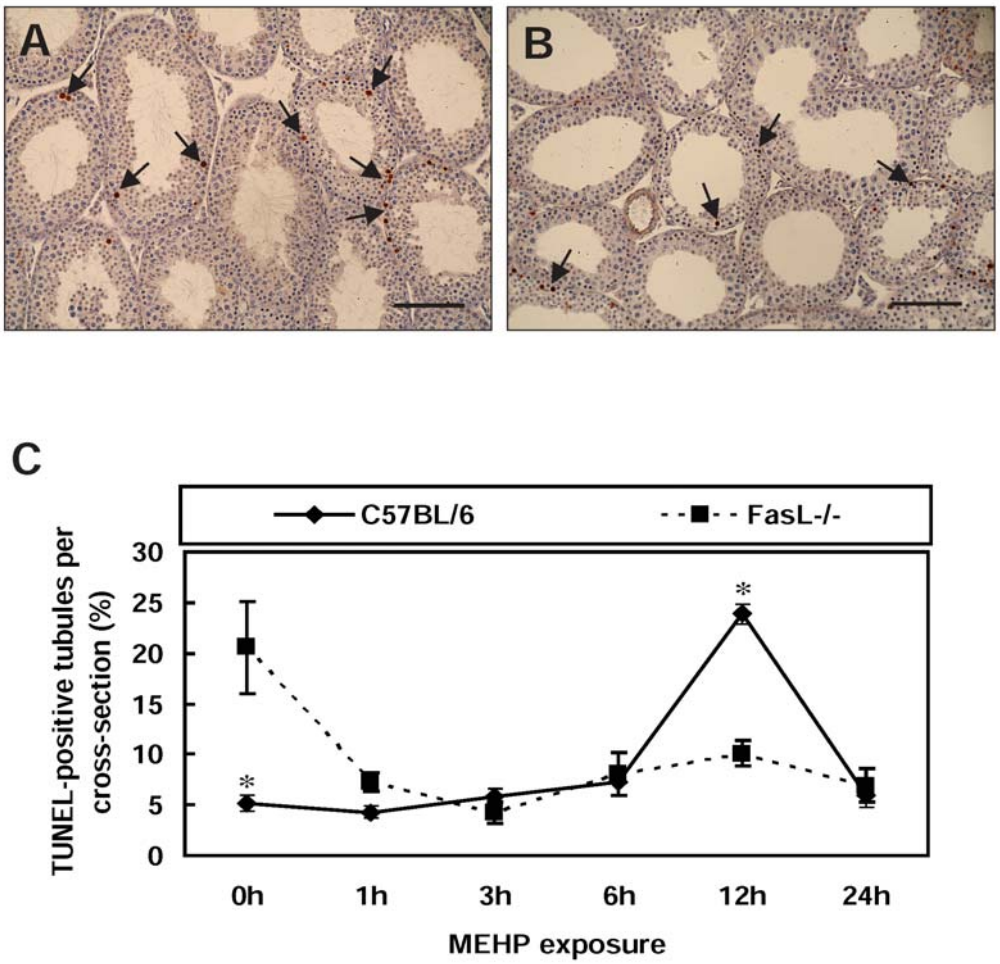

Fig 3.3 Germ cell apoptotic index (AI) in peripubertal FasL gene-deficient mice after MEHP exposure. The AI in mouse paraffin-embedded testis cross sections was determined by TUNEL assay. PND 28 mice were treated with MEHP for various periods of time. Testicular cross-sections show TUNEL-positive germ cells as brown spots (arrows) in MEHP-treated C57BL/6J mice (A) and $FasL^{-/-}$ mice (B) at 12 h of exposure. The bar represents 100 μm. (C) C57BL/6J wild-type mice displayed an increase in germ cell apoptosis at 12 h of MEHP exposure. The apoptotic rate of germ cell in $FasL^{-/-}$ mice significantly decreased after MEHP exposure (*<0.05, Student *t*-test).

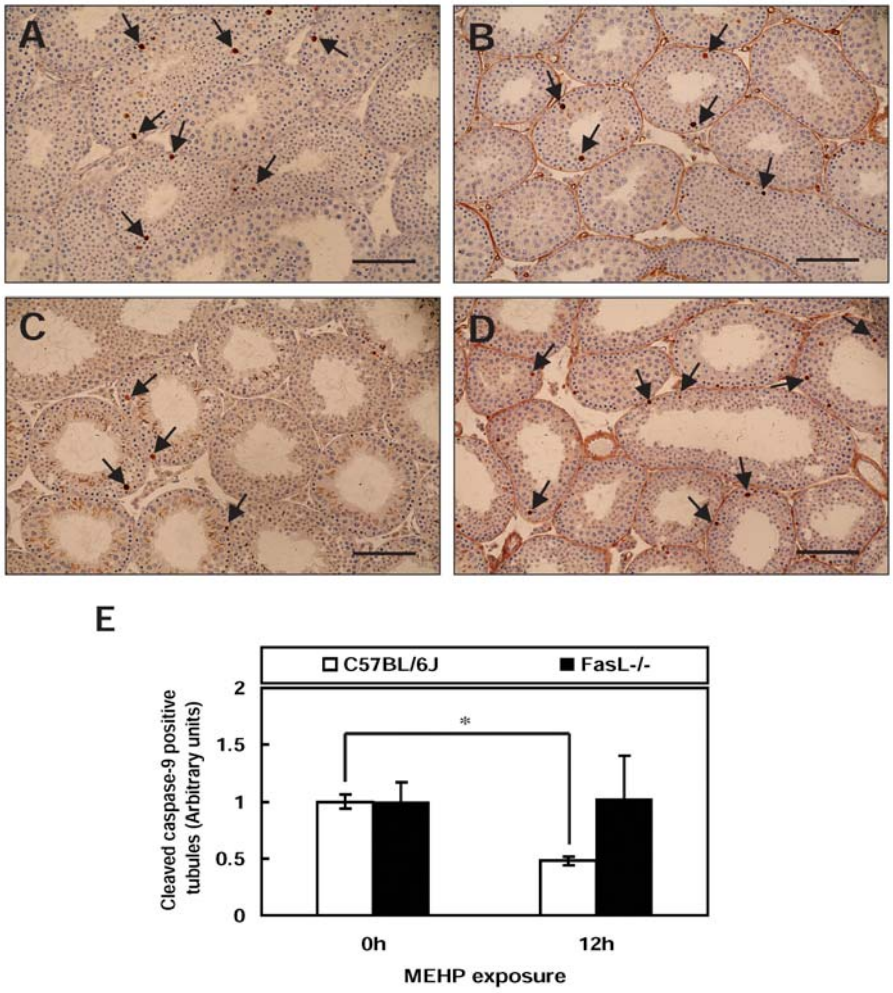

Fig 3.4 Immunohistochemical detection of cleaved caspase-9 in mice testes. Cross-sections (5 µm) of paraffin-embedded testis tissues from C57BL/6J and FasL$^{-/-}$ mice (PND 28) were analyzed. (A) Non-treated C57BL/6J mice; (B) C57BL/6J mice treated with MEHP for 12 h; (C) Non-treated C57BL/6J mice; (D) C57BL/6J mice treated with MEHP for 12 h. The arrows indicate the cleaved-caspase-9-positive germ cells. The bar represents 100 µm. (E) Testis cross-sections showed that the level of cleaved caspase-9 was reduced in C57BL/6J mice after MEHP exposure but remained the same expression when FasL signaling was absent (*<0.05, Student *t*-test).

3.2.6 *Expression of TRAIL protein in the testis of young FasL$^{-/-}$ mice*

Western blot analysis of testis samples from FasL$^{-/-}$ (PND 28) mice showed that the expression of TRAIL was 1.3-fold higher than that seen in C57BL/6J (PND 28) mice (Fig 3.5A and 3.5B). After MEHP exposure, TRAIL levels increased at 12 hours in the testis of C57BL/6J mice but no significant changes in TRAIL levels were measured in the testis of FasL$^{-/-}$ mice at any time point.

3.2.7 *Increased c-FLIP expression in FasL$^{-/-}$ mice after MEHP exposure*

Western blot analysis of testis samples from both C57BL/6J (PND 28) and FasL$^{-/-}$ (PND 28) mice indicated that the basal levels of c-FLIP was very low (Fig 3.5A and 3.5C). However, in response to MEHP exposure, the levels of c-FLIP were found to be significantly increased in the FasL$^{-/-}$ mice (~2.3-fold) at each of the measured time points but not at any of the time points in C57BL/6J mice.

3.2.8 *Localization of c-FLIP in the seminiferous tubules*

Immunofluorescence detection of c-FLIP in testis cross-sections revealed that it is localized within the cytoplasm of spermatocytes and round spermatids but not in spermatogonia in PND 28 C57BL/6J mouse testes (Fig 3.6A). However, PND 28 FasL$^{-/-}$ mice had a very low expression level of c-FLIP in the seminiferous tubule as compared to

C57BL/6J mice (Fig 3.6B). The c-FLIP expression in MEHP-treated C57BL/6J mice remained similar to that observed in non-treated mice (Fig 3.6C). However, its expression increased in treated- $FasL^{-/-}$ mouse testis compared to non-treated groups (Fig 3.6D).

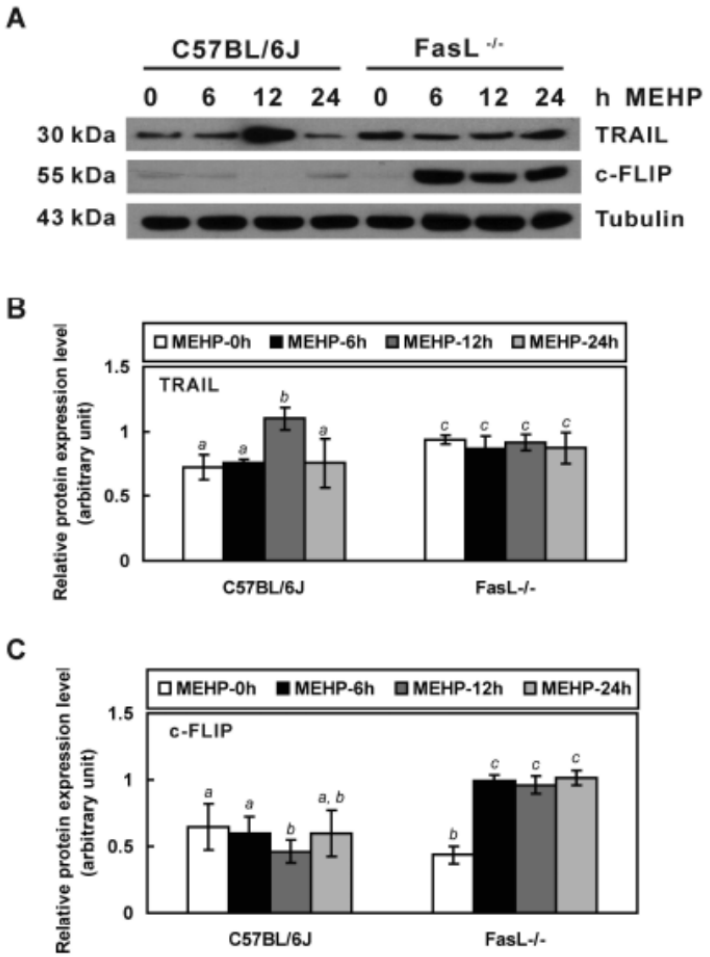

Fig 3.5 Western blot analyses of TRAIL and c-FLIP protein expression in PND 28 FasL gene-deficient mice. Total cellular proteins from whole testis tissues were detected using primary antibodies against TRAIL (1:250) and c-FLIP (1:1000). FasL$^{-/-}$ mice showed a significant increase in TRAIL expression compared to C57BL/6J mice. TRAIL expression in C57BL/6J wild-type mice was enhanced by 12 h MEHP exposure while there was no significant difference between control or MEHP-treated FasL$^{-/-}$ mice. C57BL/6J mice had a very low expression level of c-FLIP. FasL$^{-/-}$ mice showed a higher level of c-FLIP protein after MEHP treatment. A: western blot; B: the quantified measurement of TRAIL expression level; C: the quantified measurement of c-FLIP expression level. Significant differences between groups are denoted by bars with different letters (p<0.05, ANOVA). For example, if any bar shows the same letter, it means that they do not show significant between each other.

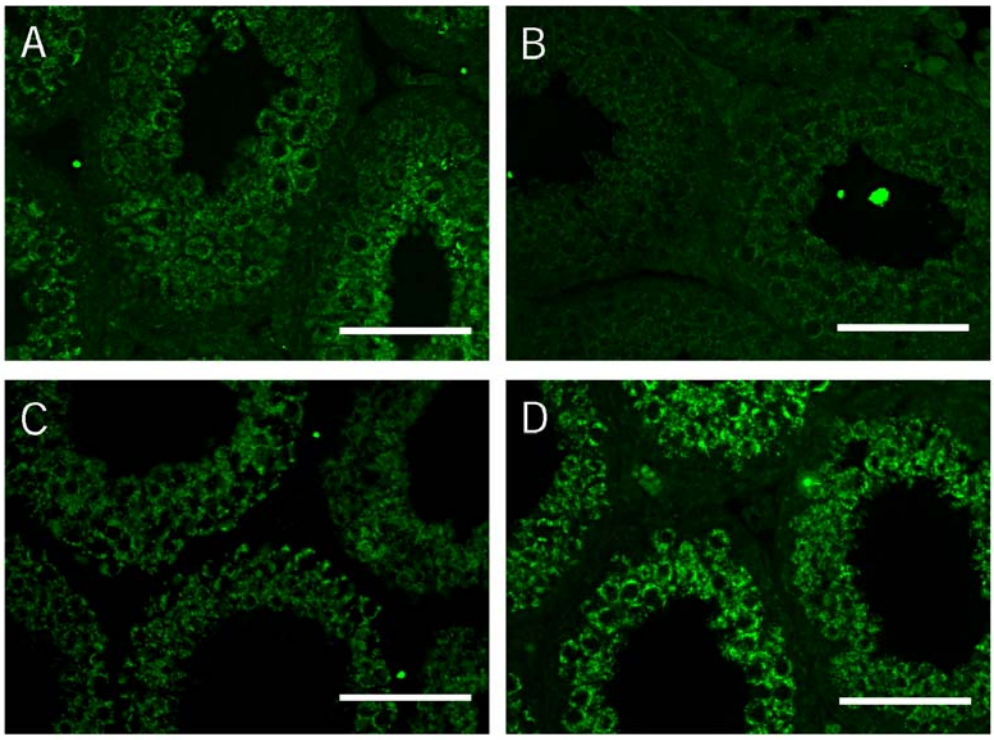

Fig 3.6 The expression and localization of c-FLIP in the seminiferous epithelium by immunofluorescence analysis. A: Non-treated C57BL/6J mice (PND 28), B: Non-treated FasL$^{-/-}$ mice (PND 28), C: MEHP-treated C57BL/6J mice (PND 28), D: MEHP-treated FasL$^{-/-}$ mice (PND 28). Testis cross-sections showed that c-FLIP is expressed in the cytoplasm of spermatocytes and spermatids. MEHP-treated FasL mice had a higher level of c-FLIP expression in the testis than non-treated mice. The bar represents 50 μm.

3.3 Discussion

The FasL/Fas signaling pathway has been described by our laboratory [51,122,123,130] and others [43,102,131] to serve as a means to regulate germ cell apoptosis in the testis as part of a physiologic mechanism to match germ cell numbers to the Sertoli cell supportive capacity. In agreement with this concept are our previous observations that *gld* mice expressing a mutant form of the FasL protein show a decreased sensitivity to germ cell apoptosis triggered by MEHP-induced Sertoli cell injury, as compared to wild-type mice [51]. Nevertheless, despite this clear indication of the participation of the Fas-signaling system after toxicant-induced Sertoli cell injury, the *gld* mice are fertile and show normal spermatogenesis indicating that this mutant form of FasL does not drastically disrupt the physiological control of apoptosis and functional spermatogenesis [51]. It is possible that the single amino acid mutant form of FasL in *gld* mice retains a limited ability to bind to and trigger Fas-mediated apoptosis but cannot activate Fas-signaling robustly after toxicant-induced Sertoli cell injury. Therefore, the intent of this study was to evaluate if the complete loss of the FasL expression in the testis would influence the normal physiologic regulation of germ cell apoptosis as well as alter the ability of germ cells to undergo apoptosis after MEHP-induced Sertoli cell injury.

Although adult $FasL^{-/-}$ mice were fertile and displayed typical testis histology (Fig 3.2C and 3.2D), these mice surprisingly showed a significant reduction in the number of mature sperm they produced. In contrast, we discovered that peripubertal (PND 28) mice displayed many seminiferous tubules with a drastic disorganization of the seminiferous

epithelium (Fig 3.1C and 3.1D). The histological analysis of these peripubertal FasL$^{-/-}$ mouse testis revealed a dramatic loss of germ cells (Fig 3.1C and 3.1D) in some seminiferous tubules as indicated by the absence of differentiating spermatocytes with only the presence of Sertoli cells and spermatogonia in the seminiferous epithelium. However, in adult FasL$^{-/-}$ mice, after the first wave of spermatogenesis was completed, a partial repopulation of these severely affected tubules apparently occurred (Fig 3.2C and 3.2D) as indicated by near normal histology; although adult FasL$^{-/-}$ mice produced fewer mature elongated spermatids. These observations suggest a more prominent functional role of FasL in early testis development rather than in the adult testis and the maintenance of spermatogenesis.

The incidence of germ cell apoptosis in FasL$^{-/-}$ (PND 28) mice is about 4 times higher than that of wild-type mice (Fig 3.1G). In adult FasL$^{-/-}$ (PND 44) mice, the basal germ cell apoptotic index (5.26) was lower than that seen in the peripubertal FasL$^{-/-}$ mice (20.58), but higher than age-matched adult wild-type C57BL/6J (PND 44) mice (1.5). This increase in the basal incidence of germ cell apoptosis may explain the slight decrease in testis weight measured in these peribuertal mice as well as the decrease in the number of spermatid produced in the adult FasL$^{-/-}$ mice (Table 3.1). On the other hand, these findings also suggest that compensatory mechanisms, such as other death ligands/receptors may exist in FasL$^{-/-}$ mice to regulate germ cell apoptosis, since it appears that MEHP exposure does not trigger the intrinsic apoptotic signaling (Fig 3.4).

In order to understand how germ cell apoptosis is triggered in FasL$^{-/-}$ mice, we further evaluated the participation of TRAIL, another member of the TNF family.

Western blot analysis revealed that TRAIL is strongly expressed in the testis of peripubertal FasL$^{-/-}$ mice, but at relatively low levels in wild-type mice (Fig 3.5A and 3.5B). Therefore, it is plausible that the increased level of TRAIL in peripubertal FasL$^{-/-}$ mice may account for, and provide *in vivo* evidence for, the observed high basal levels of germ cell apoptosis seen in these mice.

In order to assess the sensitivity of FasL$^{-/-}$ mice to toxicant-triggered apoptosis, the MEHP-induced exposure model of prepubertal mice was used. MEHP specifically injures the Sertoli cells of the testis, inducing FasL expression, which leads to initiation of germ cell apoptosis through the extrinsic signaling pathway [103]. In wild-type mice, the basal level of germ cell apoptosis is low and is significantly induced after MEHP exposure (Fig 3.3), which is consistent with our previous studies [51,122]. Since no increase in the cleavage of caspase-9 occurred in the testis of FasL$^{-/-}$ mice after MEHP exposure (Fig 3.4), it does not appear that the intrinsic pathway participates in the initiation of germ cell apoptosis in the FasL$^{-/-}$ mice after Sertoli cell injury. We have also previously shown that peripubertal *gld* mice have a similar basal germ cell apoptotic index as the wild-type controls. However, in *gld* mice, the increase in MEHP-induced germ cell apoptosis is significantly diminished as compared to wild-type mice [51], indicating that the expression of the single amino acid mutation in FasL affords these mice only partial protection against germ cell apoptosis. However, the germ cells of FasL$^{-/-}$ mice showed a much different response to MEHP exposure than either C57BL/6J or *gld* mice. After exposure of FasL$^{-/-}$ mice to MEHP, a dramatic decrease in the high basal germ cell AI of 20.58 to an AI of 8.04 occurred within 6 hours of MEHP exposure and remained at this

level for 24 hours (Fig 3.3). Since no significant changes in the levels of TRAIL protein were observed in FasL$^{-/-}$ mice after MEHP exposure (Fig 3.5), it would appear that the negative effect of MEHP on germ cell apoptosis in FasL$^{-/-}$ mice lies downstream of TRAIL.

c-FLIP is a well-described inhibitor of caspase-8 [132], and we have previously suggested that c-FLIP is involved in regulating MEHP-triggered germ cell apoptosis [133]. The testis of the PND 28 C57BL/6J and FasL$^{-/-}$ mice were found to display low levels of c-FLIP, while large increases in the levels of c-FLIP were measured in the testis of only FasL$^{-/-}$ mice following MEHP treatment (Fig 3.5A, 3.5C and 3.6). Although increases in c-FLIP levels in FasL$^{-/-}$ mice after MEHP can provide a logical mechanism to account for the observed decreases in germ cell apoptosis, the mechanism underlying this specific increase in c-FLIP protein levels in these mice after MEHP exposure is not readily apparent.

There are several intriguing reports suggesting that the FasL protein itself has an inverse influence on c-FLIP expression. These studies indicate that FasL induces the degradation of c-FLIP via the ubiquitin-proteasomal pathway after the simulation of nitric oxide (NO) or reactive oxygen species (ROS)[134,135]. Therefore, it would be expected that in FasL$^{-/-}$ mice, the absence of FasL and its negative influence on c-FLIP expression would allow for a buildup of c-FLIP in the cell. Moreover, our group previously reported that c-FLIP is induced in p53 gene-deficient (p53$^{-/-}$) mice after MEHP exposure [136] and that c-FLIP is also induced as a result of the FasL/Fas interaction *in vitro* when p53 is not activated [133]. It appears that p53 serves as a

positive regulator to stimulate the FasL/Fas signaling pathway which facilitates the activation of caspase-8 and the degradation of c-FLIP following MEHP exposure, leading to an increase in germ cell apoptosis [136]. These data suggest that linkages may exist in the testis by which FasL/Fas signaling can influence p53-dependent processes that subsequently act to modulate the levels of c-FLIP in germ cells and their sensitivity to undergo death-receptor mediated apoptosis.

Taken together, the present study demonstrates that: 1) loss of FasL protein expression results in decreased production of mature spermatids in the adult testis, likely as a result of alterations in germ cell homeostatsis during the first wave of spermatogenesis, 2) the high baseline incidence of germ cell apoptosis in peripubertal $FasL^{-/-}$ mice is correlated with increases in the levels of TRAIL and/or the decrease in the levels of c-FLIP and, 3) a decline in germ cell apoptosis observed after MEHP treatment in $FasL^{-/-}$ mice closely corresponds to the occurrence of increased levels. These novel findings provide new insights into the functional roles of FasL in the testis at distinct developmental periods and further indicate that FasL itself is required for the regulation of c-FLIP levels in the testis.

Chapter 4: TRAIL gene-deficient mice show a disorganization of spermatogenesis during the peripubertal period of testicular development

4.1 Introductions and Rationale

We demonstrated in Chapter 3 a possible mechanism that increases the expression of FLAR in FasL gene-deficient mice to reduce the apoptotic index in the testis after MEHP treatment. In this chapter, the TRAIL gene-deficiency will be discussed to provide further information for a comparison with FasL gene-deficient mice.

Another member of the TNF family, a tumor necrosis factor related to apoptosis-inducing ligand (TRAIL/Apo2L/TNFSF10) [34], is expressed in human and rodent testis [35,36,37]. TRAIL is a Type II transmembrane protein that binds to two receptors in humans, DR4 (TRAIL-R1/TNFRSF10A) and DR5 (TRAIL-R2/ TNFRSF10B), whereas there is only one TRAIL death receptor in mice, called TRAIL-R (MK/mDR5), and it is equally homologous to both human death receptors. [38,39]. The interaction between TRAIL and DR5 triggers a signaling pathway similar to the Fas-FasL system by transmitting signals through DISC. [40]. In our lab, a previous study showed that the combined addition of recombinant TRAIL and anti-DR5 antibody (MD5) together caused significant increases in germ cell apoptosis *in vitro,* thereby implicating a role for TRAIL in testes [137]. Although recent studies have focused on the application of TRAIL in autoimmune diseases [138], anti-cancer therapy [139,140,141], and Type I diabetes

[142], the role of TRAIL in the immune system and its functional mechanisms are controversial [99]. TRAIL gene-deficient mice contain a partial deletion of exon 2 and a complete deletion in exon 3 in the TRAIL gene, resulting in spontaneous tumor formation [99,142,143,144].

In order to more rigorously define the role of the DR5/TRAIL signaling system in the physiological regulation of germ cells in the testis, we describe here the testicular phenotype of TRAIL gene-deficient mice. Since the highest level of "physiological" germ cell apoptosis in mice occurs during the peri-pubertal period, we include here a detailed evaluation of the testis of these gene-deficient mice both during the peri-pubertal period (28 days of age) as well as in adult mice (44 days of age). We also show in this chapter for the first time, evidence for the requirement of TRAIL for functional spermatogenesis.

4.2. Results

4.2.1 *Physiological characterization of the testis of TRAIL$^{-/-}$ mice*

In order to understand the physiological differences between the wild type C57Bl/6J and TRAIL gene-deficient mice, the testis weight and body weight were recorded. At 28 days of age, C57BL/6J mice had a statistically higher testis/body weight ratio (g/kg) as compared with the TRAIL$^{-/-}$ mice (3.6±0.4, 3.3±0.2, and 3.5±0.1; respectively) (Figure 4.1A, left group), while there were no differences in the body weight of the mice examined (Figure 4.1B, left group). In adults (44 days of age), no differences, however, were observed in the testis/body weight ratio in any of the mice examined (Figure 4.1A, right group).

4.2.2 *TRAIL$^{-/-}$ mice showed an increase in germ cell apoptosis*

Contrary to our expectations, TRAIL$^{-/-}$ mice were found to have a drastically greater increase in basal incidence in TUNEL-positive germ cells compared to wild-type C57BL/6J mice at both 28 days and 44 days of age (Figure 4.2). TRAIL$^{-/-}$ mice had a high germ cell apoptotic index at 28 days (21.54%) and continued to maintain a high incidence of germ cell apoptosis at 44 days of age (20.2%).

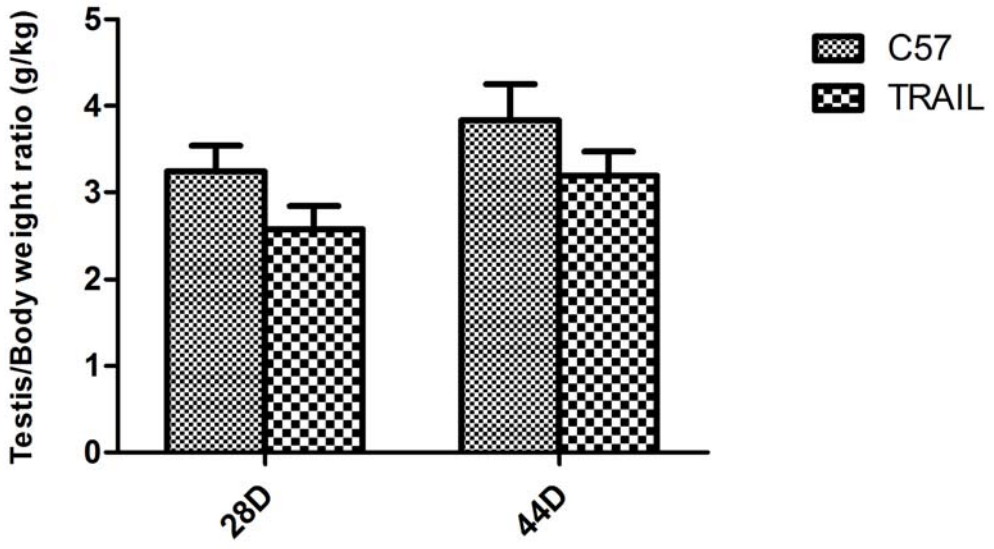

Figure 4.1 Physiological parameters of the testis in wild-type C57BL/6J mice and TRAIL gene-deficient mice. The testis weight and body weight of various strains of mice at 28 and 44 days were measured. A: The testis/body weight ratio. B: The body weight. Left group represents 28-day-old mice and the right group represents 44-day-old mice.

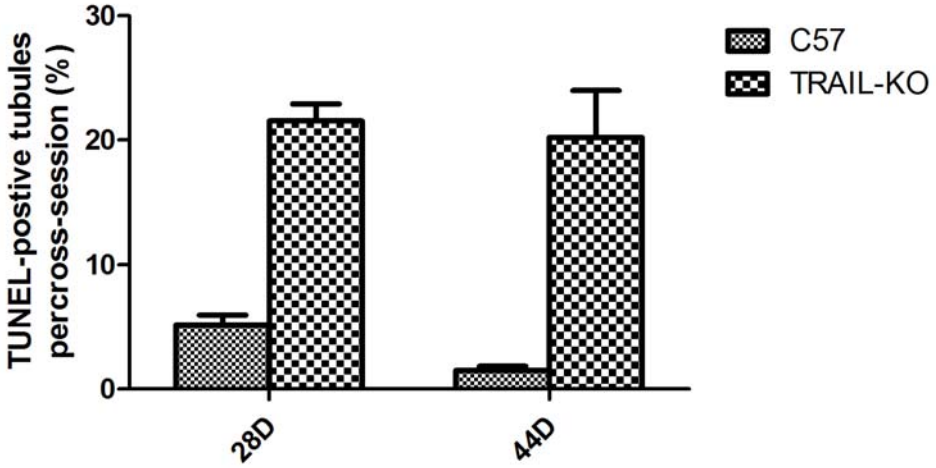

Figure 4.2 Apoptotic rate in germ cells of 28- and 44-day-old gene-deficient mice. The apoptotic rate in cross-sections from paraffin-embedded mouse testes was determined by TUNEL assay. At least two testicular cross-sections per mouse were analyzed. Left group represents 28-day-old mice and right group represents 44-day-old mice.

4.2.3 *Differences in FasL protein expression in wild-type and gene deficient mice*

A comparison between C57BL/6J and TRAIL gene-deficient mice revealed differences in the expression pattern of TRAIL mice at 28 days and 44 days of age. In 28-day-old mice, FasL expression was significantly increased in TRAIL$^{-/-}$ mice (1.56-fold) (Figure 4.3, left group). At 44 days of age, no significant differences in FasL expression were observed (Figure 4.3, right group).

4.2.4 *Testicular histology revealed a spermatogenic delay, cell cycle arrest, and high germ cell apoptotic index in the testis of TRAIL$^{-/-}$ mice*

Evaluation of the testicular histology in peri-pubertal mice with an increased incidence of spermatocytes showed an arrest during the meiotic phase and spermatogenic disorganization was observed in 28-day-old TRAIL$^{-/-}$ mice (Figure 4.4C and 4.4D) as compared with the wild-type C57BL/6J mice (Figure 4.4A and 4.4B). The testis of adult 44 day-old TRAIL$^{-/-}$ mice showed cell cycle arrests and disorganization of germ cells was observed (Figure 4.4G and 4.4H).

4.2.5 *Decreased spermatid head formation in gene deficient mice*

Measurements of spermatid head counts revealed that adult (44 day-old) FasL- and TRAIL-gene deficient mice had a dramatic decrease in the production of mature

spermatids compared with C57BL/6J mice (reduced to 51% and 39% of production in FasL$^{-/-}$ and TRAIL$^{-/-}$ mice, respectively) (Figure 4.5).

4.2.6 *TRAIL$^{-/-}$ mice had a prolonged pregnancy interval between litters*

In order to examine breeding success, the period of time between the day the mating cage was set up to the day of confirmed birth was recorded. The box-plot shows different pregnancy intervals among the gene-deficient mice. Wild-type C57BL/6J and FasL$^{-/-}$ mice showed similar pregnancy intervals (23 days and 21 days, respectively), while TRAIL$^{-/-}$ mice displayed the longest pregnancy interval (~29 days) (Figure 4.6).

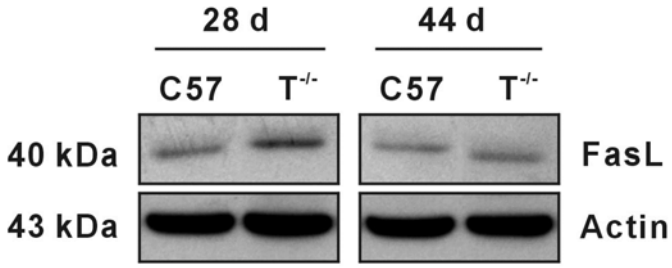

Figure 4.3 Differences in FasL expression in TRAIL$^{-/-}$ mice at PND28. FasL expression in total cellular proteins from whole testis homogenates at 28 and 44 days were detected using primary antibodies against FasL (1:500). β-actin was the loading control.

C: C57BL/6J mice; T$^{-/-}$: TRAIL$^{-/-}$ mice.

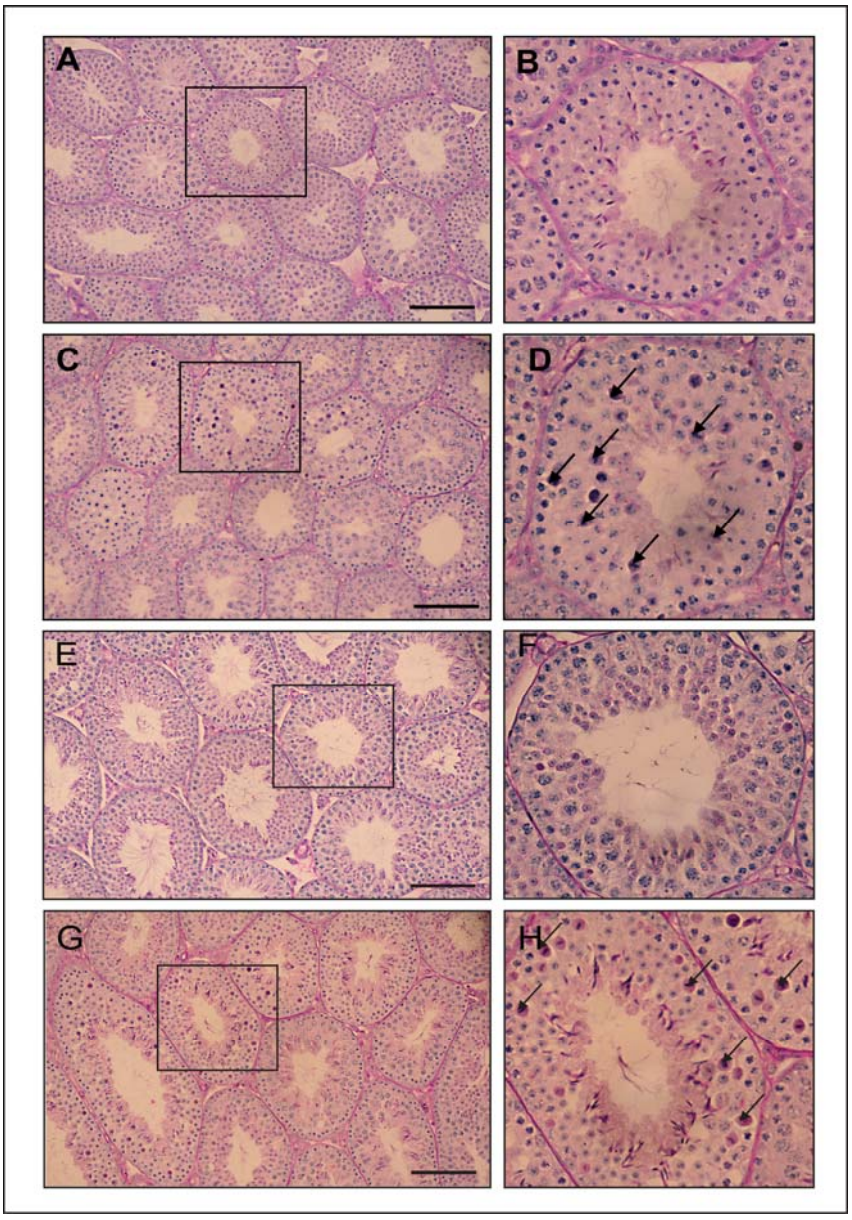

Figure 4.4 Testicular histopathology. Cross-sections (5 μm) of paraffin-embedded testis tissues were evaluated for morphological changes by using periodic acid-Schiffs-Hematoxylin (PAS-H) staining. A, B, E, F: wild-type C57BL/6J mice; C D, G, H: TRAIL$^{-/-}$ mice. A-D: 28-day-old mice; and E-H: 44-day-old mice. Arrows indicate cell cycle arrest in spermatocytes in TRAIL$^{-/-}$ mice. The bar represents 100 μm.

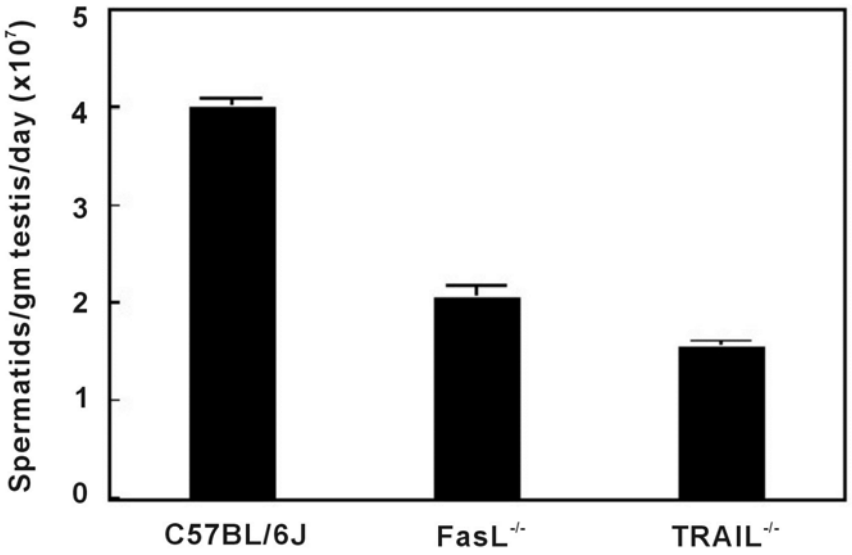

Figure 4.5 The number of mature spermatid heads at 44 days. Testes from 44-day-old mice were homogenized in DMSO/saline solution, and spermatid heads were counted using a hemocytometer. Each testis sample was counted three times.

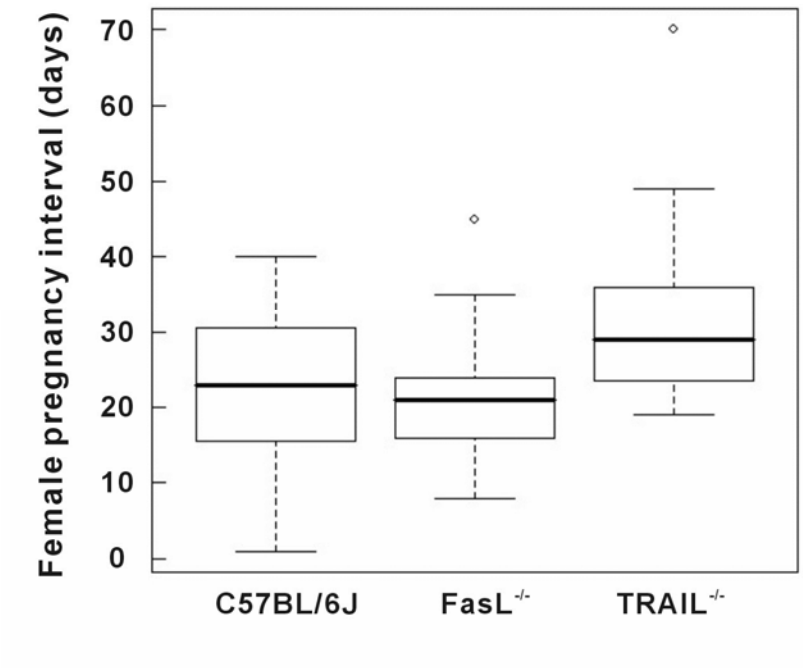

Figure 4.6 The pregnancy interval of gene deficient mice. The interval between two litters was evaluated by maintaining the breeding pairs of various gene deficient mice strains. Each breeding pair was established as mating 6-week-old mice, and continued breeding for at least 4 litters. The hollow circle spot indicates the out-of-range results that were excluded from calculation in $FasL^{-/-}$ and $TRAIL^{-/-}$ mice.

4.3 Discussion

In Chapter 3, we discussed how the extrinsic pathway plays an important role during normal testis development and requires FasL-Fas stimulated signaling to initiate germ cell apoptosis [50,144,145]. In Chapter 4, in order to define the functional contribution of TRAIL/DR5 on normal testis development, as well as in controlling apoptosis of germ cells in the testis during spermatogenesis, we evaluated the testis of TRAIL-gene deficient mice during the peri-pubertal period (28 days of age) and during adulthood (44 days of age).

The testes and body weights of wild-type C57BL/6J and $TRAIL^{-/-}$ mice were examined (Figure 4.1). C57BL/6J mice had a higher testis/body weight ratio at 28 days. No significant differences were observed in the body weight of the various 28-day-old mice, but $FasL^{-/-}$ mice showed a slight increase in body weight at 44 days (Table 3.1). Similarly, it was shown that the loss of Bax, another proapoptotic protein, caused no significant changes in the testis weight of young mice [146]. However, the loss of Bcl-2 resulted in a dramatic decrease in testis weight [147]. These findings suggest that the loss of anti-apoptotic proteins may be more detrimental than the loss of pro-apoptotic proteins for developmental functions in the testis.

$TRAIL^{-/-}$ mice carry a partial deletion of exon 2 and a complete deletion of exon 3 in the TRAIL gene [142]. Interestingly, others have reported that HeLa cell line transfected with two alternative splicing transcripts of TRAIL (TRAIL-β and TRAIL-γ) that revealed a decrease in DNA fragmentation and cell death due to the loss of exon 3, thereby

resulting in a truncated TRAIL protein lacking the extracellular domain in both splicing variants [148]. Our results show a different observation in that the mutation in the TRAIL gene was caused by an increase in germ cell apoptosis. It is possible that this increase in germ cell apoptosis may result from another death receptor signaling family member or may point to the participation of the intrinsic apoptotic signaling pathway in order to compensate for the loss of TRAIL and to maintain homeostasis during testis development. On the other hand, there are differences in the basal apoptotic rates between the young and adult mice. The 44-day-old TRAIL$^{-/-}$ mice continued to maintain a high apoptotic index, while the adult FasL$^{-/-}$ mice showed a significant decrease in germ cell apoptosis compared with levels observed at 28 days. These observations suggest that TRAIL may play a more dominant role than FasL in controlling the population of germ cells after the first wave of spermatogenesis, while FasL may be more critical during the peri-pubertal period than during adulthood.

Recent studies have indicated that Fas is an important regulator of spermatocyte apoptosis in rats during the first wave of spermatogenesis as a mechanism to maintain appropriate populations of spermatocytes [50]. Interestingly, FasL-deficient mice (*gld* mice), carrying a single mutation in the c-terminus of the FasL protein, show an increase in germ cell apoptosis in 8 weeks old adult mice [51], suggesting that Fas system is not required for spermatogenesis in adult mice.

Our results here indicate that those gene-deficient mice that lack one death ligand display no obvious morphological changes and no protection from apoptosis of testicular germ cells. In order to explain this, the protein levels of FasL and TRAIL were

determined by western blot analysis in the various deficient mice. Interestingly, at 28 days, FasL$^{-/-}$ mice showed a higher level of TRAIL protein (Figure 3.5), while TRAIL$^{-/-}$ mice showed only a small increase in the FasL protein, a finding that is in agreement with the hypothesis that FasL and TRAIL can functionally compensate for the loss of the other in the testis during peri-pubertal age *in vivo* (Figure 4.3). Although these two death ligands appear to compensate for each other, we predicted that complete compensation would result in a wild type phenotype. However, the sperm counts were still lower compared to C57 (Figure 4.5).

The histological analysis of testicular cross sections suggested that FasL and TRAIL expression may be critical for the development of germ cells during the peri-pubertal age. In 28-day-old FasL$^{-/-}$ mice, some seminiferous tubules showed a dramatic loss of germ cells (Figure 3.1, 4.4) that may have led to a delay in germ cell development. The abnormal spermatogenesis was caused by an absence of differential spermatocytes and only with Sertoli cells and spermatogonia in the seminiferous epithelium. However, at 44 days old, after the first wave spermatogenesis, those immature tubules may have automatically repopulated in FasL$^{-/-}$ mice (Figure 3.2 and 4.4). An increase in cell cycle arrest was detected in spermatocytes in 28-day-old TRAIL$^{-/-}$ mice (Figure 4.4), but not in FasL$^{-/-}$ and wild-type mice (Figure 3.1 and 3.2). At 44 days, TRAIL$^{-/-}$ mice still showed cell cycle arrest and apoptosis (Figure 4.2 and 4.4) that were higher than C57BL/6J wild-type or FasL$^{-/-}$ mice. These observations further suggest that TRAIL may be more important than FasL for long term maintenance of spermatogenesis by controlling germ cell apoptosis, as mentioned above.

Finally, in order to determine whether the loss of either FasL or TRAIL can alter the ability of reproduction, the numbers of mature spermatid heads were counted in the different gene-deficient mice. Adult (44-day-old) $FasL^{-/-}$ mice displayed a decrease in mature spermatid formation (Figure 4.5), which could be due to the increase in apoptosis seen at 28 days (Figure 4.2). Adult $TRAIL^{-/-}$ mice produced the lowest number of mature spermatid heads, possibly due to the continued high germ cell apoptotic rate as well as cell cycle arrest. The decreased number of spermatid heads did not dramatically influence the productivity of these death-ligands deficient mice. However, recent reports suggest a lower reproductive efficiency in humans with decreased sperm counts because humans require a minimum number of sperm in order to maintain a normal reproductive function [149,150]. Even though all of the gene-deficient mice were fertile, the female mice showed different intervals between pregnancies. $TRAIL^{-/-}$ female mice had the longest delay between pregnancies (~29 days) compared to C57BL/6J wild-type mice (~23 days) (Figure 4.6). These observations suggest that the loss of TRAIL causes difficulty in reproduction, possibly resulting from lower levels of mature spermatids, but how this processes influences of intervals between pregnancies in the female remains unknown.

Taken together, the findings presented in this study provide evidence for the first time that FasL and TRAIL may partly compensate for each other to regulate germ cell apoptosis during the first wave of spermatogenesis. These findings also point to a more predominant role of FasL than TRAIL in controlling the proper number of germ cells during the first wave of spermatogenesis that occurs in peri-pubertal mice. TRAIL is

more critical for maintaining long-term homeostasis of the germ cell population in the adult testis as well as in the reproductive function.

Chapter 5: A comparison of FasL and TRAIL gene deficient mice during development and following MEHP treatment

5.1 Introduction and Rationale

In Chapter 3, we identified c-FLIP as a potential mechanism responsible for the decrease in apoptosis in FasL gene deficient mice after MEHP exposure. We continued to examine the normal physiological function of another death ligand, TRAIL, using TRAIL gene deficient mice. To test whether TRAIL is also involved the regulation of c-FLIP after MEHP exposure, the germ cell apoptosis were measured in TRAIL$^{-/-}$ mice with/without MEHP exposure.

From previous results, both FasL and TRAIL gene deficient mice had decreased testis/body weight ratios and spermatid head counts, but showed an increase in germ cell apoptosis during the first wave of spermatogenesis. To further understand the delay in spermatogenesis in both FasL and TRAIL gene deficient mice, we performed a microarray analysis to compare the gene profiles of death ligand gene deficient and wild-type mice.

5.2. Results

5.2.1 *Germ cell apoptosis not significnat increased in TRAIL$^{-/-}$ mice after MEHP exposure*

To evaluate the effect of MEHP on germ cell apoptosis, PND 28 TRAIL$^{-/-}$, FasL$^{-/-}$, and C57BL/6J mice were treated with 1 g/kg of MEHP for various time periods. In TRAIL$^{-/-}$ mice, increases in the number of apoptotic germ cells were apparent in a time-dependent manner starting from the high basal apoptotic index (AI) after MEHP exposure (Fig 5.1). Findings consistent with the previous study, an increased expression of FasL can increase germ cell apoptosis after MEHP exposure. [51,122]. As described in previous chapters (Chapters 3 and 4), the basal AI in the testis of FasL$^{-/-}$ and TRAIL$^{-/-}$ mice were significantly higher compared with C57BL/6J mice (20.58%, 21.54%, and 5.16%, respectively). In response to MEHP exposure, the high basal AI in TRAIL$^{-/-}$ mice was found to increase significantly at 6 hours after exposure and remained at that high level at both the 12 and 24-hour time points (Fig 5.1). The maximal difference in the AI between the two types of gene deficient mice was observed at 12-hour time points with +/- ~50% difference (FasL$^{-/-}$ mice decreased from 20.58% to 10.09%; TRAIL$^{-/-}$ mice increased from 21.54% to 31.96%). The maximal difference in the AI between the FasL$^{-/-}$ and C57BL/6J mice was observed at the 12-hour time point with ~50% difference (10.09 and 23.86, respectively).

5.2.2 *No obvious increase in c-FLIP expression in TRAIL$^{-/-}$ mice compared to FasL$^{-/-}$ mice following MEHP exposure*

Western blot analysis of testis samples from 28-day-old C57BL/6J, TRAIL$^{-/-}$ and FasL$^{-/-}$ mice indicated that the basal levels of c-FLIP were very low (Fig 5.2). As discussed in Chapter 3, FasL$^{-/-}$ mice responded to MEHP exposure with increased the levels of c-FLIP, while TRAIL$^{-/-}$ mice were found to have only slightly increased levels at each of the measured time points.

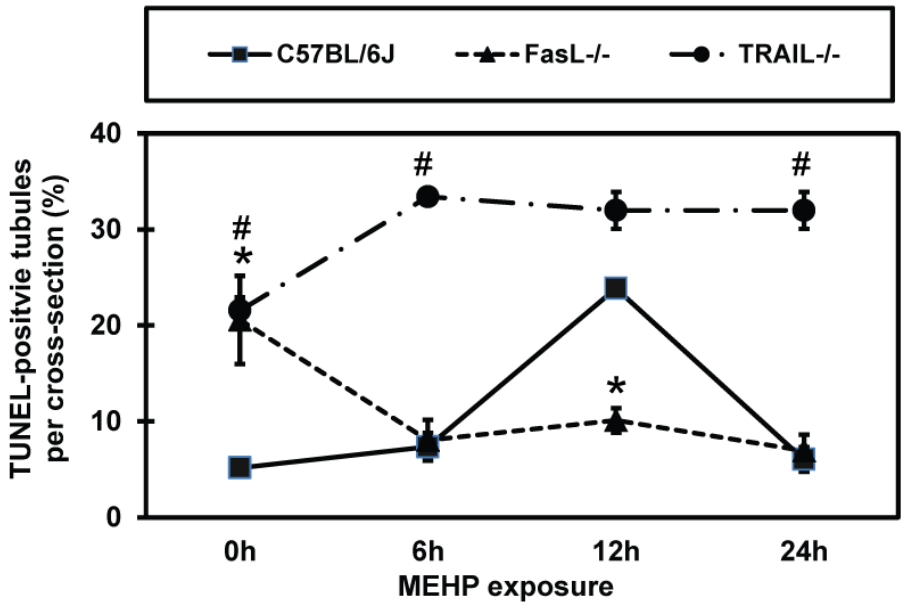

Figure 5.1 Germ cell apoptotic index (AI) in peri-pubertal TRAIL and FasL gene-deficient mice after MEHP exposure. The AI in mouse paraffin-embedded testis cross sections were determined by TUNEL assay. PND 28 mice were treated with MEHP for various periods of time. C57BL/6J wild-type mice and TRAIL$^{-/-}$ mice displayed an increase in germ cell apoptosis at 12 hours of MEHP exposure. The apoptotic rate of germ cell in FasL$^{-/-}$ mice was significantly lower after MEHP exposure compared with C57BL/6J mice (* and # <0.05, Student *t*-test; * indicate FasL$^{-/-}$ vs C57; # indicate TRAIL$^{-/-}$ vs C57).

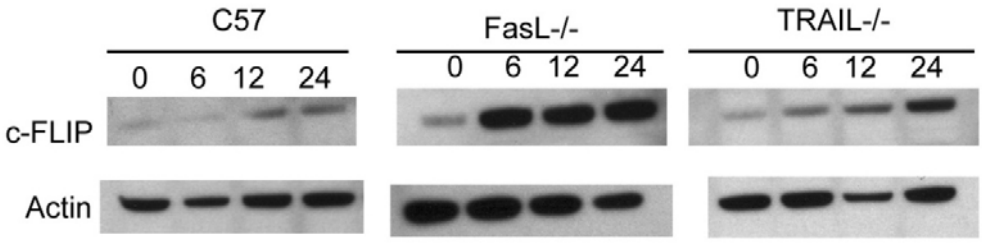

Figure 5.2 Western blot analyses of c-FLIP protein expression in PND 28 C57BL/6J, FasL gene-deficient, and TRAIL gene-deficient mice. Total cellular proteins from whole testis tissues were detected using primary antibodies against c-FLIP (1:1000). C57BL/6J mice had a very low expression level of c-FLIP. $FasL^{-/-}$ mice showed a higher level of c-FLIP protein after MEHP treatment, which $TRAIL^{-/-}$ mice demonstrated only a gradual increase following MEHP treatment.

5.2.3 *Microarray analysis of FasL and TRAIL gene deficient mice*

Out of nearly 28,000 putative probes, there were 281 genes, with 99 genes unknown, in the $FasL^{-/-}$ mice that had a 4-fold difference as compared to C57BL/6J mice (Table 5.1). There were 200 genes, with 70 unknown, in $TRAIL^{-/-}$ mice that showed 4-fold changes as compared with C57BL/6J mice (Table 5.2). $FasL^{-/-}$ and $TRAIL^{-/-}$ mice shared in common 169 genes with 4-fold changes, including 65 unknown genes, compared with C57BL/6J mice (Table 5.3). There were 104 genes grouped in 7 categories by their functions in the testis, including biosynthesis, cytoskeletal, immune, metabolism, signal transduction, spermatogenesis/development, and unknown (Table 5.4 and Fig 5.3). The delayed of spermatogenesis was observed in FasL and TRAIL gene deficient mice, as described in previous chapters. These results led us to check those genes that showed a difference with C57BL/6J and that may be involved in the spermatogenesis/development categories (Fig 5.4).

Among the 7 categories, spermatogenesis/development appears to be the major group to show strongly altered gene expression in death ligand gene deficient mice (Fig 5.3). The genes include a disintergrin and metallopeptidase domain 7 (Adam7), arginine decarboxylase (Adc), complement component 4 binding protein (C4bp), CUB and zona pellucida-like domain 1 (Cuzd1), cyclin-dependent kinase 5, regulatory subunit 1 (p35) (cdk5r1), cyclin, basic protein of sperm head cytoskeleton 2 (cylc2), cysteine-rich secretory protein 1 (Crisp1), fascin homolog 3, actin-bundling protein, testicular (Fscn3), germ cell-specific gene 1 (Gsg1), neuropeptide Y (Npy) outer dense fiber of sperm tails

3B (Odf3b), REX1, RNA exonulcease 1 homolog (Rexo1), serine peptidase inhibitor, Kazal type 8 (Spink8), serine peptidase inhibitor, Kunitz type 3(Spint3), sperm maturation 1 (Spem1), spermatogenesis and centriole associated 1 (Spatc1), spermatogenesis associated 18 (Spata 18), spermatogenesis associated 3 (Spata3), tctex1 domain containing 1 (Tcte1d1), testicular haploid expressed gene (Theg), testis-specific serine kinase 3 (Tssk3), testis-specific serine kinase 6 (Tssk6), ubiquitin-like (Ubqlnl), ubiquitin-like 4B (Ubl4b).

Table 5.1

Genes significantly different between C57BL/6J and FasL gene deficient mice

Array ID	Gene	Entrez_gene	Fold change (Log2 scale)	P-value	RefSeq
PH_mM_0008100	Agpat2	67512	-3.11	0.00	NM_026212.1
PH_mM_0013901	Oxct2a	64059	-3.35	0.00	NM_022033.3
PH_mM_0014490	Adam4	11498	-2.00	0.00	NM_009620.1
mMC019261	Adam7	11500	5.23	0.00	NM_007402.2
PH_mM_0007832	Abhd16b	241850	-2.61	0.00	NM_183181.2
mMC018239	Acta1	11459	2.39	0.00	NM_009606.2
PH_mM_0007685	Acbd7	78245	3.31	0.00	NM_030063.2
PH_mM_0012448	Arl2bp	107566	-2.24	0.00	NM_024269.3
mMR026559	Arl9	384185	-2.85	0.00	NM_206935.1
mMC010060	Akr1b7	11997	2.70	0.00	NM_009731.2
PH_mM_0004216	Ahsg	11625	2.36	0.00	NM_013465.1
PH_mM_0001251	Agt	11606	-2.33	0.00	NM_007428.3
mMC005531	Adc	242669	-3.40	0.00	NM_172875.2
mMR026859	Atg4a	666468	2.11	0.00	NM_174875.3
PH_mM_0014216	Bcmo1	63857	-2.66	0.00	NM_001163028.1
mMC013786	Calml4	75600	-2.54	0.00	NM_138304.2
mMC010796	Cad	69719	2.11	0.00	NM_023525.1
PH_mM_0014563	Ces5a	67935	6.64	0.00	NM_001003951.1
mMC013527	Ceacam10	26366	3.80	0.00	NM_007675.4
mMC003243	Casp7	12369	-3.39	0.00	NM_007611.2
mMC024713	Ctnna3	216033	-2.14	0.00	NM_001164376.1
PH_mM_0003640	Cd164l2	69655	-2.02	0.00	NM_027152.1
mMC026451	Cd52	23833	6.64	0.00	NM_013706.2
mMC000821	Cd96	84544	-2.09	0.00	NM_032465.2
PH_mM_0004772	Cwh43	231293	3.60	0.00	NM_181323.2
PH_mM_0011226	Cby3	76653	-3.97	0.00	XM_484016.4
PH_mM_0009165	Ch25h	12642	3.38	0.00	NM_009890.1
PH_mM_0012528	Cpsf4l	52670	-2.38	0.00	NM_029794.2
PH_mM_0009005	Cdrt4	66338	-2.61	0.00	NM_025496.1
PH_mM_0003221	Ccdc159	67119	-2.14	0.00	NM_025977.3
PH_mM_0008848	Ccdc57	71276	-2.59	0.00	NM_027745.1
PH_mM_0009593	Col1a2	12843	3.10	0.00	NM_007743.2
PH_mM_0004326	C4bp	12269	3.43	0.00	NM_007576.3
mMC009101	Cuzd1	16433	4.96	0.00	NM_008411.3
mMR031232	Cux2	13048	-2.28	0.00	NM_007804.2
PH_mM_0001409	Cdk5r1	12569	3.25	0.00	NM_009871.2

Table 5.1-continued

Array ID	Gene	Entrez_gene	Fold change (Log2 scale)	P-value	RefSeq
PH_mM_0000031	Cylc2	74914	-2.03	0.00	NM_001162865.1
mMC018400	Cstl1	228756	-3.19	0.00	NM_177655.3
PH_mM_0003392	Crisp1	11571	6.64	0.00	NM_009638.3
PH_mM_0013099	Cyp2a12	13085	-3.06	0.00	NM_133657.1
PH_mM_0005867	Defb2	13215	5.38	0.00	NM_010030.1
PH_mM_0008623	Defb21	403172	-2.86	0.00	NM_207276.2
mMC007896	Defb37	353320	5.64	0.00	NM_181683.2
PH_mM_0009190	Defb38	360212	5.51	0.00	NM_183036.1
mMC002785	Defb40	360217	6.56	0.00	NM_183039.3
PH_mM_0005654	Defb42	619548	4.20	0.00	NM_001034910.3
PH_mM_0008476	Dnajb8	56691	-2.52	0.00	NM_019964.1
PH_mM_0009718	Dnajc5b	66326	-2.28	0.00	NM_001163537.1
PH_mM_0007033	Dydc2	71200	-3.38	0.00	NM_027717.1
mMC023498	Elf3	13710	2.01	0.00	NM_001163131.1
PH_mM_0005876	Efcab1	66793	-2.28	0.00	NM_025769.3
PH_mM_0009631	Eddm3b	219026	2.07	0.00	NM_203508.1
mMC006344	Esrp1	207920	2.00	0.00	NM_194055.2
mMC013655	Fasl	14103	-2.34	0.00	NM_010177.3
PH_mM_0003129	Fez1	235180	-2.24	0.00	NM_183171.4
PH_mM_0007905	Fscn3	56223	-3.33	0.00	NM_019569.2
PH_mM_0016216	Fbxo39	628100	-2.41	0.00	NM_001099688.2
PH_mM_0008011	Fcrla	98752	2.10	0.00	NM_145141.2
PH_mM_0008087	Fxyd3	17178	2.24	0.00	NM_008557.2
PH_mM_0017479	Gprc5c	70355	2.47	0.00	NM_001110337.1
PH_mM_0006150	Gsdmd	69146	-2.47	0.00	NM_026960.4
PH_mM_0016293	Gsg1	14840	-2.76	0.00	NM_010352.2
PH_mM_0001002	Gpx3	14778	4.32	0.00	NM_001083929.1
PH_mM_0016195	Gpx4	625249	-2.23	0.00	NM_001037741.2
PH_mM_0006314	Gstcd	67553	-2.40	0.00	NM_026231.2
PH_mM_0006326	Gapdhs	14447	-2.07	0.00	NM_008085.1
mMC017921	1700022A21Rik	72252	-2.02	0.00	NR_003953.1
PH_mM_0003574	Gp1bb	14724	-2.12	0.00	NM_010327.2
PH_mM_0006445	Glt6d1	71103	-2.86	0.00	NM_001039095.1
PH_mM_0005506	Gramd2	546134	-2.58	0.00	NM_001033498.1
PH_mM_0001530	Gmps	229363	3.91	0.00	NM_001033300.2
PH_mM_0000197	Gucy2d	14918	-2.13	0.00	NM_001130693.1
mMC001823	Hspa1l	15482	-2.20	0.00	NM_013558.2
PH_mM_0014524	Hbb-b1	15129	2.48	0.00	NM_008220.4
mMR001167	Hk1	15275	-2.10	0.00	NM_010438.3

Table 5.1-continued

Array ID	Gene	Entrez_gene	Fold change (Log2 scale)	P-value	RefSeq
PH_mM_0015866	LOC100047146	100047146	-2.90	0.00	XM_001473694.2
PH_mM_0003363	Irgc1	210145	-2.00	0.00	NM_199013.2
mMC025253	Ido1	15930	2.62	0.00	NM_008324.1
PH_mM_0006924	Iqcf6	100041096	-2.10	0.00	NM_001101628.1
PH_mM_0003498	Ica1	15893	-2.13	0.00	NM_010492.3
PH_mM_0008043	Klhl24	75785	-2.06	0.00	NM_029436.3
mMC020164	Krt15	16665	2.45	0.00	NM_008469.2
PH_mM_0000659	Klc3	232943	-2.22	0.00	NM_146182.3
PH_mM_0006784	Kcnip2	80906	-3.12	0.00	NM_030716.2
PH_mM_0007225	Lelp1	69332	-3.08	0.00	NM_027042.1
mMC021607	Lemd1	213409	-2.05	0.00	NM_001033250.4
PH_mM_0009010	Lrrc69	73314	-2.28	0.00	NM_028499.2
PH_mM_0005345	Lrrc8b	433926	-2.92	0.00	NM_001033550.2
mMR026555	Lhx1	16869	-2.23	0.00	NM_008498.2
mMC014819	Lcn2	16819	-2.34	0.00	NM_008491.1
PH_mM_0003059	Lum	17022	2.16	0.00	NM_008524.2
mMC011770	Ly6g6c	68468	-2.27	0.00	NM_023463.3
mMC022185	Mboat1	218121	2.54	0.00	NM_153546.4
mMC006485	Mgst2	211666	-2.04	0.00	NM_174995.2
mMC011249	Mical3	194401	-2.64	0.00	NM_153396.2
PH_mM_0016111	Map2k7	26400	-2.26	0.00	NM_001042557.2
PH_mM_0010566	LOC100047953	100047953	-2.27	0.00	XM_001479514.2
PH_mM_0012595	Mlf1	17349	-3.28	0.00	NM_001039543.2
PH_mM_0015068	Nqo2	18105	-3.09	0.00	NM_001163241.1
PH_mM_0016090	Naca	17938	-2.21	0.00	NM_013608.3
PH_mM_0015482	Neurl1b	240055	2.08	0.06	NM_001081656.2
mMC013235	Npy	109648	6.12	0.00	NM_023456.2
PH_mM_0009408	Nos2	18126	-2.40	0.00	NM_010927.3
mMC025836	Nfe2	18022	-2.45	0.00	NM_008685.2
PH_mM_0007159	Odam	69592	3.79	0.00	NM_027128.2
mMC005441	Odf3b	70113	-3.14	0.00	NM_001013022.1
mMR026715	Osgin1	71839	-2.70	0.00	NM_027950.1
PH_mM_0001494	Ptx4	68509	-2.67	0.00	NM_026747.1
mMC007063	Padi6	242726	-2.29	0.00	NM_153106.2
mMC008262	Ptrh1	329384	-2.13	0.00	NM_178595.3
PH_mM_0008786	Perp	64058	2.56	0.00	NM_022032.4
PH_mM_0004075	Phospho1	237928	-2.59	0.00	NM_153104.3
PH_mM_0014989	Pldi	73616	-2.04	0.00	NR_033616.1
mMC020960	Kctd16	383348	-2.07	0.00	NM_026135.1
PH_mM_0005312	Kcnk7	16530	-2.50	0.00	NM_010609.2

Table 5.1-continued

Array ID	Gene	Entrez_gene	Fold change (Log2 scale)	P-value	RefSeq
PH_mM_0015888	Paqr9	75552	-2.14	0.00	NM_198414.2
PH_mM_0009053	Ptgs1	19224	2.80	0.00	NM_008969.3
PH_mM_0003579	Pate2	330921	2.04	0.00	NM_001033421.3
mMC015224	Prss37	67690	-2.11	0.00	NM_026317.2
PH_mM_0009328	Prss52	73382	-2.27	0.00	NM_028525.2
mMC022760	Prss55	71037	-2.11	0.00	NM_001081063.1
mMC016079	Proc	19123	-2.40	0.00	NM_008934.2
PH_mM_0016190	Pwwp2b	101631	-2.16	0.00	NM_001033206.2
mMR029146	Pdpr	319518	-2.04	0.00	NM_198308.1
mMC011943	Rabgef1	56715	-2.96	0.00	NM_019983.2
mMC008409	Reep6	70335	-2.45	0.00	NM_139292.1
PH_mM_0010144	Rgsl1	240816	-2.19	0.00	XM_994482.3
PH_mM_0012710	Rexo1	66932	-2.68	0.00	NM_025852.3
PH_mM_0002842	Rnase12	497106	5.97	0.00	NM_001011875.1
PH_mM_0008304	Rnase9	328401	2.64	0.00	NM_183032.2
PH_mM_0007365	Rnf148	71300	-2.02	0.00	NM_027754.1
PH_mM_0006463	Rundc3a	51799	-3.06	0.00	NM_016759.3
mMC006813	S100a14	66166	2.39	0.00	NM_001163525.2
mMC016579	Slfnl1	194219	-2.45	0.00	NM_177570.3
PH_mM_0006920	Scpppq1	100271704	-2.84	0.00	NM_001163772.1
PH_mM_0004314	Serpina3a	74069	-2.12	0.00	NM_001167705.1
PH_mM_0001660	Spink13	100038417	2.36	0.00	NM_001168423.2
PH_mM_0007762	Spink8	78709	6.49	0.00	NM_183136.2
PH_mM_0005443	Spint3	629747	4.11	0.00	NM_001177401.1
mMC021428	LOC100504162	100504162	-3.04	0.00	XM_003085010.1
mMR031068	Sh3d20	70559	-2.06	0.00	NM_183288.2
PH_mM_0007777	Slamf9	98365	-2.00	0.00	NM_029612.4
PH_mM_0005970	Srgap1	117600	-2.59	0.00	NM_001081037.1
mMC002188	Spem1	74288	-3.28	0.00	NM_028855.1
PH_mM_0003210	Spert	67926	-2.09	0.00	NM_001164140.1
PH_mM_0004196	Spatc1	74281	-3.22	0.00	NM_028852.1
mMC004094	Spata18	73472	-2.53	0.00	NM_178387.3
PH_mM_0012342	Spata3	70060	-3.00	0.00	NM_027029.2
PH_mM_0014840	Sat1	20229	2.06	0.00	NM_009121.3
PH_mM_0004702	St6galnac2	20446	-2.14	0.00	NM_009180.3
mMC012015	St8sia5	225742	-2.34	0.00	NM_013666.2
mMC018552	Soat1	20652	3.13	0.00	NM_009230.3
PH_mM_0016223	Synj2	20975	-2.08	0.00	NM_001113351.1
PH_mM_0014001	Tctex1d1	67344	-2.85	0.00	NM_001163767.1
PH_mM_0012549	Theg	21830	-2.46	0.00	NM_011583.3

Table 5.1-continued

Array ID	Gene	Entrez_gene	Fold change (Log2 scale)	P-value	RefSeq
mMC023686	Tspy-ps	22109	-2.01	0.00	NR_027507.1
mMR027860	Tssk3	58864	-2.20	0.00	NM_080442.2
mMC014962	Tssk6	83984	-3.00	0.00	NM_032004.1
PH_mM_0013088	Gm5334	384639	-2.79	0.00	NR_003648.2
mMC015309	Ttc24	214191	-3.43	0.00	NM_172526.3
PH_mM_0007513	Tmsb15a	78478	-2.29	0.00	NM_030106.2
mMC015474	Trp53tg5	73603	-2.18	0.00	XR_035042.2
mMC020942	Trpm5	56843	-2.03	0.00	NM_020277.2
mMC006780	Tm4sf4	229302	-2.17	0.00	NM_145539.2
PH_mM_0015434	Tmem156	243025	-2.08	0.00	XM_144292.8
mMC003564	Trim42	78911	-2.39	0.00	NM_030219.2
mMC016927	Tmod4	50874	-3.17	0.00	NM_016712.3
PH_mM_0002232	Tppp2	219038	-3.17	0.00	NM_001128634.1
PH_mM_0013731	Tuba4a	22145	-2.70	0.00	NM_009447.3
PH_mM_0000965	Tuba8	53857	-2.18	0.00	NM_017379.1
mMC024820	Ubqlnl	244179	-3.11	0.00	NM_198624.3
PH_mM_0013440	Ubl4b	67591	-3.20	0.00	NM_026261.2
PH_mM_0008023	B3gnt3	72297	-2.36	0.00	NM_028189.3
PH_mM_0010872	LOC100503879	100503879	-2.22	0.00	XM_003084721.1
mMC011659	Vasp	22323	-2.49	0.00	NM_009499.2
PH_mM_0000489	Wfdc13	408190	3.92	0.00	NM_001012704.1
PH_mM_0008282	Wfdc15b	192201	5.81	0.00	NM_001045554.1
PH_mM_0006159	Wbp2nl	74716	-2.19	0.00	NM_029066.1
mMC005905	Wdr64	75820	-2.26	0.00	NM_029453.2
PH_mM_0007047	Wbscr28	76629	-2.24	0.00	NM_194065.2
PH_mM_0013579	Wwp2	66894	-2.50	0.00	NM_025830.3

Table 5.2
Genes significantly different between C57BL/6J and TRAIL gene deficient mice

Array ID	Gene	Entrez_gene	Fold change (Log2 scale)	P-value	RefSeq
PH_mM_0008100	Agpat2	67512	-2.55	0.00	NM_026212.1
PH_mM_0013901	Oxct2a	64059	-2.80	0.00	NM_022033.3
PH_mM_0009512	Adam21	56622	-2.18	0.00	NM_020330.4
mMC019261	Adam7	11500	3.12	0.00	NM_007402.2
PH_mM_0012476	Adamts20	223838	-2.08	0.00	NM_001164786.1
PH_mM_0007832	Abhd16b	241850	-2.17	0.00	NM_183181.2
PH_mM_0006457	Acsbg2	328845	-2.26	0.00	NM_001039114.1
mMR026559	Arl9	384185	-2.74	0.00	NM_206935.1
PH_mM_0004216	Ahsg	11625	2.80	0.00	NM_013465.1
PH_mM_0013352	Agt	11606	-2.29	0.00	NM_007428.3
mMC017518	Ankrd53	75305	-2.12	0.00	NM_029245.3
mMC005531	Adc	242669	-3.01	0.00	NM_172875.2
mMC022312	Bcl2l14	66813	-2.01	0.00	NM_025778.3
PH_mM_0014216	Bcmo1	63857	-2.44	0.00	NM_001163028.1,NM_021486.3
PH_mM_0004515	Bhmt	12116	-2.14	0.00	NM_016668.3
PH_mM_0014563	Ces5a	67935	5.17	0.00	NM_001003951.1
mMC013527	Ceacam10	26366	2.03	0.00	NM_007675.4
mMC023526	Csnka2ip	224291	-2.16	0.00	NM_173861.2
mMC003243	Casp7	12369	-2.95	0.00	NM_007611.2
mMC026451	Cd52	23833	4.52	0.00	NM_013706.2
PH_mM_0004772	Cwh43	231293	2.35	0.00	NM_181323.2
PH_mM_0011226	Cby3	76653	-2.63	0.00	XM_484016.4
PH_mM_0012528	Cpsf4l	52670	-2.08	0.00	NM_029794.2
PH_mM_0009005	Cdrt4	66338	-2.18	0.00	NM_025496.1
PH_mM_0008848	Ccdc57	71276	-2.44	0.00	NM_027745.1
PH_mM_0005353	Ccdc70	67929	-2.17	0.00	NM_026459.3
PH_mM_0009593	Col1a2	12843	2.45	0.00	NM_007743.2
PH_mM_0004326	C4bp	12269	2.27	0.00	NM_007576.3
mMC009101	Cuzd1	16433	3.34	0.00	NM_008411.3
mMR031232	Cux2	13048	-2.06	0.00	NM_007804.2

Table 5.2-continued

Array ID	Gene	Entrez_gene	Fold change (Log2 scale)	P-value	RefSeq
PH_mM_0001409	Cdk5r1	12569	2.01	0.00	NM_009871.2
PH_mM_0000031	Cylc2	74914	-2.82	0.00	NM_001162865.1
mMC018400	Cstl1	228756	-2.61	0.00	NM_177655.3
PH_mM_0003392	Crisp1	11571	6.64	0.00	NM_009638.3
PH_mM_0013099	Cyp2a12	13085	-2.42	0.00	NM_133657.1
PH_mM_0005867	Defb2	13215	2.89	0.00	NM_010030.1
PH_mM_0008623	Defb21	403172	-2.71	0.00	NM_207276.2
mMC007896	Defb37	353320	4.28	0.00	NM_181683.2
PH_mM_0009190	Defb38	360212	4.01	0.00	NM_183036.1
mMC002785	Defb40	360217	4.09	0.00	NM_183039.3
PH_mM_0005654	Defb42	619548	2.02	0.00	NM_001034910.3
PH_mM_0008476	Dnajb8	56691	-2.23	0.00	NM_019964.1
PH_mM_0007033	Dydc2	71200	-2.33	0.00	NM_027717.1
PH_mM_0005876	Efcab1	66793	-2.03	0.00	NM_025769.3
PH_mM_0002521	BB014433	434285	-2.08	0.00	NM_001007591.2
PH_mM_0016323	Fam71d	70897	-2.26	0.00	NM_027597.4
PH_mM_0002154	Fam71f2	245884	-2.89	0.00	NM_001101486.1
PH_mM_0003129	Fez1	235180	-2.08	0.00	NM_183171.4
PH_mM_0007905	Fscn3	56223	-2.95	0.00	NM_019569.2
PH_mM_0016216	Fbxo39	628100	-2.12	0.00	NM_001099688.2
mMC007046	Fxyd2	11936	-2.57	0.00	NM_007503.3
PH_mM_0016293	Gsg1	14840	-2.42	0.00	NM_010352.2
PH_mM_0001002	Gpx3	14778	2.65	0.00	NM_001083929.1
PH_mM_0016195	Gpx4	625249	-2.05	0.00	NM_001037741.2
PH_mM_0006314	Gstcd	67553	-2.27	0.00	NM_026231.2
PH_mM_0006445	Glt6d1	71103	-2.05	0.00	NM_001039095.1
PH_mM_0001530	Gmps	229363	2.50	0.00	NM_001033300.2
PH_mM_0014524	Hbb-b1	15129	2.47	0.00	NM_008220.4
mMR001167	Hk1	15275	-2.32	0.00	NM_010438.3
PH_mM_0003363	Irgc1	210145	-2.06	0.00	NM_199013.2
mMC023153	Ifltd1	74071	-2.06	0.00	NM_028742.2
mMC008241	Iqcf4	67320	-2.04	0.00	NM_026090.2
PH_mM_0003498	Ica1	15893	-2.10	0.00	NM_010492.3
PH_mM_0006784	Kcnip2	80906	-2.79	0.00	NM_030716.2

Table 5.2-continued

Array ID	Gene	Entrez_gene	Fold change (Log2 scale)	P-value	RefSeq
PH_mM_0007225	Lelp1	69332	-2.91	0.00	NM_027042.1
PH_mM_0009010	Lrrc69	73314	-2.12	0.00	NM_028499.2
PH_mM_0005345	Lrrc8b	433926	-2.84	0.00	NM_001033550.2
mMC014819	Lcn2	16819	-2.19	0.00	NM_008491.1
mMC011770	Ly6g6c	68468	-2.45	0.00	NM_023463.3
PH_mM_0014286	Ms4a14	383435	-2.02	0.00	XM_357051.5
mMC011249	Mical3	194401	-2.64	0.00	NM_153396.2
PH_mM_0016111	Map2k7	26400	-2.22	0.00	NM_001042557.2
PH_mM_0010566	LOC100047953	100047953	-2.20	0.00	XM_001479514.2
mMC003608	Mpzl2	14012	2.09	0.00	NM_007962.4
PH_mM_0012595	Mlf1	17349	-2.53	0.00	NM_001039543.2
PH_mM_0015068	Nqo2	18105	-2.32	0.00	NM_001163241.1
PH_mM_0016090	Naca	17938	-2.37	0.00	NM_013608.3
mMC013235	Npy	109648	4.11	0.00	NM_023456.2
PH_mM_0001706	Olfr59	18359	3.00	0.01	NM_011002.2
mMC005441	Odf3b	70113	-2.39	0.00	NM_001013022.1
mMR026715	Osgin1	71839	-2.42	0.00	NM_027950.1
mMC017452	Pdzk1	59020	-2.11	0.00	NM_001146001.1,
PH_mM_0004075	Phospho1	237928	-2.44	0.00	NM_153104.3
mMC015166	Plcz1	114875	-2.12	0.00	NM_054066.4
PH_mM_0014989	Pldi	73616	-2.44	0.00	NR_033616.1
PH_mM_0009071	Prnd	26434	-2.16	0.00	NM_023043.2
PH_mM_0015888	Paqr9	75552	-2.28	0.00	NM_198414.2
mMC014816	Ptgds	19215	-2.94	0.00	NM_008963.2
mMC016079	Proc	19123	-2.04	0.00	NM_008934.2
mMC023111	Ppp2r2b	72930	-2.39	0.00	NM_027531.1
mMC011943	Rabgef1	56715	-2.31	0.00	NM_019983.2
mMC008409	Reep6	70335	-2.20	0.00	NM_139292.1
PH_mM_0010144	Rgsl1	240816	-2.33	0.00	XM_994482.3
PH_mM_0012710	Rexo1	66932	-2.45	0.00	NM_025852.3
PH_mM_0002842	Rnase12	497106	4.21	0.00	NM_001011875.1
PH_mM_0007365	Rnf148	71300	-2.11	0.00	NM_027754.1
PH_mM_0006463	Rundc3a	51799	-2.98	0.00	NM_016759.3
mMC016579	Slfnl1	194219	-2.29	0.00	NM_177570.3

Table 5.2-continued

Array ID	Gene	Entrez_gene	Fold change (Log2 scale)	P-value	RefSeq
PH_mM_0006920	Scpppq1	100271704	-2.13	0.00	NM_001163772.1
PH_mM_0007762	Spink8	78709	4.54	0.00	NM_183136.2
PH_mM_0005443	Spint3	629747	2.87	0.00	NM_001177401.1
mMC021428	LOC100504162	100504162	-2.26	0.00	XM_003085010.1
PH_mM_0005970	Srgap1	117600	-2.13	0.00	NM_001081037.1
mMC002188	Spem1	74288	-2.91	0.00	NM_028855.1
PH_mM_0004196	Spatc1	74281	-2.82	0.00	NM_028852.1
mMC004094	Spata18	73472	-2.49	0.00	NM_178387.3
mMC009674	Spata3	70060	-2.23	0.00	NM_001122732.1
PH_mM_0012342	Spata3	70060	-2.90	0.00	NM_027029.2
PH_mM_0004702	St6galnac2	20446	-2.36	0.00	NM_009180.3
PH_mM_0005808	Sult1e1	20860	-2.32	0.00	NM_023135.2
PH_mM_0014001	Tctex1d1	67344	-2.62	0.00	NM_001163767.1
PH_mM_0012549	Theg	21830	-2.42	0.00	NM_011583.3
mMR027860	Tssk3	58864	-2.06	0.00	NM_080442.2
mMC014962	Tssk6	83984	-2.49	0.00	NM_032004.1
PH_mM_0013088	Gm5334	384639	-2.46	0.00	NR_003648.2
mMC015309	Ttc24	214191	-2.89	0.00	NM_172526.3
mMC016927	Tmod4	50874	-2.50	0.00	NM_016712.3
PH_mM_0002232	Tppp2	219038	-2.71	0.00	NM_001128634.1
PH_mM_0013731	Tuba4a	22145	-2.41	0.00	NM_009447.3
mMC024820	Ubqlnl	244179	-3.05	0.00	NM_198624.3
mMC013491	Usp50	75083	-2.01	0.00	NM_029163.3
PH_mM_0013440	Ubl4b	67591	-2.90	0.00	NM_026261.2
PH_mM_0008023	B3gnt3	72297	-2.27	0.00	NM_028189.3
mMC011659	Vasp	22323	-2.46	0.00	NM_009499.2
PH_mM_0000489	Wfdc13	408190	3.01	0.00	NM_001012704.1
PH_mM_0008282	Wfdc15b	192201	4.04	0.00	NM_001045554.1
PH_mM_0004833	Wdr38	76646	-2.12	0.00	NM_029687.3
mMC005905	Wdr64	75820	-2.03	0.00	NM_029453.2
PH_mM_0007047	Wbscr28	76629	-2.42	0.00	NM_194065.2
PH_mM_0013579	Wwp2	66894	-2.03	0.00	NM_025830.3

Table 5.3

Genes significantly different between C57BL/6J and FasL/TRAIL gene deficient mice

			Fold Change log2 (Ratio)		P value		
ID	Gene	Entrez_gene	F/C	T/C	F/C	T/C	RefSeq
PH_mM_0008100	Agpat2	67512	-3.11	-2.55	0.00	0.00	NM_026212.1
PH_mM_0013901	Oxct2a	64059	-3.35	-2.80	0.00	0.00	NM_022033.3
mMC019261	Adam7	11500	5.23	3.12	0.00	0.00	NM_007402.2
PH_mM_0007832	Abhd16b	241850	-2.61	-2.17	0.00	0.00	NM_183181.2
mMR026559	Arl9	384185	-2.85	-2.74	0.00	0.00	NM_206935.1
PH_mM_0004216	Ahsg	11625	2.36	2.80	0.00	0.00	NM_013465.1
PH_mM_0013352	Agt	11606	-2.48	-2.29	0.00	0.00	NM_007428.3
mMC005531	Adc	242669	-3.40	-3.01	0.00	0.00	NM_172875.2
PH_mM_0014216	Bcmo1	63857	-2.66	-2.44	0.00	0.00	NM_001163028.1
PH_mM_0014563	Ces5a	67935	6.64	5.17	0.00	0.00	NM_001003951.1
mMC013527	Ceacam10	26366	3.80	2.03	0.00	0.00	NM_007675.4
mMC003243	Casp7	12369	-3.39	-2.95	0.00	0.00	NM_007611.2
mMC026451	Cd52	23833	6.64	4.52	0.00	0.00	NM_013706.2
PH_mM_0004772	Cwh43	231293	3.60	2.35	0.00	0.00	NM_181323.2
PH_mM_0011226	Cby3	76653	-3.97	-2.63	0.00	0.00	XM_484016.4
PH_mM_0012528	Cpsf4l	52670	-2.38	-2.08	0.00	0.00	NM_029794.2
PH_mM_0009005	Cdrt4	66338	-2.61	-2.18	0.00	0.00	NM_025496.1
PH_mM_0008848	Ccdc57	71276	-2.59	-2.44	0.00	0.00	NM_027745.1
PH_mM_0009593	Col1a2	12843	3.10	2.45	0.00	0.00	NM_007743.2
PH_mM_0004326	C4bp	12269	3.43	2.27	0.00	0.00	NM_007576.3
mMC009101	Cuzd1	16433	4.96	3.34	0.00	0.00	NM_008411.3
mMR031232	Cux2	13048	-2.28	-2.06	0.00	0.00	NM_007804.2
PH_mM_0001409	Cdk5r1	12569	3.25	2.01	0.00	0.00	NM_009871.2
PH_mM_0000031	Cylc2	74914	-2.03	-2.82	0.00	0.00	NM_001162865.1
mMC018400	Cstl1	228756	-3.19	-2.61	0.00	0.00	NM_177655.3
PH_mM_0013099	Cyp2a12	13085	-3.06	-2.42	0.00	0.00	NM_133657.1
PH_mM_0005867	Defb2	13215	5.38	2.89	0.00	0.00	NM_010030.1
PH_mM_0008623	Defb21	403172	-2.86	-2.71	0.00	0.00	NM_207276.2
mMC007896	Defb37	353320	5.64	4.28	0.00	0.00	NM_181683.2
PH_mM_0009190	Defb38	360212	5.51	4.01	0.00	0.00	NM_183036.1
mMC002785	Defb40	360217	6.56	4.09	0.00	0.00	NM_183039.3
PH_mM_0005654	Defb42	619548	4.20	2.02	0.00	0.00	NM_001034910.3
PH_mM_0008476	Dnajb8	56691	-2.52	-2.23	0.00	0.00	NM_019964.1
PH_mM_0007033	Dydc2	71200	-3.38	-2.33	0.00	0.00	NM_027717.1
PH_mM_0005876	Efcab1	66793	-2.28	-2.03	0.00	0.00	NM_025769.3
PH_mM_0003129	Fez1	235180	-2.24	-2.08	0.00	0.00	NM_183171.4
PH_mM_0007905	Fscn3	56223	-3.33	-2.95	0.00	0.00	NM_019569.2
PH_mM_0016216	Fbxo39	628100	-2.41	-2.12	0.00	0.00	NM_001099688.2
PH_mM_0016293	Gsg1	14840	-2.76	-2.42	0.00	0.00	NM_010352.2

Table 5.3-contiuned

ID	Gene	Entrez_gene	Fold Change log2 (Ratio) F/C	Fold Change log2 (Ratio) T/C	P value F/C	P value T/C	RefSeq
PH_mM_0001002	Gpx3	14778	4.32	2.65	0.00	0.00	NM_001083929.1
PH_mM_0016195	Gpx4	625249	-2.23	-2.05	0.00	0.00	NM_001037741.2
PH_mM_0006314	Gstcd	67553	-2.40	-2.27	0.00	0.00	NM_026231.2
PH_mM_0006445	Glt6d1	71103	-2.86	-2.05	0.00	0.00	NM_001039095.1
PH_mM_0001530	Gmps	229363	3.91	2.50	0.00	0.00	NM_001033300.2
PH_mM_0014524	Hbb-b1	15129	2.48	2.47	0.00	0.00	NM_008220.4
mMR001167	Hk1	15275	-2.10	-2.32	0.00	0.00	NM_010438.3
PH_mM_0003363	Irgc1	210145	-2.00	-2.06	0.00	0.00	NM_199013.2
PH_mM_0003498	Ica1	15893	-2.13	-2.10	0.00	0.00	NM_010492.3
PH_mM_0006784	Kcnip2	80906	-3.12	-2.79	0.00	0.00	NM_030716.2
PH_mM_0007225	Lelp1	69332	-3.08	-2.91	0.00	0.00	NM_027042.1
PH_mM_0009010	Lrrc69	73314	-2.28	-2.12	0.00	0.00	NM_028499.2
PH_mM_0005345	Lrrc8b	433926	-2.92	-2.84	0.00	0.00	NM_001033550.2
mMC014819	Lcn2	16819	-2.34	-2.19	0.00	0.00	NM_008491.1
mMC011770	Ly6g6c	68468	-2.27	-2.45	0.00	0.00	NM_023463.3
mMC011249	Mical3	194401	-2.64	-2.64	0.00	0.00	NM_153396.2
PH_mM_0016111	Map2k7	26400	-2.26	-2.22	0.00	0.00	NM_001042557.2
PH_mM_0010566	LOC100047953	100047953	-2.27	-2.20	0.00	0.00	XM_001479514.2
PH_mM_0012595	Mlf1	17349	-3.28	-2.53	0.00	0.00	NM_001039543.2
PH_mM_0015068	Nqo2	18105	-3.09	-2.32	0.00	0.00	NM_001163241.1
PH_mM_0016090	Naca	17938	-2.21	-2.37	0.00	0.00	NM_013608.3
mMC013235	Npy	109648	6.12	4.11	0.00	0.00	NM_023456.2
mMC005441	Odf3b	70113	-3.14	-2.39	0.00	0.00	NM_001013022.1
mMR026715	Osgin1	71839	-2.70	-2.42	0.00	0.00	NM_027950.1
PH_mM_0004075	Phospho1	237928	-2.59	-2.44	0.00	0.00	NM_153104.3
PH_mM_0014989	Pldi	73616	-2.04	-2.44	0.00	0.00	NR_033616.1
PH_mM_0015888	Paqr9	75552	-2.14	-2.28	0.00	0.00	NM_198414.2
mMC016079	Proc	19123	-2.40	-2.04	0.00	0.00	NM_008934.2
mMC011943	Rabgef1	56715	-2.96	-2.31	0.00	0.00	NM_019983.2
mMC008409	Reep6	70335	-2.45	-2.20	0.00	0.00	NM_139292.1
PH_mM_0010144	Rgsl1	240816	-2.19	-2.33	0.00	0.00	XM_994482.3
PH_mM_0012710	Rexo1|	66932|	-2.68	-2.45	0.00	0.00	NM_025852.3
PH_mM_0002842	Rnase12	497106	5.97	4.21	0.00	0.00	NM_001011875.1
PH_mM_0007365	Rnf148	71300	-2.02	-2.11	0.00	0.00	NM_027754.1
PH_mM_0006463	Rundc3a	51799	-3.06	-2.98	0.00	0.00	NM_016759.3
mMC016579	Slfnl1	194219	-2.45	-2.29	0.00	0.00	NM_177570.3
PH_mM_0006920	Scpppq1	100271704	-2.84	-2.13	0.00	0.00	NM_001163772.1
PH_mM_0007762	Spink8	78709	6.49	4.54	0.00	0.00	NM_183136.2
PH_mM_0005443	Spint3	629747	4.11	2.87	0.00	0.00	NM_001177401.1
mMC021428	LOC100504162	100504162	-3.04	-2.26	0.00	0.00	XM_003085010.1

Table 5.3-contiuned

ID	Gene	Entrez_gene	Fold Change log2 (Ratio) F/C	Fold Change log2 (Ratio) T/C	P value F/C	P value T/C	RefSeq
PH_mM_0005970	Srgap1	117600	-2.59	-2.13	0.00	0.00	NM_001081037.1
mMC002188	Spem1	74288	-3.28	-2.91	0.00	0.00	NM_028855.1
PH_mM_0004196	Spatc1	74281	-3.22	-2.82	0.00	0.00	NM_028852.1
mMC004094	Spata18	73472	-2.53	-2.49	0.00	0.00	NM_178387.3
PH_mM_0012342	Spata3	70060	-3.00	-2.90	0.00	0.00	NM_027029.2
PH_mM_0004702	St6galnac2	20446	-2.14	-2.36	0.00	0.00	NM_009180.3
PH_mM_0014001	Tctex1d1	67344	-2.85	-2.62	0.00	0.00	NM_001163767.1
PH_mM_0012549	Theg	21830	-2.46	-2.42	0.00	0.00	NM_011583.3
mMR027860	Tssk3	58864	-2.20	-2.06	0.00	0.00	NM_080442.2
mMC014962	Tssk6	83984	-3.00	-2.49	0.00	0.00	NM_032004.1
PH_mM_0013088	Gm5334	384639	-2.79	-2.46	0.00	0.00	NR_003648.2
mMC015309	Ttc24	214191	-3.43	-2.89	0.00	0.00	NM_172526.3
mMC016927	Tmod4	50874	-3.17	-2.50	0.00	0.00	NM_016712.3
PH_mM_0002232	Tppp2	219038	-3.17	-2.71	0.00	0.00	NM_001128634.1
PH_mM_0013731	Tuba4a	22145	-2.70	-2.41	0.00	0.00	NM_009447.3
mMC024820	Ubqlnl	244179	-3.11	-3.05	0.00	0.00	NM_198624.3
PH_mM_0013440	Ubl4b	67591	-3.20	-2.90	0.00	0.00	NM_026261.2
PH_mM_0008023	B3gnt3	72297	-2.36	-2.27	0.00	0.00	NM_028189.3
mMC011659	Vasp	22323	-2.49	-2.46	0.00	0.00	NM_009499.2
PH_mM_0000489	Wfdc13	408190	3.92	3.01	0.00	0.00	NM_001012704.1
PH_mM_0008282	Wfdc15b	192201	5.81	4.04	0.00	0.00	NM_001045554.1
mMC005905	Wdr64	75820	-2.26	-2.03	0.00	0.00	NM_029453.2
PH_mM_0007047	Wbscr28	76629	-2.24	-2.42	0.00	0.00	NM_194065.2
PH_mM_0013579	Wwp2	66894	-2.50	-2.03	0.00	0.00	NM_025830.3

Table 5.4

Functional Categorization of Genes Significantly Altered between Wild-type (C57Bl/6J) and Gene deficient mice (FasL-KO and TRAIL-KO)

Gene symbol	One array #	Functional category
Agpat2	PH_mM_0008100	Biosynthesis
Ces5a	PH_mM_0014563	Biosynthesis
Cstl1	mMC018400	Biosynthesis
Fbxo39	PH_mM_0016216	Biosynthesis
Mical3	mMC011249	Biosynthesis
Tppp2	PH_mM_0002232	Biosynthesis
Wfdc13	PH_mM_0000489	Biosynthesis
Wfdc15b	PH_mM_0008282	Biosynthesis
Wwp2	PH_mM_0013579	Biosynthesis
Ceacam10	mMC013527	Cytoskeletal
Cwh43	PH_mM_0004772	Cytoskeletal
Col1a2	PH_mM_0009593	Cytoskeletal
Dnajb8	PH_mM_0008476	Cytoskeletal
Fez1	PH_mM_0003129	Cytoskeletal
Gmps	PH_mM_0001530	Cytoskeletal
Lrrc8b	PH_mM_0005345	Cytoskeletal
St6galnac2	PH_mM_0004702	Cytoskeletal
Gm5334	PH_mM_0013088	Cytoskeletal
Tuba4a	PH_mM_0013731	Cytoskeletal
Vasp	mMC011659	Cytoskeletal
Cd52	mMC026451	Immune
Defb2	PH_mM_0005867	Immune
Defb21	PH_mM_0008623	Immune
Defb37	mMC007896	Immune
Defb38	PH_mM_0009190	Immune
Defb40	mMC002785	Immune
Defb42	PH_mM_0005654	Immune
Ly6g6c	mMC011770	Immune
Naca	PH_mM_0016090	Immune
Rnase12	PH_mM_0002842	Immune
Oxct2a	PH_mM_0013901	Metabolism
Bcmo1	PH_mM_0014216	Metabolism

Table 5.4-continued

Functional Categorization of Genes Significantly Altered between Wild-type (C57Bl/6J) and Gene deficient mice (FasL-KO and TRAIL-KO)

Gene symbol	One array #	Functional category
Gpx4	PH_mM_0016195	Metabolism
Glt6d1	PH_mM_0006445	Metabolism
Hk1	mMR001167	Metabolism
Nqo2	PH_mM_0015068	Metabolism
Casp7	mMC003243	Signal transducer activity
Arl9	mMR026559	Signal transducer activity
Ahsg	PH_mM_0004216	Signal transducer activity
Cux2	mMR031232	Signal transducer activity
Ica1	PH_mM_0003498	Signal transducer activity
Map2k7	PH_mM_0016111	Signal transducer activity
Osgin1	mMR026715	Signal transducer activity
Rundc3a	PH_mM_0006463	Signal transducer activity
B3gnt3	PH_mM_0008023	Signal transducer activity
Adam7	mMC019261	Spermatogenesis/development
Adc	mMC005531	Biosynthesis
C4bp	PH_mM_0004326	Spermatogenesis/development
Cuzd1	mMC009101	unknown
Cdk5r1	PH_mM_0001409	Spermatogenesis/development
Cylc2	PH_mM_0000031	Spermatogenesis/development
Crisp1	PH_mM_0003392	Spermatogenesis/development
Fscn3	PH_mM_0007905	Spermatogenesis/development
Gsg1	PH_mM_0016293	Spermatogenesis/development
Npy	mMC013235	Spermatogenesis/development
Odf3b	mMC005441	Spermatogenesis/development
Rexo1|	PH_mM_0012710	cell signal
Spink8	PH_mM_0007762	Spermatogenesis/development
Spint3	PH_mM_0005443	Spermatogenesis/development
Spem1	mMC002188	Spermatogenesis/development
Spatc1	PH_mM_0004196	Spermatogenesis/development
Spata18	mMC004094	Spermatogenesis/development
Spata3	PH_mM_0012342	Spermatogenesis/development
Tctex1d1	PH_mM_0014001	unknown

Table 5.4-continued

Functional Categorization of Genes Significantly Altered between Wild-type (C57Bl/6J) and Gene deficient mice (FasL-KO and TRAIL-KO)

Gene symbol	One array #	Functional category
Theg	PH_mM_0012549	Spermatogenesis/development
Tssk3	mMR027860	Spermatogenesis/development
Ubqlnl	mMC024820	Metabolism
Ubl4b	PH_mM_0013440	Spermatogenesis/development
Abhd16b	PH_mM_0007832	Unknown
Agt	PH_mM_0013352	Unknown
Cby3	PH_mM_0011226	Unknown
Cpsf4l	PH_mM_0012528	Unknown
Cdrt4	PH_mM_0009005	Unknown
Ccdc57	PH_mM_0008848	Unknown
Cyp2a12	PH_mM_0013099	Unknown
Dydc2	PH_mM_0007033	Unknown
Efcab1	PH_mM_0005876	Unknown
Gstcd	PH_mM_0006314	Unknown
Hbb-b1	PH_mM_0014524	Unknown
Irgc1	PH_mM_0003363	Unknown
Lelp1	PH_mM_0007225	Unknown
Lrrc69	PH_mM_0009010	Unknown
Lcn2	mMC014819	Unknown
Mlf1	PH_mM_0012595	Unknown
Phospho1	PH_mM_0004075	Unknown
Pldi	PH_mM_0014989	Unknown
Paqr9	PH_mM_0015888	Unknown
Proc	mMC016079	Unknown
Rabgef1	mMC011943	Unknown
Reep6	mMC008409	Unknown
Rgsl1	PH_mM_0010144	Unknown
Rnf148	PH_mM_0007365	Unknown
Slfnl1	mMC016579	Unknown
Scpppq1	PH_mM_0006920	Unknown
Srgap1	PH_mM_0005970	Unknown
Ttc24	mMC015309	Unknown
Tmod4	mMC016927	Unknown

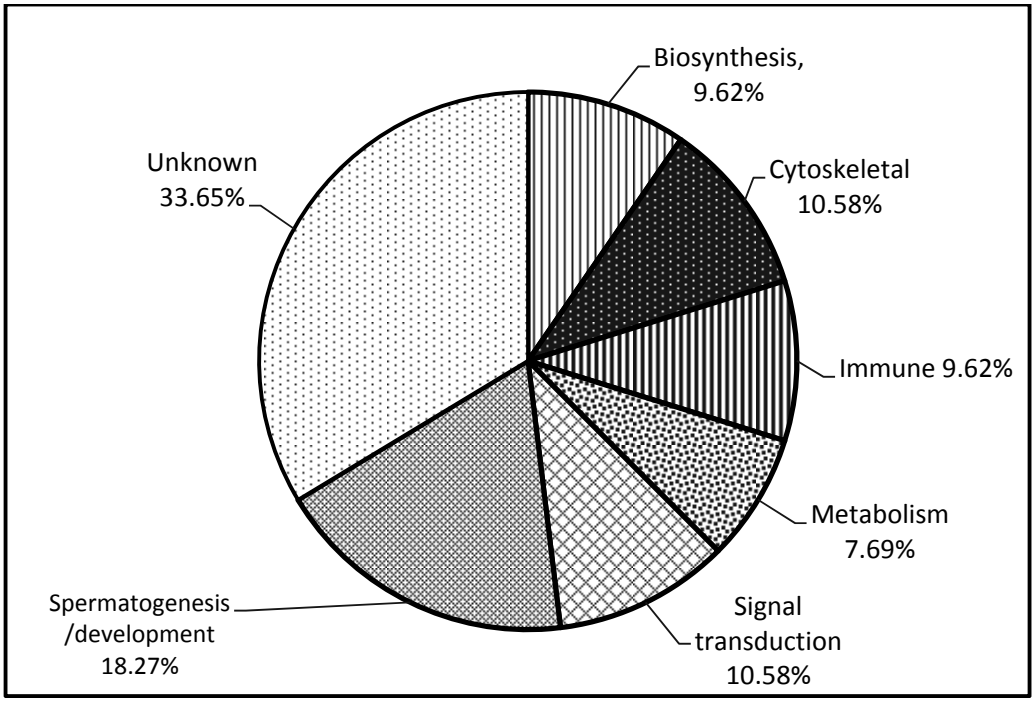

Figure 5.3 Categories of differential gene expression between death ligands gene deficient and C57BL/6J wild type mice. There are 104 differentially expressed genes (more than 4-fold) in C57BL/6J mice compared to FasL/TRAIL gene deficient mice. Genes were grouped in 7 categories based on their known biological functions in the testis.

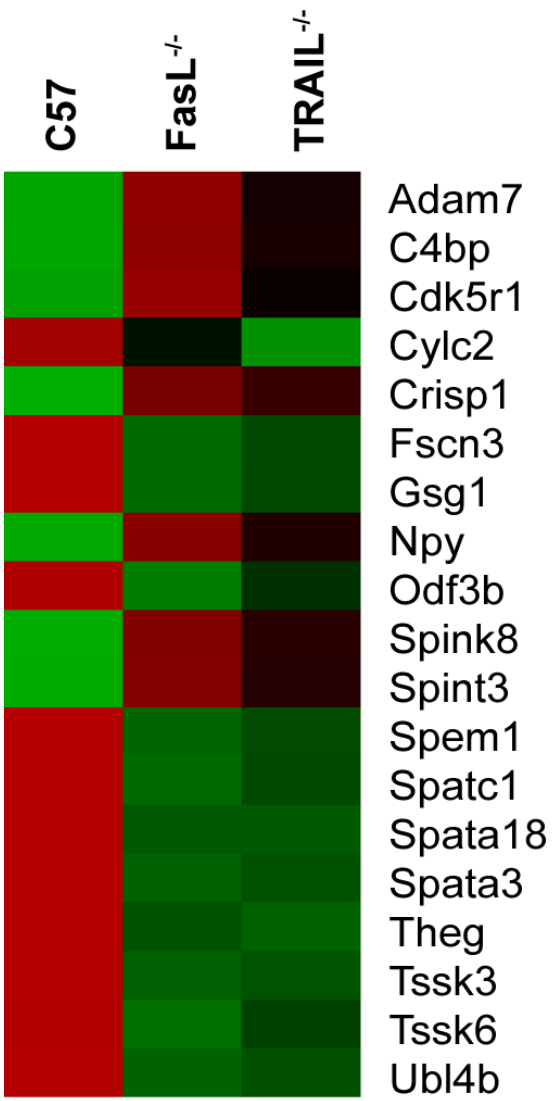

Figure 5.4 Microarray analysis of the gene expression profile in C57BL/6J and FasL/TRAIL gene deficient mice. There were19 differentially expressed genes (more than 4-fold) in C57BL/6J mice compared to FasL/TRAIL gene deficient mice. These genes are involved in spermatogenesis and development of the testis.

5.3 Discussion

In Chapter 3 we hypothesized that different death ligands may have the ability to compensate for each other when either FasL or TRAIL is missing in the testis. In our toxicant model, we identified c-FLIP as an important regulator of germ cell apoptosis in FasL gene deficient mice after MEHP exposure. FasL may be responsible for regulating the expression of c-FLIP in TRAIL gene deficient mice, as in the model of degradation of c-FLIP after nitric oxide (NO) or reactive oxygen species (ROS)[134,135]. TRAIL gene deficient mice, however, do not reveal a similar reduction of AI following MEHP exposure, as observed in FasL gene deficient mice (Fig 5.1). This may be due to TRAIL not being involved in regulating the levels of c-FLIP in our toxicant model (Fig 5.2), as we discussed in Chapter 3. At the same time, the TRAIL gene deficient mice were found to have higher AI than FasL gene deficient mice or C57BL/6J mice, and that increase may be due to the presence of FasL in the testis without efficient levels of c-FLIP to reduce germ cells apoptosis. Therefore, the results in this study agree with our previous hypothesis that FasL is the primary factor that accounts for the increased germ cell apoptosis in the testis after MEHP treatment.

Most studies have focused on how death ligands play a role in apoptosis in germ cells, but little is known about the non-apoptotic role of FasL or TRAIL in the testis. Based on our observations in FasL/TRAIL gene deficient mice, we found morphological alterations that may not be directly connected to apoptosis. For example, there is a delay of the first wave of spermatogenesis in FasL/TRAIL gene deficient mice. Also, more

metaphase cell cycle arrest was observed during spermatogenesis in the TRAIL gene deficient mice. These observations led us to explore the possible non-apoptotic roles of FasL and TRAIL in the testis, which may influence development of regulation in spermatogenesis. Therefore, we performed a microarray analysis to gain more information about the gene alteration when FasL or TRAIL is lost in the testis.

We categorized 169 genes with 4-fold changes in 7 categories (Fig 5.3). To explore how genes alter spermatogenesis in FasL and TRAIL gene deficient mice, we will discuss the 19 genes involving spermatogenesis and testis development. The following discussion will present gene functions in their order as part of the whole process of spermatogenesis and development of spermatocyte, spermatid, and spermatozoa.

Three of these 19 genes that are involved in spermatogenesis include neuropeptide Y (Npy), Spermatogenesis and centriole associated 1 (Spatc1), and spermatogenesis-associated 18 (Spata18). Npy is a neuropeptide that is widely expressed in the central nervous system and influences many physiological processes, including cortical excitability, stress response, food intake, circadian rhythms, and cardiovascular function. Recently, Npy has been added to the list of secretagogues that influence reproductive functions [151], and it can influence Leydig cell activity by inhibiting testosterone secretion [113]. This may infer that death ligand gene deficient mice may have altered levels of testosterone, which result in delayed spermatogenesis. Spatc1, also known as speriolin, is a novel centrosomal protein present in the connecting piece region of mouse and human sperm. It is transmitted to the mouse zygote and can be detected

throughout the first mitotic division by regulating or stabilizing the folding of Cdc20 during meiosis in spermatogenic cells. [152,153]. Spata18 is a novel p53 transcriptional target that is expressed in seminiferous tubules, and reports indicate that Spata18 may be regulated by p53 and p63,and that deficiency may cause spermatogenesis defects [154].

Cyclin-dependent kinase 5 regulatory subunit 1(P35) (Cdk5r1) and Spermatogenesis-associated 3 (Spata3) may have important influence during spermatocyte development. Cdk5r1(P35) is a neuron specific activator of CDK5[155], which is known to be involved in the control of the cell cycle, and it is also found in Sertoli cells, Leydig cells, and metaphase spermatocytes[156]. The possible function of CDK5 in the testis may as a regulator of the luteinizing hormone (LH), follicle-stimulating hormone (FSH), and epidermal growth factor (EGF)[157]. P35 activity is observed in isolated elongated spermatids and at the time when elongated spermatids appear in the developing testis, suggesting a role for Cdk5 [158]. Spata3, also known as the musculus testis and spermatogenesis cell apoptosis-related gene 1 (Mtsarg1), is mainly located in spermatocyte, and it may have an important role in spermatocyte development [159].

When spermatocytes gradually form spermatids, Cylicin, basic protein of sperm head cytoskeleton 2 (Cylc2), spermatid-specific murine paralog of the actin-bundling protein fascin (FSCN1), germ cell-specific gene 1 **(**GSG1**),** spermatid maturation 1 (Spem 1), and ubiquitin-like protein 4B (Ubl4b) may affect the development and differentiation in this step. Cylc2 may play a role to format the structure of spermatids and help differentiation during spermatogenesis [160]. FSCN1 possibly functions during

terminal elongation of the spermatid head and in the microfilament rearrangements that accompany fertilization [161]. GSG1 is a protein that interacts with testis-specific poly(A) polymerase (TPAP), which is highly expressed in round spermatids [162]. TPAP deficient mice were shown to have impaired expression of haploid-specific genes that are required for the morphogenesis of germ cells [163]. Spem 1 is a protein exclusively expressed in the cytoplasm of elongated spermatids in the testis, and loss of Spem 1 results in sperm deformation and male infertility in mice [164]. Theg is 42 kDa protein specifically expressed in spermatid cells. Although its function is not clearly understood, it may interact with Sertoli cells during spermatogenesis [165]. It also can be a good marker for spermatid cells. Ubl4b is a testis-specific autosomal gene, and it is restricted to post-meiotic germ cells and can be detected only in elongated spermatids but not in spermatocytes [166].

The last step for spermatogenesis is to form spermatozoa to transfer sperm to the epididymis. A disintegrin and metallopeptidase domain 7 (Adam7) is one member of the ADAMs family of zinc proteases, which are expressed in the caput region of the epididymis and on the surface of the spermatozoa, and can be redistributed in the sperm head during the acrosome reaction [167]. Complement C4b-binding protein (C4BP) is a plasma protein synthesized in the liver that plays a regulatory role in the host defense complement system. Recently, it was also found in epididymis epithelial cells and the surfaces of spermatozoa, and may be an androgen-dependent promoter binding protein. C4bp may be involved in sperm maturation [168,169]. Cysteine-Rich Secretory Protein 1 (Crisp1) is one epididymal protein, belonging to the Cysteine-RIch Secretory Protein

(CRISP) family, and can play a role in the mammalian fertilization process by participating in both sperm-zona pellucida interaction and gamete fusion by binding to egg-complementary sites [170]. The outer dense fibers 3B (Odf3b) is a member of the Odf family of proteins. In animals with internal fecundation, Odfs are the main cytoskeletal structures of the sperm tail and an expanding group of proteins co-assembled along the axoneme during the development of the sperm tail [171].

Serine peptidase inhibitor, Kazal type3 and 8 (Spink 8 and Spint3) belong to the Kazal protease inhibitors and may have a function for the regulation of sperm maturation by regulating the proteolytic processing of the sperm membrane during epididymal transit [172,173]. Testis-specific serine/threonine kinase 3 and 6 (Tssk3 and Tssk6) are members of the testis-specific serine/threonine kinases (Tssk) family and may regulate sperm differentiation in the testis and/or fertilization [174]. Tssk-3 is induced at puberty, persists during adulthood and is restricted to the interstitial Leydig cells of post-pubertal males [175].

Taken together, this chapter demonstrates that: 1) FasL is the main death ligand to regulate the level of c-FLIP in the testis in response to MEHP exposure. 2) Loss of one death ligand may cause impairment of the first wave of spermatogenesis and further reduce sperm counts in the testis. 3) There are several possible genes involved in the altered spermatogenesis and development in the testis of gene-deficient mice. If we can confirm that these candidate genes have similar results at RNA and protein levels, this information will help us to understand more about the non-apoptotic roles in FasL and TRAIL in the testis.

Chapter 6: MEHP promotes invasion and migration of testicular embryonic carcinoma cells

6.1 Introduction and Rationale

We previously discovered that MEHP exposure induces the activation of matrix metalloproteinase-2 (MMP-2) in the seminiferous tubule [122], consequently leading to impaired spermatogenesis. The ratio between MMP-2 and its endogenous inhibitor, tissue inhibitor of matrix metalloproteinase-2 (TIMP-2), is critical for maintaining normal germ cell development [122,176] and also for influencing the tumor progression in different types of tumors [177,178]. Interestingly, it has been shown that the serum level of MMP-2 increases in patients diagnosed with testicular germ cell tumors [179]. These findings led us to test whether MEHP-activated MMP-2 in the testis plays a role in regulating testicular cancer progression. We show that MEHP-induced c-Myc is partially responsible for the down-regulation of TIMP-2 in the testis [180]. It has been widely appreciated that c-Myc functions as a switch on tumor promotion by regulating proliferation or tumor suppression by modulating apoptosis [181]. Therefore, studying the functional significance of c-Myc on testicular cancer progression in response to phthalate is a logical extension of this work.

In this chapter, the effect of MEHP on stimulating cell invasion and migration of testicular embryonal carcinoma cells is investigated in vitro using the NT2/D1 teratoma cell line. The data indicate that one mechanism to account for the increase in invasion and

migration following MEHP exposure is through the MMP-2 activation. Microarray analysis also demonstrates that cell adhesion molecules and transcription factors may also be responsible for tumor progression in the testis after MEHP exposure.

6.2. Results

6.2.1 *MEHP treatment up-regulates MMP-2 and c-Myc expression in NT2/D1 cells*

The changes in MMP-2, MMP-9, and c-Myc expression in response to MEHP exposure were determined by western blots. The MMP-2 protein level in NT2/D1 cells was found to increase significantly at 3 hours after MEHP exposure and remain steady until 24 hours of incubation (2.53-fold, compared to non-treated group) (Fig 6.1A). Low doses of MEHP treatment showed no significant effects on MMP-2 expression, while 200 μM of MEHP strongly induced MMP-2 protein levels after 12 hours of incubation (2.38-fold, compared to non-treated group) (Fig 6.1B). No significant changes in MMP-9 expression were observed after MEHP exposure. The protein level of c-Myc in NT2/D1 cells was up-regulated shortly after MEHP treatment (1.52-fold, compared to non-treated cells), decreased at 3 hours and then increased after 12 hours of incubation (Fig 6.1A). In addition, high doses of MEHP treatment significantly enhanced c-Myc levels (3.22-fold at 200 μM, compared to the non-treated cells) (Fig 6.1B), indicating that the induction of c-Myc by MEHP exposure is dose-dependent.

6.2.2 *MEHP treatment up-regulates MMP-2 activity in NT2/D1 cells*

The amount of soluble MMP-2 secreted from NT2/D1 cells was measured by ELISA. Figures 6.2A and 6.2B show the time-dependent increases in the soluble MMP-2

level after MEHP exposure (4.89-fold at 24 hours of incubation, compared to the non-treated group). High doses of MEHP treatment stimulated significant production of soluble MMP-2 (3.97-fold at 200 μM, compared to the non-treated group), even though soluble MMP-2 production decreased at 400 μM of dosage (2.06-fold, compared to the non-treated group). The activities of MMP-2 and MMP-9 *in vitro* were determined by gelatin zymography (Fig 6.3A and Fig 6.3B), indicating that MMP-2 is time- and dose-dependently activated by MEHP treatment. The MMP-9 level was relatively low to MMP-2 and was slightly increased by MEHP, suggesting that MEHP exposure has major effects on MMP-2 activity, but not on MMP-9.

6.2.3 *SB-3CT suppressed MEHP-induced MMP-2 activation in NT2/D1 cells*

Specific gelatinase inhibitor, SB-3CT, and MEHP were applied to NT2/D1 cells. After 12 hours of incubation, conditioned media were collected and MMP-2 activity were further analyzed. ELISA results indicated that low doses of SB-3CT treatment (5 μM) significantly reduced the amount of soluble MMP-2 compared to MEHP treatment alone (Fig 6.4A). Fig 6.4B reveals that MMP-2 gelatinase activity was enhanced by MEHP, but decreased dose-dependently when SB-3CT was added

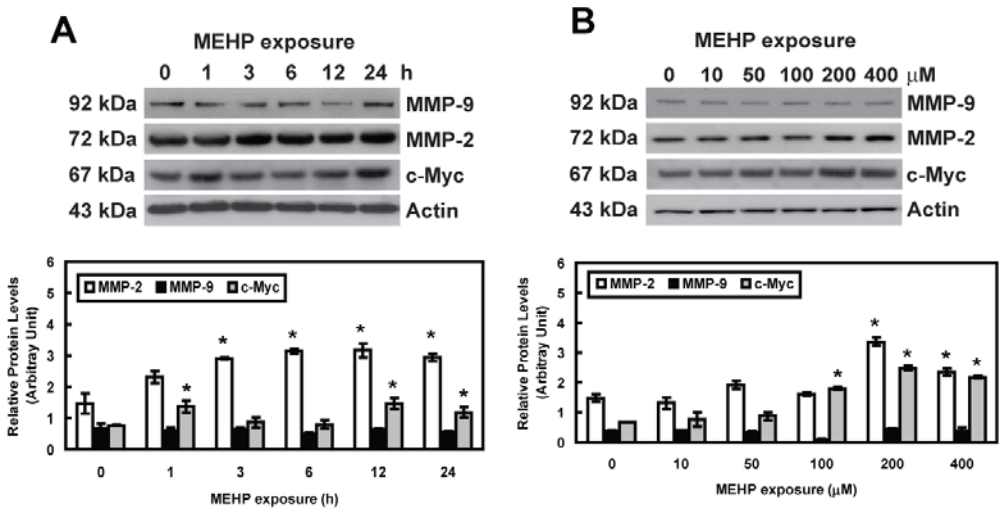

Figure 6.1 MMP-2 protein expression in NT2/D1 cells is increased with MEHP exposure. Total protein (30 μg) from NT2/D1 cells treated with or without MEHP was analyzed by western blot analysis. Time dependent inductions of MMP-2 were detected following MEHP exposure (Figure 6-1A). Dose-dependent induction of MMP-2 was detected following MEHP exposure (Figure 6-1B). Actin served as the loading control. The quantified relative protein levels of MMP-2 and MMP-9 are shown under the blot images. Values represent the mean ± SEM. Asterisks denote significant differences between the treatment and control groups (*p<0.05, Student t-test).

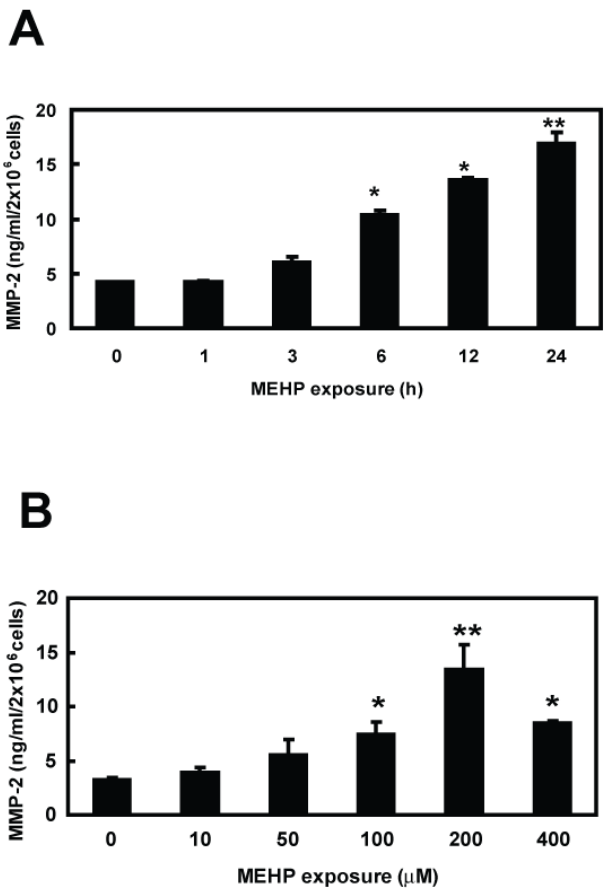

Figure 6.2 MMP-2 activity in NT2/D1 cells increased after MEHP exposure. The amount of soluble MMP-2 released from NT2/D1 cells was measured by ELISA. Time- and dose-dependent inductions of soluble MMP-2 were detected in response to MEHP exposure (Figure 6-2A and 6-2B), respectively. Values represent the mean ± SEM. Asterisks denote significant differences between the treatment and control groups (*p<0.05, Student t-test).

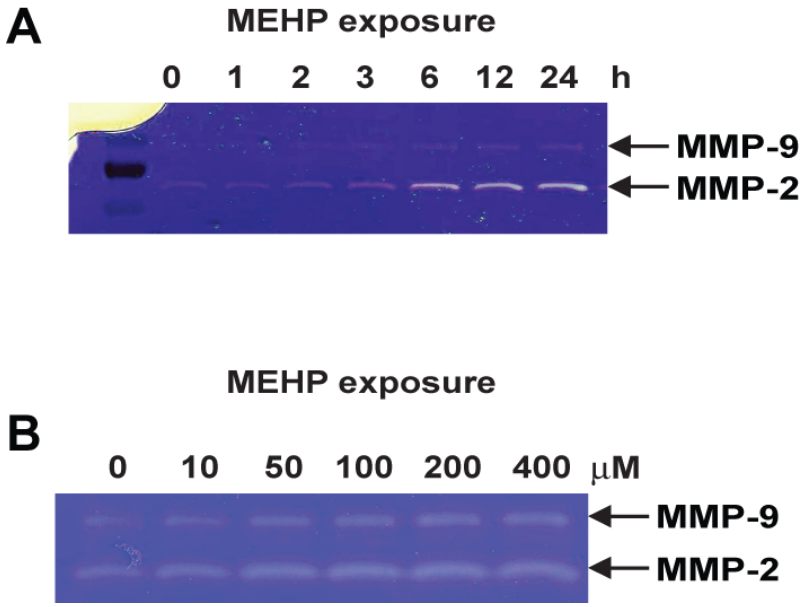

Figure 6.3 MMP-2 Gelatinolytic activity in NT2/D1 cells increased with MEHP exposure. Gelatinolytic activities of MMP-2 and MMP-9 in the media were determined by gelatin zymography. Clear bends shown on the blue background indicate the enzyme activity. MEHP treatment caused an increase in MMP-2 activity in a time- and dose-dependent manner. MMP-9 activity was relatively weaker than MMP-2, while it increased with MEHP exposure, as well.

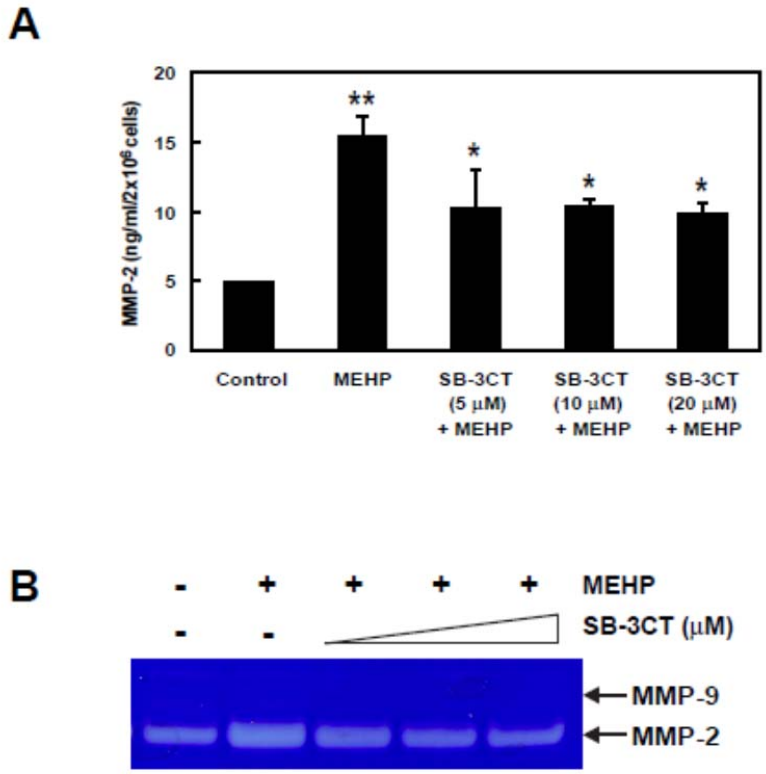

Figure 6.4 SB-3CT inhibited MEHP-induced MMP-2 activation in NT2/D1 cells. NT2/D1 cells were treated with various doses of SB-3CT and 200 μM of MEHP for 12 hours, and the conditioned media were collected. (A) The amount of soluble MMP-2 released from NT2/D1 cells was measured by ELISA. SB-3CT treatment slightly decreased the amount of free MMP-2. Values represent the mean ± SEM. Asterisks denote significant differences between the treatment and control groups (*p<0.05, **p<0.01, Student t-test). (B) Gelatinolytic activities of MMP-2 and MMP-9 in the media were determined by gelatin zymography. MMP-2 activity was reduced by SB-3CT and MEHP co-treatment compared to MEHP treatment only in a dose dependent manner. No change in MMP-9 activity was observed.

6.2.4 *MEHP exposure promoted the invasive activity and the migration capability of NT2/D1 cells*

In order to estimate the effect of MEHP treatment on cell invasion, non-treated or MEHP-treated NT2/D1 cells were tested by transwell invasion assay. Interestingly, after MEHP exposure, NT2/D1 cells had a stronger ability to digest and pass through Matrigel. Fig 6.5 shows that the number of invasive cells significantly increased in the MEHP-treated group (3.23-fold) compared to the non-treated group. In addition to invasive ability, the number of cells that migrated into the cell-free zone were counted. More cells were observed in the cell-free zone after MEHP treatment (1.59-fold at 36 hours, compared to the control group), indicating that MEHP facilitates the migration of NT2/D1 cells (Fig 6.6).

6.2.5 *SB-3CT showed inhibitory effects on MEHP-enhanced invasion and migration in Nt2/D1 cells*

To determine whether the activated MMP-2 was necessary for MEHP-enhanced cell invasion and migration, SB-3CT was applied to NT2/D1 cells in the presence of MEHP. The addition of SB-3CT and MEHP co-treatment suppressed the number of invasive cells (down to 0.68-fold compared to MEHP-treated groups, Fig 6.5). SB-3CT treatment was also able to decrease the number of migrated cells in the presence of MEHP (down to 0.81-fold compared to MEHP-treated group, Fig 6.6). These results suggest that gelatinases play an essential role in testicular cancer invasion and migration stimulated by MEHP exposure.

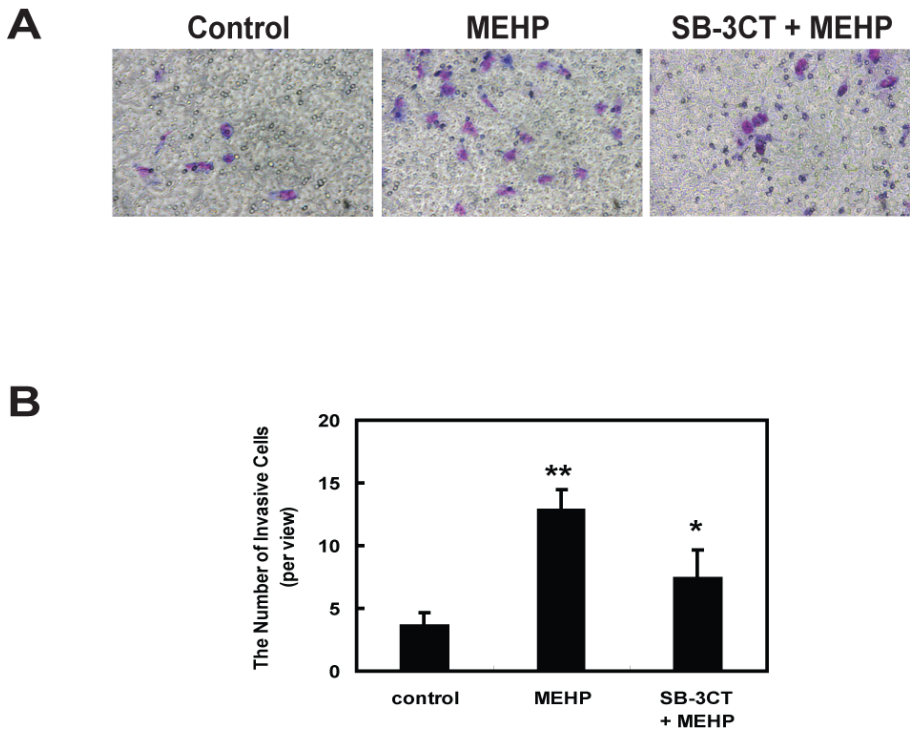

Figure 6.5 The invasion activities of NT2/D1 cells were enhanced by MEHP exposure and suppressed by SB-3CT, showing the compensation effect on MEHP treatment. (A) *In vitro* invasion assays were performed using transwell chambers (8 μm pore size) coated with Matrigel. Non-treated, MEHP-treated and SB-3CT/MEHP co-treated cells ($2x10^5$) were seeded on the Matrigel and incubated overnight. Invasive cells were stained with 20% Giemsa solution. Cells attached to the lower surface of the filter were photographed by Canon-5D digital camera attached to a light microscope (x200). (B) The quantified number of cells penetrating Matrigel was counted. Values represent the mean ± SEM. Asterisks denote significant differences between the treatment and control groups (**p<0.01, Student t-test).

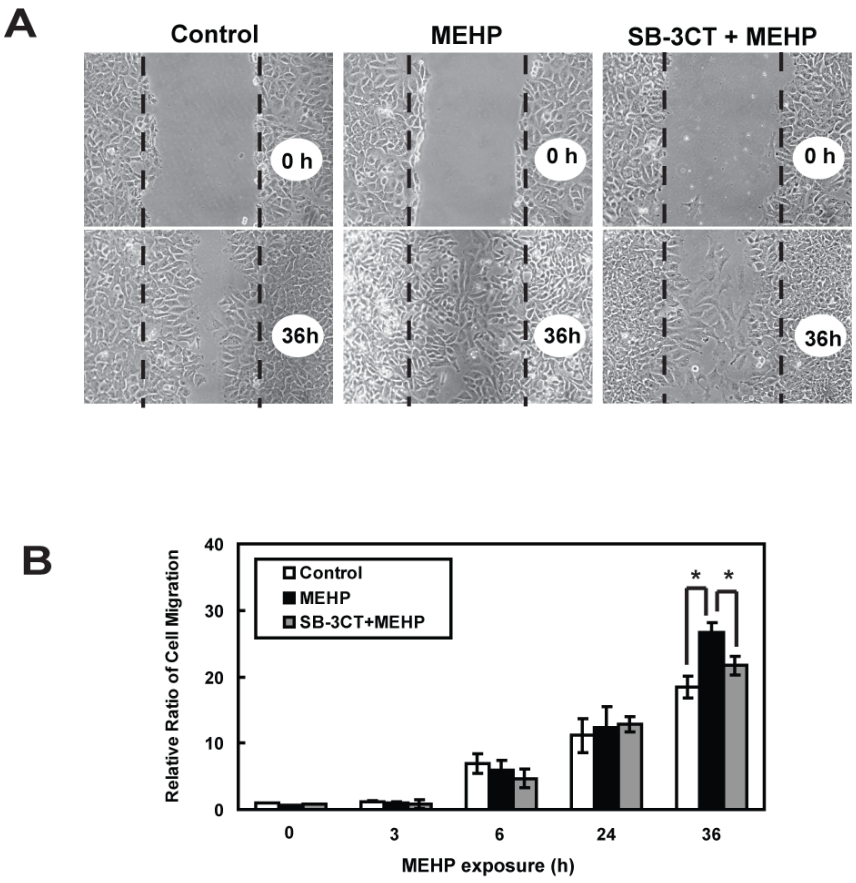

Figure 6.6 The migration activities of NT2/D1 cells were enhanced by MEHP exposure and suppressed by SB-3CT, showing the compensation effect on MEHP treatment. (A) Wound-healing migration assay was performed to determine the change in migration rate of NT2/D1 cells after MEHP treatment or SB-3CT/MEHP co-treatment. Cells were photographed by Canon-5D digital camera attached to a light microscope (x200). (B) The number of cells migrating into the cell-free zone was evaluated. Values represent the mean ± SEM. Asterisks denote significant differences between the treatment and control groups (*p<0.05, Student t-test).

6.2.6 *Microarray analysis of gene expression in NT2/D1 cells following MEHP exposure*

Of nearly 30,000 putative probes, 1,289 genes in the testicular embryonic carcinoma cell line, NT2/D1, were significantly altered by MEHP exposure. There were 45 genes that displayed more than 2-fold changes in mRNA levels following MEHP exposure (Fig 6.7). The genes are grouped in 7 categories on the bases of their biological functions, including adhesion molecules, metabolism modifiers, transcription factors, translation components, cell-cycle regulators, signal transduction mediators, and miscellanea (Fig 6.8). Among these categories, cell adhesion molecules (9 genes out of 45, 19%) appear to be the major group that is strongly altered in response to MEHP treatment. These genes include pleckstrin homology domain containing family O member 1 (PLEKHO1), vinculin (VCL), gap junction protein alpha 1 (GJA1), WD repeat domain 1 (WD1), leucine rich repeat containing 8 family member A (LRC8A), N-cadherin (CDH2), claudin 6 (CLDN6), catenin-beta 1 (CTNNB1) and matrix metalloproteinase-2 (MMP-2). Seven genes (16%) are grouped as transcription factors, including inhibitor of DNA binding 1 (ID1), inhibitor of DNA binding 2 (ID2), inhibitor of DNA binding 3 (ID3), TEA domain family member 4 (TEAD4), polyhomeotic homolog 1 (PHC1), zinc finger protein 429 (ZHF429) and DNA-damage-inducible transcript 3 (DDIT3).

Semi-quantitative RT-PCR was performed to verify the mRNA expression of 11 MEHP-regulated genes (6 for down-regulation and 5 for up-regulation) which were randomly selected from microarray results, including NTS, ID1, VCL, GJA1, LFNG, IL17RD, CLDN6, CTNNB1, MARS, MMP2 and DDIT3 (Fig 6.9). Among adhesion

molecules, semi-quantitative RT-PCR confirmed that GJA1 is significantly down-regulated by MEHP treatment (0.54-fold, at 24 hours, compared with 0 hour group), while CLDN6 and CTNNB1 were up-regulated (2.77- and 1.38-fold, at 24 h). RT-PCR confirmed that VCL expression is reduced by MEHP at 3 hours (0.79-fold), while no changes were observed at 24 hours that is not consistent with microarray data. Among transcription factors, RT-PCR results showed that ID1 and PHC decreased after MEHP treatment (0.45- and 0.78-fold, at 3 hours), and DDIT3 increased (1.81-fold, at 3 hours). However, NTS expression pattern was not consistent according to microarray and RT-PCR results. Microarray analysis and RT-PCR data both revealed that MMP-2 mRNA expression in NT2/D1 cells was significantly increased at 24 hours after MEHP stimulation (2.87- and 1.61-fold, respectively). Even though RT-PCR showed that MMP-2 level was strongly induced at 3 hours of incubation, microarray analysis indicated that MMP-2 levels were not induced at 3 hours.

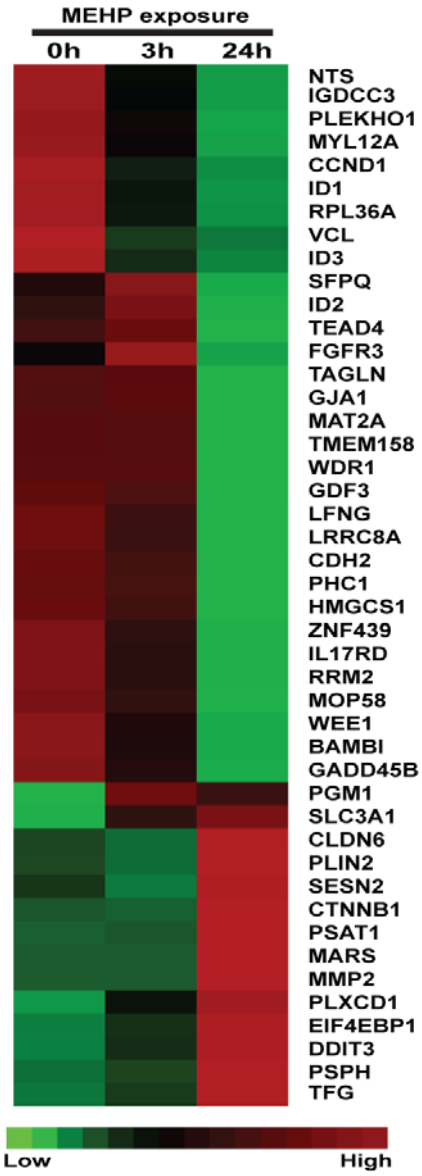

Figure 6.7 Microarray analysis of the gene expression profile in NT2/D1 cells treated with or without MEHP. Microarray analysis was performed using Human Whole Genome One Array Chips v.5 produced by Phalanx Biotech Group, carrying 29,187 human genome probes and 1,088 experimental control probes. NT2/D1 cells were treated with MEHP for 0, 3 and 24 hours. (A) There were 45 differentially expressed genes (more than 2-fold) in response to MEHP exposure that were identified and their mRNA levels were shown as hierarchical clustering. Relative expression levels of these genes are color-coded on the bottom.

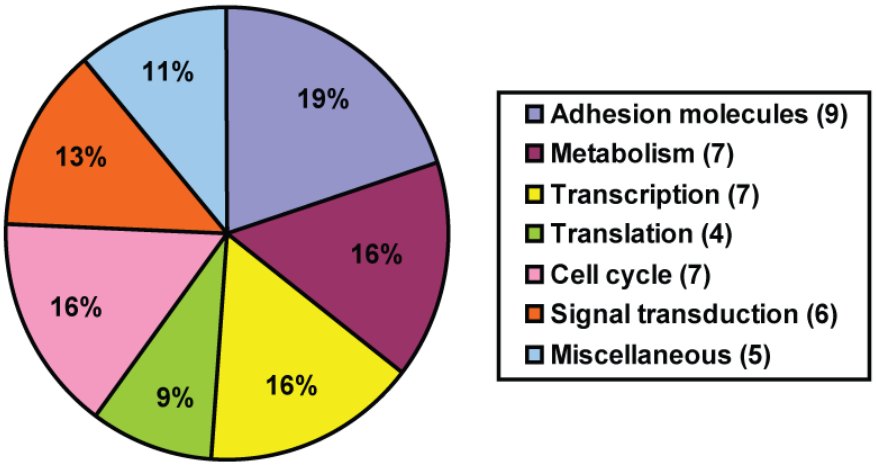

Figure 6.8 The categories of gene expression profiles in microarray analysis. There were 45 differentially expressed genes grouped in 7 categories on the basis of biological functions.

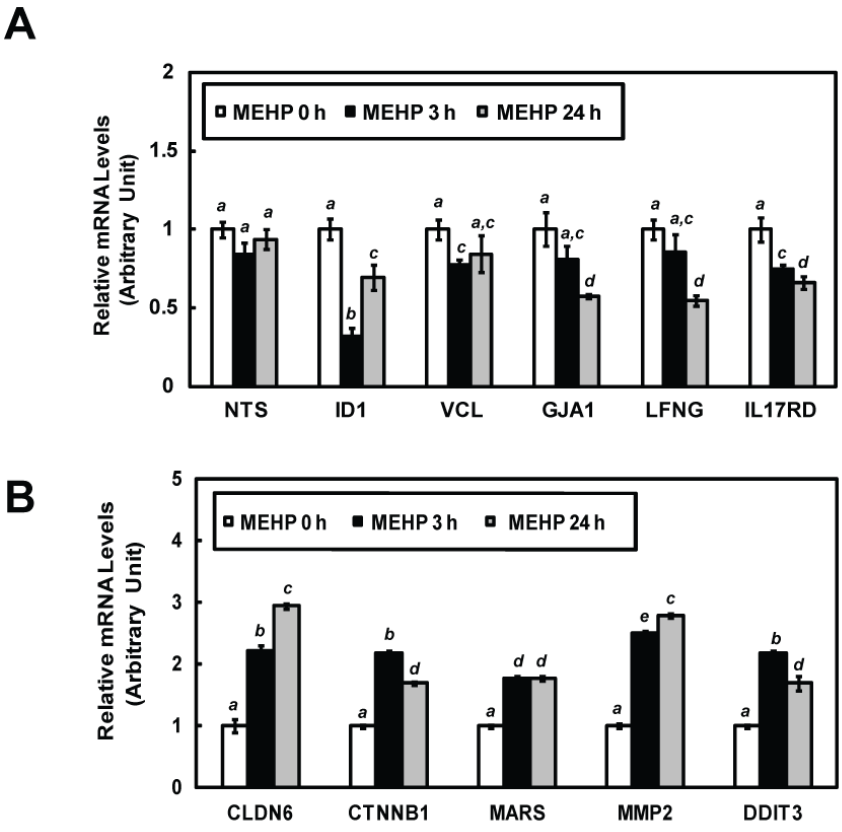

Figure 6.9 Semi-quantitative RT-PCR was performed in order to confirm the results derived from the microarray analysis. There were 7 randomly selected genes assayed and GAPDH served as a control. Values represent the mean ± SEM. Significant difference between groups are denoted by bars with different letters (*p<0.05, ANONA).

6.3 Discussion

Testicular dysgenesis syndrome (TDS) is a common human health problem that refers to symptoms including poor semen quality, undescended testis (cryptorchidism), hypospadias, and testicular cancer. The incidence of these diseases has dramatically increased over the past 50 years, and it has been hypothesized that environmental influences rather than genetic defects account for this increase [182,183,184]. Phthalate exposure has been linked to reproductive dysfunction and has been shown to adversely affect normal germ cell development. Exposure to high levels of DEHP results in liver lesions and an increased incidence of hepatocellular carcinoma in rodents [185,186], and studies also suggest that DHEP is a potential tumor promoter but not genotoxic. A recent study indicates that di-(n-butyl) phthalate (DBP) exposure promotes the vulnerability of fetal germ cells, and is possibly related to testicular germ cell tumor formation [187]. Therefore, the effect of phthalate exposure on the regulation of testicular cancer progression is of interest.

We previously identified several important molecular factors that are critical for controlling normal germ cell development, including c-Myc and MMP-2, which are altered following phthalate exposure [122,180] and have been shown to be tightly associated with tumor metastasis and tumor progression [188,189,190]. Since c-Myc controls cell proliferation, cell differentiation and self-renewal [191,192], the up-regulation of c-Myc seen in testicular embryonal carcinoma following MEHP exposure may suggest that phthalates affect both normal cell differentiation and tumor cell

development. Matrigel invasion and wound-healing migration assays are well-developed methods to observe the ability of tumor cells to metastasize, and are strongly related to MMP-2 and MMP-9 activities [193,194,195]. In this study, after MEHP exposure, NT2/D1 cells had the stronger ability to digest and pass through the Matrigel. In addition, our data also show that MEHP promotes the migration of cancer cells. These results suggest that MEHP exposure may enhance the potential of testicular cancer cells to become more metastatic and malignant. It is then reasonable to conclude that the molecular mechanism that accounts for this alteration can be explained by the activation of MMP-2. Using specific a MMP-2 inhibitor, SB-3CT, we were able to suppress endogenous MMP-2 activity stimulated by MEHP both *in vitro* and *in vivo* [122,176]. We found that the addition of SB-3CT to NT2/D1 cells partially inhibited MEHP-induced invasion and migration. Therefore, MEHP-induced MMP-2 activation appears to be important in regulating the metastasis status of testicular germ cell tumors.

In addition to MMP-2 and c-Myc activation, we performed microarray analysis in order to examine the gene expression patterns altered by MEHP exposure on a genome-wide basis. Phthalate exposure has been demonstrated to impair junctional connection in the seminiferous tubule by altering the junctional protein expression [176,196]. Interestingly, MEHP primarily influences cell adhesion molecules and transcription factors, which are also closely related to tumorigenesis. Hence, we further discuss the functional significance of distinct genes in testicular cancers following toxicant exposure.

Gap junctional intercellular communication (GJIC) controls cell growth, development, and differentiation [197]. The inhibition of gap junctional communication

has been proposed to be related to tumor promotion [198,199]. GJA1 gene encodes protein connexin 43 (Cx43), forming the main structure of gap junction. Mutation or deficiency in GJA1 gene leads to a variety of human diseases or disorders [200,201]. Interestingly, it has been shown that the reduction of Cx43 enhances the invasion capacity of human glioblastoma cells [202]. In the mouse testis, a decrease in Cx43 protein level and the change in Cx43 localization have been observed after DEHP exposure [196]. Similar results also have demonstrated that DEHP treatment inhibits gap junctional communication *in vitro* [203]. Our current results indicate that MEHP exposure leads to a decrease in GJA1 mRNA expression in NT2/D1 cells. The reduction of GJA1 following MEHP exposure may partially explain the mechanism of MEHP-enhanced invasion in NT2/D1 cells. On the other hand, although DEHP-induced tumorigenesis in the liver is strongly correlated with the inhibition of gap junctional communication in rodents, it appears that this phenomenon is species-specific [112,204]. Therefore, the role of suppressed GJA1 in human testicular cancer progression by phthalates remains an open question.

The focal adhesion molecule, vinculin, is important for maintaining the structure of adherens junction through the interaction with actin filament and integrin [205,206]. We previously showed that MEHP exposure breaks down laminin/integrin complex at the ectoplasmic specialization [176]. In this study, we further found that MEHP treatment reduces vinculin mRNA levels in the testicular cancer cells, suggesting that phthalate primarily impairs the junctional connection in the testis. Overexpression of vinculin has been shown to suppress the tumorigenesis [207]. Immunostaining results also

demonstrate that vinculin expression is negatively correlated with the metastasis of squamous cell tumor [208], indicating that reduced cellular adhesiveness is strongly associated with the metastasis of malignant tumors. Therefore, MEHP-decreased viculin may be involved in regulating the invasive and migration ability of testicular cancer cells in parallel to the activation of MMP-2.

β1-catenin, an oncogene, has been demonstrated to be involved in various biological processes, including cell adhesion, cell growth, and tumorigenesis. The accumulation of β1-catenin in the germ cell nuclei associated with the abnormal OCT3/4 expression leads to the malignant transformation of seminoma [209]. The activation of β1-catenin signaling may cause Sertoli cell tumor formation [210]. DEHP induces the up-regulation of α-catenin and N-cadherin in rat testes [211]. Fetal exposure to DEHP in mice causes the delay in liver development and the alteration of glycogen metabolism through the activation of Wnt/β1-catenin signaling [212]. Here, we show that the β1-catenin mRNA level is up-regulated by MEHP in NT2/D1 cells, demonstrating that phthalate has the potential to promote tumor progression by up-regulation of oncogenes. In addition, c-Myc expression can be regulated by the Wnt/β1-catenin/TCF signaling pathway, resulting in colorectal and skin carcinogenesis [213,214]. Therefore, we speculate that MEHP-induced β1-catenin up-regulation may play a role in modulating the differentiation status of testicular cells by influencing c-Myc expression.

Claudin-6, which belongs to the claudin superfamily, is a key component of tight junctions. Several studies have suggested that claudin-6 functions as a tumor suppressor in breast cancer, accompanied by the alteration of MMP activity [215,216,217]. The

frequency of epigenetic silencing in the claudin-6 gene by methylation is increased in esophageal squamous cell carcinomas [218]. However, overexpression of claudin-6 increases the invasiveness, migration and proliferation rate of human gastric adenocarcinoma cell line [219]. Claudin-6 is also potentially a diagnostic marker for atypical teratoid/rhabdoid tumors (AT/RT) [220]. These observations demonstrate that the function of claudin-6 in promoting or suppressing tumor progression may be cell-specific. In testicular embryonal carcinoma, we found that MEHP exposure increased the mRNA level of clausin-6. Interestingly, claudin-6 expression appears to be limited in some testicular embryonal carcinoma and immature epithelial teratocarcinoma [221], and developmentally regulates adipogenesis and epithelialization of embryos [222,223,224]. Therefore, claudin-6 not only serves as a basis of tight junction structure, but also is important for cell differentiation that may be c-Myc-dependent.

Inhibitor of DNA binding (ID) proteins are transcription factors, which are important for cell cycle, cell development, and tumorigenesis [225,226]. Surprisingly, MEHP exposure significantly reduces the mRNA level of three ID proteins in testicular embryonal carcinoma, demonstrating that phthalates influence the dynamic expression of transcriptomes in the tumor. In the murine testis, ID3 expression is regulated by the follicle-stimulating hormone (FSH) [227]. MEHP has been shown to disrupt FSH signaling [89,228]. Hence, impaired FSH signaling may be responsible for decreases in ID proteins after MEHP exposure.

The findings of the current study indicate cellular mechanisms triggered by MEHP exposure that act to enhance tumor progression/metastasis in testicular embryonal

carcinoma cells (NT2/D1). We observed that: 1) NT2/D1 cells have an increased ability to digest and migrate into the Matrigel matrix following MEHP exposure and that this was dependent on increased activity of MMP2, as the enhancing effects of MEHP exposure can be partially inhibited by addition of the specific MMP2 inhibitor SB-3CT. 2) We showed that MEHP not only increases the activation of MMP2, but also down-regulates the expression of both the tight-junction (*GJA1*) and adherens junction (*VCL*) genes, which could further aid in the capacity for the invasion and migration of the NT2/D1 cells. Finally, 3) we described the activation of the MYC transcription factor after MEHP exposure. Since MYC plays a role in promoting the expression of CLDN6 and inhibits TIMP2 expression, disruption in MYC expression could provide an underlying mechanism to account for MMP2 activation after MEHP treatment. Taken together, these novel findings provide important mechanistic insights by which exposure to environmental toxicants, such as the phthalates, can enhance testicular cancer metastasis and invasion.

Chapter 7: Concluding Remarks

Spermatogenesis is an important physiological process in the male reproductive system. The number of spermatozoa that can be formed depend on the supportive capacity of Sertoli cells that provide an adaptive environment and nutrition for germ cells growth and development but that may be disrupted by genetic effects and environmental stresses. In this research, a toxicant exposure model (MEHP treatment) test was used to determine if loss of death ligands can protect or reduce the impact from MEHP exposure. The results revealed a partial reduction of germ cell apoptosis after toxicant treatment; however, the reduction of apoptosis may not occur directly through the original mechanism that we hypothesized. The lack of FasL expression maybe not be the main factor to reduce germ cell apoptosis in the testes because even before MEHP treatment a high apoptotic rate was observed in FasL gene deficient mice. Apoptosis was greatly decreased after treatment that led to the assumption that FasL may directly contribute to bind Fas to form DISC and, further, regulate levels of cFLIP to enhance the process of apoptosis. Based on that observation, it was important to examine in detail the mechanism by which cFLIP is regulated by FasL via gene expression/inhibition or protein degradation. In order to answer that question, a cell model was employed but is still under design because it was not a good fit for the experiment. Future research will focus on development of a better method to understand the mechanism.

TG-interacting factor (TGIF), originally identified for its ability to bind a specific retinoid element, is considered to repress transcription by competing with retinoid

receptors for binding to this element [229]. Subsequent studies found that TGIF represses transcription in different biological processes through its ability as a DNA-binding repressor or as a co-repressor in association with other DNA-binding proteins. For example, TGIF can interact with the transcriptional factor Smad2 to restrict the expression of transforming growth factor beta (TGF-b)-responsive genes [230] . More recently, TGIF has been identified as a component of the TNF-a signaling pathway that integrates cytotoxicity [231]. TGIF is demonstrated to act in concert with the E3 ubiquitin ligase Itch to promote ubiquitin-dependent degradation of cFLIP. Itch can enhance the stability of TGIF, which in turn facilitates the access of cFLIP for ubiquitin-dependent degradation by Itch. In order to investigate in detail the mechanism by which cFLIP is regulated in FasL gene deficient mice, we performed IHF to detect the expression of TGIF in C57BL/6J and FasL gene deficient mice with MEHP treatment. The preliminary results (data not presented in this dissertation) show that C57BL/6J has a higher expression than FasL gene deficient mice after MEHP treatment, and in terms of cFLIP may be partially controlled by TGIF. The upstream genes of TGIF are cJun and cFos, and the expression of cJun and cFos was shown to increase also in C57BL/6J mice with MEHP treatment, but no significant expression was observed in FasL gene deficient mice. The phosphorylation of ERK also increased in C57BL/6J, and the results indicate that the MAPK pathway may involve regulation of cFLIP. More research is needed to to confirm that the MAPK pathway is an upstream regulatory factor in controlling the expression of cFLIP.

The delay of spermatogenesis and development of abnormal germ cells were found in FasL and TRAIL gene deficient mice. Most of our previous research focused mainly on how death ligands influence the extrinsic pathway during germ cell apoptosis, but those death ligands may also play different roles in early testes development as well as in later homeostatsis of the spermatogenesis. In order to gain more information about non-apoptosis roles of death ligands, we performed a microarray analysis of the testis of FasL or TRAIL gene deficient mouse to gain more gene information, which may be important for regulating spermatogenesis. Many genes were found to be involved in spermatogenesis and may be influenced by the loss of one of the death ligands in the testes. However, more research is needed, for example, to confirm gene expressions by real-time RTPCR and western blot and to verify gene expression alteration due to loss of one of the death ligands. Further, samples of different age gene deficient mice samples need to be compared for changes during development. The number of Sertoli cells need to be counted and the concentration of testosterone need to be measured to understand whether the reduction of spermatid head counts is due to a decrease in the number of Sertoli cells or quantity of testosterone. Those results can provide a better understanding about the non-apoptosis role of FasL/TRAIL death ligands in the testes.

In our study about ways that MEHP influences male reproduction, we found that several genes are involved tumor progression. Most toxicology research has focused on adverse effects of chemical compounds to learn how substances may harm humans, for example, cause cancer. However, other studies that have sought to determine if a substance is carcinogenetic have overlooked non-carcinogens that may enhance tumor

progression. This an important area of research because our environment includes many different types of chemical compounds defined as non-carcinogens. We need to avoid exposure to both carcinogens as well as non-carcinogens that may promote tumor progression. For example, primary tumors may become more aggressive in testicular cancer patients, who are exposed to phthalate products that may promote tumorigenesis.

In Chapter 6, we discussed how our hypothesis was tested in a cell model and our findings that MEHP enhanced tumor progression, leading to the question of whether dose phthalate may account for tumor promotion *in vivo*. To answer that question, we need to test our hypothesis in an animal model and with other types of cancer cells that may share a similar pathway to tumor progression. For example, up-regulation in c-Myc is commonly found in many types of cancer cells, such as skin, lung, breast, and others. In addition, it is important to know whether phthalates impact male reproduction and enhance tumor progression in testicular cancer.

The goal of toxicology research is identify toxicants in the environment and to prevent human disease and provide better treatment without adverse effects. The research on which this dissertation is based represents a small contribution to our understanding about how toxicants impact male reproduction. As a toxicologist, I hope my work will help prevent humans disease caused by environmental toxicants and reduce adverse effects of compounds used for therapeutic purposes.

Reference

1. Lonnie D. Russell, Robert A. Ettlin, Amiya P. Sinha Hikim, Clegg ED (1990) Histological and histopathological evaluation of the testis: Cache River Press.

2. Nicander L (1967) An electron microscopical study of cell contacts in the seminiferous tubules of some mammals. Z Zellforsch Mikrosk Anat 83: 375-397.

3. Kerr JB, Loveland, K.L., O'Bryan. & de Kretser, D. M. (2005) Cytology of the testis and intrinsic control mechanisms. In Knobil and Neill's physiology of reproduction. New York: NY: Elsevier. 827-947 p.

4. Wessel GM (2011) Accessorizing the testis. Enrico Sertoli and the "mother cell" of the testis. Mol Reprod Dev 78: Fmi.

5. Skinner MK, Griswold MD (2005) Sertoli cell biology. San Diego: CA: Elsevier Academic Press.

6. Sertoli E (1865) Dell'esistenza di particolari cellule ramificate nei canalicoli seminiferi del testicolo umano. Morgagni 7: 3.

7. Skinner MK, Griswold MD (2005) Sertoli cell biology. Amsterdam ; Boston: Elsevier Academic Press. xv, 494 p. p.

8. de Rooij DG, Russell LD (2000) All you wanted to know about spermatogonia but were afraid to ask. J Androl 21: 776-798.

9. Kerr JF, Wyllie AH, Currie AR (1972) Apoptosis: a basic biological phenomenon with wide-ranging implications in tissue kinetics. Br J Cancer 26: 239-257.

10. Xu G, Shi Y (2007) Apoptosis signaling pathways and lymphocyte homeostasis. Cell Res 17: 759-771.

11. Lindsten T, Ross AJ, King A, Zong WX, Rathmell JC, et al. (2000) The combined functions of proapoptotic Bcl-2 family members bak and bax are essential for normal development of multiple tissues. Mol Cell 6: 1389-1399.

12. Wei MC, Zong WX, Cheng EH, Lindsten T, Panoutsakopoulou V, et al. (2001) Proapoptotic BAX and BAK: a requisite gateway to mitochondrial dysfunction and death. Science 292: 727-730.

13. Cheng EH, Wei MC, Weiler S, Flavell RA, Mak TW, et al. (2001) BCL-2, BCL-X(L) sequester BH3 domain-only molecules preventing BAX- and BAK-mediated mitochondrial apoptosis. Mol Cell 8: 705-711.

14. Zou H, Henzel WJ, Liu X, Lutschg A, Wang X (1997) Apaf-1, a human protein homologous to C. elegans CED-4, participates in cytochrome c-dependent activation of caspase-3. Cell 90: 405-413.

15. Zou H, Li Y, Liu X, Wang X (1999) An APAF-1.cytochrome c multimeric complex is a functional apoptosome that activates procaspase-9. J Biol Chem 274: 11549-11556.

16. Uren AG, Pakusch M, Hawkins CJ, Puls KL, Vaux DL (1996) Cloning and expression of apoptosis inhibitory protein homologs that function to inhibit apoptosis and/or bind tumor necrosis factor receptor-associated factors. Proc Natl Acad Sci U S A 93: 4974-4978.

17. Duckett CS, Nava VE, Gedrich RW, Clem RJ, Van Dongen JL, et al. (1996) A conserved family of cellular genes related to the baculovirus iap gene and encoding apoptosis inhibitors. EMBO J 15: 2685-2694.

18. Chai J, Du C, Wu JW, Kyin S, Wang X, et al. (2000) Structural and biochemical basis of apoptotic activation by Smac/DIABLO. Nature 406: 855-862.

19. Verhagen AM, Ekert PG, Pakusch M, Silke J, Connolly LM, et al. (2000) Identification of DIABLO, a mammalian protein that promotes apoptosis by binding to and antagonizing IAP proteins. Cell 102: 43-53.

20. Locksley RM, Killeen N, Lenardo MJ (2001) The TNF and TNF receptor superfamilies: integrating mammalian biology. Cell 104: 487-501.

21. Garrido C, Galluzzi L, Brunet M, Puig PE, Didelot C, et al. (2006) Mechanisms of cytochrome c release from mitochondria. Cell Death Differ 13: 1423-1433.

22. Kluck RM, Bossy-Wetzel E, Green DR, Newmeyer DD (1997) The release of cytochrome c from mitochondria: a primary site for Bcl-2 regulation of apoptosis. Science 275: 1132-1136.

23. Gogvadze V, Orrenius S, Zhivotovsky B (2006) Multiple pathways of cytochrome c release from mitochondria in apoptosis. Biochim Biophys Acta 1757: 639-647.

24. Elmore S (2007) Apoptosis: a review of programmed cell death. Toxicol Pathol 35: 495-516.

25. Ashkenazi A, Dixit VM (1998) Death receptors: signaling and modulation. Science 281: 1305-1308.

26. Chinnaiyan AM, O'Rourke K, Tewari M, Dixit VM (1995) FADD, a novel death domain-containing protein, interacts with the death domain of Fas and initiates apoptosis. Cell 81: 505-512.

27. Kischkel FC, Hellbardt S, Behrmann I, Germer M, Pawlita M, et al. (1995) Cytotoxicity-dependent APO-1 (Fas/CD95)-associated proteins form a death-inducing signaling complex (DISC) with the receptor. Embo J 14: 5579-5588.

28. Lavrik I, Golks A, Krammer PH (2005) Death receptor signaling. J Cell Sci 118: 265-267.

29. Medema JP, Scaffidi C, Kischkel FC, Shevchenko A, Mann M, et al. (1997) FLICE is activated by association with the CD95 death-inducing signaling complex (DISC). Embo J 16: 2794-2804.

30. Thome M, Tschopp J (2001) Regulation of lymphocyte proliferation and death by FLIP. Nat Rev Immunol 1: 50-58.

31. Krueger A, Baumann S, Krammer PH, Kirchhoff S (2001) FLICE-inhibitory proteins: regulators of death receptor-mediated apoptosis. Mol Cell Biol 21: 8247-8254.

32. Hyer ML, Samuel T, Reed JC (2006) The FLIP-side of Fas signaling. Clin Cancer Res 12: 5929-5931.

33. Peter ME, Budd RC, Desbarats J, Hedrick SM, Hueber AO, et al. (2007) The CD95 receptor: apoptosis revisited. Cell 129: 447-450.

34. Wu GS, Burns TF, Zhan Y, Alnemri ES, El-Deiry WS (1999) Molecular cloning and functional analysis of the mouse homologue of the KILLER/DR5 tumor necrosis factor-related apoptosis-inducing ligand (TRAIL) death receptor. cancer research 59: 2770-2775.

35. Chaudhary PM, Eby M, Jasmin A, Bookwalter A, Murray J, et al. (1997) Death receptor 5, a new member of the TNFR family, and DR4 induce FADD-dependent apoptosis and activate the NF-kappaB pathway. Immunity 7: 821-830.

36. Schneider P, Thome M, Burns K, Bodmer JL, Hofmann K, et al. (1997) TRAIL receptors 1 (DR4) and 2 (DR5) signal FADD-dependent apoptosis and activate NF-kappaB. Immunity 7: 831-836.

37. Kuang AA, Diehl GE, Zhang J, Winoto A (2000) FADD is required for DR4- and DR5-mediated apoptosis: lack of trail-induced apoptosis in FADD-deficient mouse embryonic fibroblasts. Journal of Biological Chemistry 275: 25065-25068.

38. McKee CM, Ye Y, Richburg JH (2006) Testicular germ cell sensitivity to TRAIL-induced apoptosis is dependent upon p53 expression and is synergistically enhanced by DR5 agonistic antibody treatment. Apoptosis 11: 2237-2250.

39. Schaefer U, Voloshanenko O, Willen D, Walczak H (2007) TRAIL: a multifunctional cytokine. Front Biosci 12: 3813-3824.

40. Lamhamedi-Cherradi SE, Zheng SJ, Maguschak KA, Peschon J, Chen YH (2003) Defective thymocyte apoptosis and accelerated autoimmune diseases in TRAIL-/- mice. Nature Immunology 4: 255-260.

41. Russell LD, Goh JC, Rashed RM, Vogl AW (1988) The consequences of actin disruption at Sertoli ectoplasmic specialization sites facing spermatids after in vivo exposure of rat testis to cytochalasin D. Biol Reprod 39: 105-118.

42. Print CG, Loveland KL (2000) Germ cell suicide: new insights into apoptosis during spermatogenesis. Bioessays 22: 423-430.

43. Lee J, Richburg JH, Younkin SC, Boekelheide K (1997) The Fas system is a key regulator of germ cell apoptosis in the testis. Endocrinology 138: 2081-2088.

44. Wang RA, Nakane PK, Koji T (1998) Autonomous cell death of mouse male germ cells during fetal and postnatal period. Biol Reprod 58: 1250-1256.

45. Shaha C, Tripathi R, Mishra DP (2010) Male germ cell apoptosis: regulation and biology. Philos Trans R Soc Lond B Biol Sci 365: 1501-1515.

46. Rucker EB, 3rd, Dierisseau P, Wagner KU, Garrett L, Wynshaw-Boris A, et al. (2000) Bcl-x and Bax regulate mouse primordial germ cell survival and apoptosis during embryogenesis. Mol Endocrinol 14: 1038-1052.

47. Furuchi T, Masuko K, Nishimune Y, Obinata M, Matsui Y (1996) Inhibition of testicular germ cell apoptosis and differentiation in mice misexpressing Bcl-2 in spermatogonia. Development 122: 1703-1709.

48. Knudson CM, Tung KS, Tourtellotte WG, Brown GA, Korsmeyer SJ (1995) Bax-deficient mice with lymphoid hyperplasia and male germ cell death. Science 270: 96-99.

49. Russell LD, Chiarini-Garcia H, Korsmeyer SJ, Knudson CM (2002) Bax-dependent spermatogonia apoptosis is required for testicular development and spermatogenesis. Biol Reprod 66: 950-958.

50. Lizama C, Alfaro I, Reyes JG, Moreno RD (2007) Up-regulation of CD95 (Apo-1/Fas) is associated with spermatocyte apoptosis during the first round of spermatogenesis in the rat. Apoptosis 12: 499-512.

51. Richburg JH, Nanez A, Williams LR, Embree ME, Boekelheide K (2000) Sensitivity of testicular germ cells to toxicant-induced apoptosis in gld mice that express a nonfunctional form of Fas ligand. Endocrinology 141: 787-793.

52. Kim SK, Yoon YD, Park YS, Seo JT, Kim JH (2007) Involvement of the Fas-Fas ligand system and active caspase-3 in abnormal apoptosis in human testes with maturation arrest and Sertoli cell-only syndrome. Fertil Steril 87: 547-553.

53. Francavilla S, D'Abrizio P, Cordeschi G, Pelliccione F, Necozione S, et al. (2002) Fas expression correlates with human germ cell degeneration in meiotic and post-meiotic arrest of spermatogenesis. Mol Hum Reprod 8: 213-220.

54. Blount BC, Silva MJ, Caudill SP, Needham LL, Pirkle JL, et al. (2000) Levels of seven urinary phthalate metabolites in a human reference population. Environ Health Perspect 108: 979-982.

55. Heudorf U, Mersch-Sundermann V, Angerer J (2007) Phthalates: toxicology and exposure. Int J Hyg Environ Health 210: 623-634.

56. Castle L, Mercer AJ, Startin JR, Gilbert J (1988) Migration from plasticized films into foods. 3. Migration of phthalate, sebacate, citrate and phosphate esters from films used for retail food packaging. Food Addit Contam 5: 9-20.

57. Hubinger JC (2010) A survey of phthalate esters in consumer cosmetic products. J Cosmet Sci 61: 457-465.

58. Hubinger JC, Havery DC (2006) Analysis of consumer cosmetic products for phthalate esters. J Cosmet Sci 57: 127-137.

59. Bornehag CG, Sundell J, Weschler CJ, Sigsgaard T, Lundgren B, et al. (2004) The association between asthma and allergic symptoms in children and phthalates in house dust: a nested case-control study. Environ Health Perspect 112: 1393-1397.

60. Lovekamp-Swan T, Davis BJ (2003) Mechanisms of phthalate ester toxicity in the female reproductive system. Environ Health Perspect 111: 139-145.

61. Gentry PR, Clewell HJ, Clewell R, Campbell J, Van Landingham C, et al. (2011) Challenges in the application of quantitative approaches in risk assessment: a case study with di-(2-ethylhexyl)phthalate. Critical Reviews in Toxicology 41: 1-72.

62. Pak VM, McCauley LA, Pinto-Martin J (2011) Phthalate exposures and human health concerns: A review and implications for practice. AAOHN J 59: 228-233; quiz 234-225.

63. Wittassek M, Koch HM, Angerer J, Bruning T (2011) Assessing exposure to phthalates - the human biomonitoring approach. Mol Nutr Food Res 55: 7-31.

64. Kavlock R, Barr D, Boekelheide K, Breslin W, Breysse P, et al. (2006) NTP-CERHR Expert Panel Update on the Reproductive and Developmental Toxicity of di(2-ethylhexyl) phthalate. Reprod Toxicol 22: 291-399.

65. Grande SW, Andrade AJ, Talsness CE, Grote K, Golombiewski A, et al. (2007) A dose-response study following in utero and lactational exposure to di-(2-ethylhexyl) phthalate (DEHP): reproductive effects on adult female offspring rats. Toxicology 229: 114-122.

66. Andrade AJ, Grande SW, Talsness CE, Gericke C, Grote K, et al. (2006) A dose response study following in utero and lactational exposure to di-(2-ethylhexyl) phthalate (DEHP): reproductive effects on adult male offspring rats. Toxicology 228: 85-97.

67. Andrade AJ, Grande SW, Talsness CE, Grote K, Chahoud I (2006) A dose-response study following in utero and lactational exposure to di-(2-ethylhexyl)-phthalate (DEHP): non-monotonic dose-response and low dose effects on rat brain aromatase activity. Toxicology 227: 185-192.

68. Andrade AJ, Grande SW, Talsness CE, Grote K, Golombiewski A, et al. (2006) A dose-response study following in utero and lactational exposure to di-(2-ethylhexyl) phthalate (DEHP): effects on androgenic status, developmental landmarks and testicular histology in male offspring rats. Toxicology 225: 64-74.

69. Grande SW, Andrade AJ, Talsness CE, Grote K, Chahoud I (2006) A dose-response study following in utero and lactational exposure to di(2-ethylhexyl)phthalate: effects on female rat reproductive development. Toxicol Sci 91: 247-254.

70. Akingbemi BT, Ge R, Klinefelter GR, Zirkin BR, Hardy MP (2004) Phthalate-induced Leydig cell hyperplasia is associated with multiple endocrine disturbances. Proc Natl Acad Sci U S A 101: 775-780.

71. Akingbemi BT, Youker RT, Sottas CM, Ge R, Katz E, et al. (2001) Modulation of rat Leydig cell steroidogenic function by di(2-ethylhexyl)phthalate. Biol Reprod 65: 1252-1259.

72. Ge RS, Chen GR, Dong Q, Akingbemi B, Sottas CM, et al. (2007) Biphasic effects of postnatal exposure to diethylhexylphthalate on the timing of puberty in male rats. J Androl 28: 513-520.

73. Pant N, Shukla M, Kumar Patel D, Shukla Y, Mathur N, et al. (2008) Correlation of phthalate exposures with semen quality. Toxicol Appl Pharmacol 231: 112-116.

74. Swan SH (2008) Environmental phthalate exposure in relation to reproductive outcomes and other health endpoints in humans. Environ Res 108: 177-184.

75. Lottrup G, Andersson AM, Leffers H, Mortensen GK, Toppari J, et al. (2006) Possible impact of phthalates on infant reproductive health. Int J Androl 29: 172-180; discussion 181-175.

76. Thomas JA, Thomas MJ (1984) Biological effects of di-(2-ethylhexyl) phthalate and other phthalic acid esters. Crit Rev Toxicol 13: 283-317.

77. Albro PW, Thomas R, Fishbein L (1973) Metabolism of diethylhexyl phthalate by rats. Isolation and characterization of the urinary metabolites. J Chromatogr 76: 321-330.

78. Ito Y, Yokota H, Wang R, Yamanoshita O, Ichihara G, et al. (2005) Species differences in the metabolism of di(2-ethylhexyl) phthalate (DEHP) in several organs of mice, rats, and marmosets. Arch Toxicol 79: 147-154.

79. Sjoberg P, Bondesson U, Gray TJ, Ploen L (1986) Effects of di-(2-ethylhexyl) phthalate and five of its metabolites on rat testis in vivo and in in vitro. Acta Pharmacol Toxicol (Copenh) 58: 225-233.

80. Hauser R (2008) Urinary phthalate metabolites and semen quality: a review of a potential biomarker of susceptibility. Int J Androl 31: 112-117.

81. Hoppin JA, Brock JW, Davis BJ, Baird DD (2002) Reproducibility of urinary phthalate metabolites in first morning urine samples. Environ Health Perspect 110: 515-518.

82. Hauser R, Meeker JD, Park S, Silva MJ, Calafat AM (2004) Temporal variability of urinary phthalate metabolite levels in men of reproductive age. Environ Health Perspect 112: 1734-1740.

83. Cater BR, Cook MW, Gangolli SD, Grasso P (1977) Studies on dibutyl phthalate-induced testicular atrophy in the rat: effect on zinc metabolism. Toxicol Appl Pharmacol 41: 609-618.

84. Fukuoka M, Tanimoto T, Zhou Y, Kawasaki N, Tanaka A, et al. (1989) Mechanism of testicular atrophy induced by di-n-butyl phthalate in rats. Part 1. J Appl Toxicol 9: 277-283.

85. Creasy DM, Beech LM, Gray TJ, Butler WH (1987) The ultrastructural effects of di-n-pentyl phthalate on the testis of the mature rat. Exp Mol Pathol 46: 357-371.

86. Gray TJ, Beamand JA (1984) Effect of some phthalate esters and other testicular toxins on primary cultures of testicular cells. Food Chem Toxicol 22: 123-131.

87. Foster PM, Foster JR, Cook MW, Thomas LV, Gangolli SD (1982) Changes in ultrastructure and cytochemical localization of zinc in rat testis following the administration of di-n-pentyl phthalate. Toxicol Appl Pharmacol 63: 120-132.

88. Dostal LA, Chapin RE, Stefanski SA, Harris MW, Schwetz BA (1988) Testicular toxicity and reduced Sertoli cell numbers in neonatal rats by di(2-ethylhexyl)phthalate and the recovery of fertility as adults. Toxicol Appl Pharmacol 95: 104-121.

89. Grasso P, Heindel JJ, Powell CJ, Reichert LE, Jr. (1993) Effects of mono(2-ethylhexyl) phthalate, a testicular toxicant, on follicle-stimulating hormone binding to membranes from cultured rat Sertoli cells. Biol Reprod 48: 454-459.

90. Li LH, Jester WF, Jr., Laslett AL, Orth JM (2000) A single dose of Di-(2-ethylhexyl) phthalate in neonatal rats alters gonocytes, reduces sertoli cell proliferation, and decreases cyclin D2 expression. Toxicol Appl Pharmacol 166: 222-229.

91. Heindel JJ, Powell CJ (1992) Phthalate ester effects on rat Sertoli cell function in vitro: effects of phthalate side chain and age of animal. Toxicol Appl Pharmacol 115: 116-123.

92. Heindel JJ, Chapin RE (1989) Inhibition of FSH-stimulated cAMP accumulation by mono(2-ethylhexyl) phthalate in primary rat Sertoli cell cultures. Toxicol Appl Pharmacol 97: 377-385.

93. Williams J, Foster PM (1989) The effects of 1,3-dinitrobenzene and mono-(2-ethylhexyl)phthalate on hormonally stimulated lactate and pyruvate production by rat Sertoli cell cultures. Toxicol Lett 47: 249-257.

94. Chapin RE, Gray TJ, Phelps JL, Dutton SL (1988) The effects of mono-(2-ethylhexyl)-phthalate on rat Sertoli cell-enriched primary cultures. Toxicol Appl Pharmacol 92: 467-479.

95. Thysen B, Morris PL, Gatz M, Bloch E (1990) The effect of mono(2-ethylhexyl) phthalate on Sertoli cell transferrin secretion in vitro. Toxicol Appl Pharmacol 106: 154-157.

96. Gray TJ, Gangolli SD (1986) Aspects of the testicular toxicity of phthalate esters. Environ Health Perspect 65: 229-235.

97. Svechnikov K, Svechnikova I, Soder O (2008) Inhibitory effects of mono-ethylhexyl phthalate on steroidogenesis in immature and adult rat Leydig cells in vitro. Reprod Toxicol 25: 485-490.

98. Gunnarsson D, Leffler P, Ekwurtzel E, Martinsson G, Liu K, et al. (2008) Mono-(2-ethylhexyl) phthalate stimulates basal steroidogenesis by a cAMP-independent mechanism in mouse gonadal cells of both sexes. Reproduction 135: 693-703.

99. Rodriguez I, Ody C, Araki K, Garcia I, Vassalli P (1997) An early and massive wave of germinal cell apoptosis is required for the development of functional spermatogenesis. Embo Journal 16: 2262-2270.

100. Moreno RD, Lizama C, Urzua N, Vergara SP, Reyes JG (2006) Caspase activation throughout the first wave of spermatogenesis in the rat. Cell Tissue Res 325: 533-540.

101. Fuchs Y, Steller H (2011) Programmed Cell Death in Animal Development and Disease. Cell 147: 742-758.

102. Lee J, Richburg JH, Shipp EB, Meistrich ML, Boekelheide K (1999) The Fas system, a regulator of testicular germ cell apoptosis, is differentially up-regulated in Sertoli cell versus germ cell injury of the testis. Endocrinology 140: 852-858.

103. Richburg JH, Nanez A, Gao H (1999) Participation of the Fas-signaling system in the initiation of germ cell apoptosis in young rat testes after exposure to mono-(2-ethylhexyl) phthalate. Toxicol Appl Pharmacol 160: 271-278.

104. Giammona CJ, Sawhney P, Chandrasekaran Y, Richburg JH (2002) Death receptor response in rodent testis after mono-(2-ethylhexyl) phthalate exposure. Toxicol Appl Pharmacol 185: 119-127.

105. Richburg JH, Johnson KJ, Schoenfeld HA, Meistrich ML, Dix DJ (2002) Defining the cellular and molecular mechanisms of toxicant action in the testis. Toxicol Lett 135: 167-183.

106. Holmes L, Jr., Escalante C, Garrison O, Foldi BX, Ogungbade GO, et al. (2008) Testicular cancer incidence trends in the USA (1975-2004): plateau or shifting racial paradigm? Public Health 122: 862-872.

107. Bosl GJ, Motzer RJ (1997) Testicular germ-cell cancer. N Engl J Med 337: 242-253.

108. Chia VM, Quraishi SM, Devesa SS, Purdue MP, Cook MB, et al. (2010) International trends in the incidence of testicular cancer, 1973-2002. Cancer Epidemiol Biomarkers Prev 19: 1151-1159.

109. Skakkebaek NE, Rajpert-De Meyts E, Main KM (2001) Testicular dysgenesis syndrome: an increasingly common developmental disorder with environmental aspects. Hum Reprod 16: 972-978.

110. Cook MB, Trabert B, McGlynn KA (2011) Organochlorine compounds and testicular dysgenesis syndrome: human data. Int J Androl 34: e68-84; discussion e84-65.

111. Salvatore M, Lorenzetti S, Maranghi F, Mantovani A, Taruscio D (2008) Molecular link(s) between hepatoblastoma pathogenesis and exposure to di-(2-ethylhexyl)phthalate: a hypothesis. Folia Med (Plovdiv) 50: 17-23.

112. McKee RH (2000) The role of inhibition of gap junctional intercellular communication in rodent liver tumor induction by phthalates: review of data on selected phthalates and the potential relevance to man. Regul Toxicol Pharmacol 32: 51-55.

113. Allen CD, Waser B, Korner M, Reubi JC, Lee S, et al. (2011) Neuropeptide Y acts within the rat testis to inhibit testosterone secretion. Neuropeptides 45: 55-61.

114. Fisher JS, Macpherson S, Marchetti N, Sharpe RM (2003) Human 'testicular dysgenesis syndrome': a possible model using in-utero exposure of the rat to dibutyl phthalate. Hum Reprod 18: 1383-1394.

115. Hutchison GR, Scott HM, Walker M, McKinnell C, Ferrara D, et al. (2008) Sertoli cell development and function in an animal model of testicular dysgenesis syndrome. Biol Reprod 78: 352-360.

116. Ge RS, Chen GR, Tanrikut C, Hardy MP (2007) Phthalate ester toxicity in Leydig cells: developmental timing and dosage considerations. Reprod Toxicol 23: 366-373.

117. Hu GX, Lian QQ, Ge RS, Hardy DO, Li XK (2009) Phthalate-induced testicular dysgenesis syndrome: Leydig cell influence. Trends Endocrinol Metab 20: 139-145.

118. Karray S, Kress C, Cuvellier S, Hue-Beauvais C, Damotte D, et al. (2004) Complete loss of Fas ligand gene causes massive lymphoproliferation and early death, indicating a residual activity of gld allele. The Journal of Immunology 172: 2118-2125.

119. Sedger LM, Glaccum MB, Schuh JC, Kanaly ST, Williamson E, et al. (2002) Characterization of the in vivo function of TNF-alpha-related apoptosis-inducing ligand, TRAIL/Apo2L, using TRAIL/Apo2L gene-deficient mice. Eur J Immunol 32: 2246-2254.

120. Richburg JH, Boekelheide K (1996) Mono-(2-ethylhexyl) phthalate rapidly alters both Sertoli cell vimentin filaments and germ cell apoptosis in young rat testes. Toxicol Appl Pharmacol 137: 42-50.

121. Bhattacharya N, Dufour JM, Vo MN, Okita J, Okita R, et al. (2005) Differential effects of phthalates on the testis and the liver. Biol Reprod 72: 745-754.

122. Yao PL, Lin YC, Richburg JH (2009) TNF alpha-mediated disruption of spermatogenesis in response to Sertoli cell injury in rodents is partially regulated by MMP2. Biol Reprod 80: 581-589.

123. Yao PL, Lin YC, Sawhney P, Richburg JH (2007) Transcriptional regulation of FasL expression and participation of sTNF-alpha in response to sertoli cell injury. Journal of Biological Chemistry 282: 5420-5431.

124. Robb GW, Amann RP, Killian GJ (1978) Daily sperm production and epididymal sperm reserves of pubertal and adult rats. Journal of Reproduction and Fertilization 54: 103-107.

125. Chen JJ, Lin YC, Yao PL, Yuan A, Chen HY, et al. (2005) Tumor-associated macrophages: the double-edged sword in cancer progression. J Clin Oncol 23: 953-964.

126. Tao P, Fisher JF, Mobashery S, Schlegel HB (2009) DFT studies of the ring-opening mechanism of SB-3CT, a potent inhibitor of matrix metalloproteinase 2. Org Lett 11: 2559-2562.

127. Park HM (2008) Hypothesis Testing and Statistical Power of a Test. The University Information Technology Services (UITS) Center for Statistical and Mathematical Computing, Indiana University.

128. Cleophas TJ, Cleophas, T. J., Zwinderman, A. H., Zwinderman, A. H., Cleophas, T. F. (2006) Statistics Applied to Clinical Trials: Kluwer Academic Publishers.

129. Takahashi T, Tanaka M, Brannan CI, Jenkins NA, Copeland NG, et al. (1994) Generalized lymphoproliferative disease in mice, caused by a point mutation in the Fas ligand. Cell 76: 969-976.

130. Richburg JH (2000) The relevance of spontaneous- and chemically-induced alterations in testicular germ cell apoptosis to toxicology. Toxicol Lett 112-113: 79-86.

131. Pentikainen V, Erkkila K, Dunkel L (1999) Fas regulates germ cell apoptosis in the human testis in vitro. Am J Physiol 276: E310-316.

132. Peter ME (2004) The flip side of FLIP. Biochem J 382: e1-3.

133. Chandrasekaran Y, McKee CM, Ye Y, Richburg JH (2006) Influence of TRP53 status on FAS membrane localization, CFLAR (c-FLIP) ubiquitinylation, and sensitivity of GC-2spd (ts) cells to undergo FAS-mediated apoptosis. Biol Reprod 74: 560-568.

134. Chanvorachote P, Nimmannit U, Wang L, Stehlik C, Lu B, et al. (2005) Nitric oxide negatively regulates Fas CD95-induced apoptosis through inhibition of ubiquitin-proteasome-mediated degradation of FLICE inhibitory protein. J Biol Chem 280: 42044-42050.

135. Wang L, Azad N, Kongkaneramit L, Chen F, Lu Y, et al. (2008) The Fas death signaling pathway connecting reactive oxygen species generation and FLICE inhibitory protein down-regulation. J Immunol 180: 3072-3080.

136. Chandrasekaran Y, Richburg JH (2005) The p53 protein influences the sensitivity of testicular germ cells to mono-(2-ethylhexyl) phthalate-induced apoptosis by increasing the membrane levels of Fas and DR5 and decreasing the intracellular amount of c-FLIP. Biol Reprod 72: 206-213.

137. Zerafa N, Westwood JA, Cretney E, Mitchell S, Waring P, et al. (2005) Cutting edge: TRAIL deficiency accelerates hematological malignancies. The Journal of Immunology 175: 5586-5590.

138. Lamhamedi-Cherradi SE, Zheng S, Tisch RM, Chen YH (2003) Critical roles of tumor necrosis factor-related apoptosis-inducing ligand in type 1 diabetes. Diabetes 52: 2274-2278.

139. Cretney E, Uldrich AP, Berzins SP, Strasser A, Godfrey DI, et al. (2003) Normal thymocyte negative selection in TRAIL-deficient mice. Journal of Experimental Medicine 198: 491-496.

140. Corazza N, Brumatti G, Jakob S, Villunger A, Brunner T (2004) TRAIL and thymocyte apoptosis: not so deadly? Cell death and differentiation 11 Suppl 2: S213-215.

141. Corazza N, Brumatti G, Schaer C, Cima I, Wasem C, et al. (2004) TRAIL and immunity: more than a license to kill tumor cells. Cell death and differentiation 11 Suppl 2: S122-125.

142. Sedger LM, Glaccum MB, Schuh JC, Kanaly ST, Williamson E, et al. (2002) Characterization of the in vivo function of TNF-alpha-related apoptosis-inducing ligand, TRAIL/Apo2L, using TRAIL/Apo2L gene-deficient mice. European Journal of Immunology 32: 2246-2254.

143. Jahnukainen K, Chrysis D, Hou M, Parvinen M, Eksborg S, et al. (2004) Increased apoptosis occurring during the first wave of spermatogenesis is stage-specific and primarily affects midpachytene spermatocytes in the rat testis. Biol Reprod 70: 290-296.

144. Moreno RD, Lizama C, Urzua N, Vergara SP, Reyes JG (2006) Caspase activation throughout the first wave of spermatogenesis in the rat. Cell and Tissue Research 325: 533-540.

145. Boekelheide K, Lee J, Shipp EB, Richburg JH, Li G (1998) Expression of Fas system-related genes in the testis during development and after toxicant exposure. Toxicology Letters 102-103: 503-508.

146. Russell LD, Chiarini-Garcia H, Korsmeyer SJ, Knudson CM (2002) Bax-dependent spermatogonia apoptosis is required for testicular development and spermatogenesis. Biology of Reproduction 66: 950-958.

147. Russell LD, Warren J, Debeljuk L, Richardson LL, Mahar PL, et al. (2001) Spermatogenesis in Bclw-deficient mice. Biology of Reproduction 65: 318-332.

148. Krieg A, Krieg T, Wenzel M, Schmitt M, Ramp U, et al. (2003) TRAIL-beta and TRAIL-gamma: two novel splice variants of the human TNF-related apoptosis-inducing ligand (TRAIL) without apoptotic potential. British Journal of Cancer 88: 918-927.

149. Chong AP, Walters CA, Weinrieb SA (1983) The neglected laboratory test. The semen analysis. Journal of Andrology 4: 280-282.

150. Keel BA, Stembridge TW, Pineda G, Serafy NT, Sr. (2002) Lack of standardization in performance of the semen analysis among laboratories in the United States. Fertility and Sterility 78: 603-608.

151. Pedrazzini T, Pralong F, Grouzmann E (2003) Neuropeptide Y: the universal soldier. Cell Mol Life Sci 60: 350-377.

152. Goto M, O'Brien DA, Eddy EM (2010) Speriolin is a novel human and mouse sperm centrosome protein. Hum Reprod 25: 1884-1894.

153. Goto M, Eddy EM (2004) Speriolin is a novel spermatogenic cell-specific centrosomal protein associated with the seventh WD motif of Cdc20. J Biol Chem 279: 42128-42138.

154. Bornstein C, Brosh R, Molchadsky A, Madar S, Kogan-Sakin I, et al. (2011) SPATA18, a spermatogenesis-associated gene, is a novel transcriptional target of p53 and p63. Mol Cell Biol 31: 1679-1689.

155. Tsai LH, Delalle I, Caviness VS, Jr., Chae T, Harlow E (1994) p35 is a neural-specific regulatory subunit of cyclin-dependent kinase 5. Nature 371: 419-423.

156. Session DR, Fautsch MP, Avula R, Jones WR, Nehra A, et al. (2001) Cyclin-dependent kinase 5 is expressed in both Sertoli cells and metaphase spermatocytes. Fertil Steril 75: 669-673.

157. Musa FR, Takenaka I, Konishi R, Tokuda M (2000) Effects of luteinizing hormone, follicle-stimulating hormone, and epidermal growth factor on expression and kinase activity of cyclin-dependent kinase 5 in Leydig TM3 and Sertoli TM4 cell lines. J Androl 21: 392-402.

158. Rosales JL, Lee BC, Modarressi M, Sarker KP, Lee KY, et al. (2004) Outer dense fibers serve as a functional target for Cdk5.p35 in the developing sperm tail. J Biol Chem 279: 1224-1232.

159. Li L, Liu G, Fu JJ, Li LY, Tan XJ, et al. (2009) Molecular cloning and characterization of a novel transcript variant of Mtsarg1 gene. Mol Biol Rep 36: 1023-1032.

160. Hess H, Heid H, Zimbelmann R, Franke WW (1995) The protein complexity of the cytoskeleton of bovine and human sperm heads: the identification and characterization of cylicin II. Exp Cell Res 218: 174-182.

161. Tubb B, Mulholland DJ, Vogl W, Lan ZJ, Niederberger C, et al. (2002) Testis fascin (FSCN3): a novel paralog of the actin-bundling protein fascin expressed specifically in the elongate spermatid head. Exp Cell Res 275: 92-109.

162. Choi HS, Lee SH, Kim H, Lee Y (2008) Germ cell-specific gene 1 targets testis-specific poly(A) polymerase to the endoplasmic reticulum through protein-protein interactions. FEBS Lett 582: 1203-1209.

163. Kashiwabara S, Noguchi J, Zhuang T, Ohmura K, Honda A, et al. (2002) Regulation of spermatogenesis by testis-specific, cytoplasmic poly(A) polymerase TPAP. Science 298: 1999-2002.

164. Zheng H, Stratton CJ, Morozumi K, Jin J, Yanagimachi R, et al. (2007) Lack of Spem1 causes aberrant cytoplasm removal, sperm deformation, and male infertility. Proc Natl Acad Sci U S A 104: 6852-6857.

165. Nayernia K, von Mering MH, Kraszucka K, Burfeind P, Wehrend A, et al. (1999) A novel testicular haploid expressed gene (THEG) involved in mouse spermatid-sertoli cell interaction. Biol Reprod 60: 1488-1495.

166. Yang F, Skaletsky H, Wang PJ (2007) Ubl4b, an X-derived retrogene, is specifically expressed in post-meiotic germ cells in mammals. Gene Expr Patterns 7: 131-136.

167. Cornwall GA, Hsia N (1997) ADAM7, a member of the ADAM (a disintegrin and metalloprotease) gene family is specifically expressed in the mouse anterior pituitary and epididymis. Endocrinology 138: 4262-4272.

168. Nonaka MI, Hishikawa Y, Moriyama N, Koji T, Ogata RT, et al. (2003) Complement C4b-binding protein as a novel murine epididymal secretory protein. Biol Reprod 69: 1931-1939.

169. Nonaka MI, Wang G, Mori T, Okada H, Nonaka M (2001) Novel androgen-dependent promoters direct expression of the C4b-binding protein alpha-chain gene in epididymis. J Immunol 166: 4570-4577.

170. Da Ros VG, Maldera JA, Willis WD, Cohen DJ, Goulding EH, et al. (2008) Impaired sperm fertilizing ability in mice lacking Cysteine-RIch Secretory Protein 1 (CRISP1). Dev Biol 320: 12-18.

171. Petersen C, Aumuller G, Bahrami M, Hoyer-Fender S (2002) Molecular cloning of Odf3 encoding a novel coiled-coil protein of sperm tail outer dense fibers. Mol Reprod Dev 61: 102-112.

172. Jalkanen J, Kotimaki M, Huhtaniemi I, Poutanen M (2006) Novel epididymal protease inhibitors with Kazal or WAP family domain. Biochem Biophys Res Commun 349: 245-254.

173. Clauss A, Persson M, Lilja H, Lundwall A (2011) Three genes expressing Kunitz domains in the epididymis are related to genes of WFDC-type protease inhibitors and semen coagulum proteins in spite of lacking similarity between their protein products. BMC Biochem 12: 55.

174. Li Y, Sosnik J, Brassard L, Reese M, Spiridonov NA, et al. (2011) Expression and localization of five members of the testis-specific serine kinase (Tssk) family in mouse and human sperm and testis. Mol Hum Reprod 17: 42-56.

175. Zuercher G, Rohrbach V, Andres AC, Ziemiecki A (2000) A novel member of the testis specific serine kinase family, tssk-3, expressed in the Leydig cells of sexually mature mice. Mech Dev 93: 175-177.

176. Yao PL, Lin YC, Richburg JH (2010) Mono-(2-ethylhexyl) phthalate-induced disruption of junctional complexes in the seminiferous epithelium of the rodent testis is mediated by MMP2. Biol Reprod 82: 516-527.

177. Theret N, Musso O, Turlin B, Lotrian D, Bioulac-Sage P, et al. (2001) Increased extracellular matrix remodeling is associated with tumor progression in human hepatocellular carcinomas. Hepatology 34: 82-88.

178. Ara T, Kusafuka T, Inoue M, Kuroda S, Fukuzawa M, et al. (2000) Determination of imbalance between MMP-2 and TIMP-2 in human neuroblastoma by reverse-transcription polymerase chain reaction and its correlation with tumor progression. J Pediatr Surg 35: 432-437.

179. Diamantopoulos N, Boutis AL, Koratzis I, Andreadis C, Galaktidou G, et al. (2010) Matrix metalloproteinases and proangiogenic factors in testicular germ cell tumors. J Buon 15: 116-121.

180. Yao PL, Lin YC, Richburg JH (2011) Transcriptional Suppression of Sertoli Cell Timp2 in Rodents Following Mono-(2-Ethylhexyl) Phthalate Exposure Is Regulated by CEBPA and MYC. Biol Reprod.

181. Larsson LG, Henriksson MA (2010) The Yin and Yang functions of the Myc oncoprotein in cancer development and as targets for therapy. Exp Cell Res 316: 1429-1437.

182. Sonne SB, Hoei-Hansen CE, Fisher JS, Leffers H, Rajpert-de Meyts E, et al. (2004) Do environmental factors play a role in the aetiology of carcinoma in situ testis and the testicular dysgenesis syndrome? Verh Dtsch Ges Pathol 88: 144-151.

183. Bay K, Asklund C, Skakkebaek NE, Andersson AM (2006) Testicular dysgenesis syndrome: possible role of endocrine disrupters. Best Pract Res Clin Endocrinol Metab 20: 77-90.

184. Toppari J, Virtanen HE, Main KM, Skakkebaek NE (2010) Cryptorchidism and hypospadias as a sign of testicular dysgenesis syndrome (TDS): environmental connection. Birth Defects Res A Clin Mol Teratol 88: 910-919.

185. Doull J, Cattley R, Elcombe C, Lake BG, Swenberg J, et al. (1999) A cancer risk assessment of di(2-ethylhexyl)phthalate: application of the new U.S. EPA Risk Assessment Guidelines. Regul Toxicol Pharmacol 29: 327-357.

186. Ashby J, Brady A, Elcombe CR, Elliott BM, Ishmael J, et al. (1994) Mechanistically-based human hazard assessment of peroxisome proliferator-induced hepatocarcinogenesis. Hum Exp Toxicol 13 Suppl 2: S1-117.

187. Jobling MS, Hutchison GR, van den Driesche S, Sharpe RM (2011) Effects of di(n-butyl) phthalate exposure on foetal rat germ-cell number and differentiation: identification of age-specific windows of vulnerability. Int J Androl.

188. Jezierska A, Motyl T (2009) Matrix metalloproteinase-2 involvement in breast cancer progression: a mini-review. Med Sci Monit 15: RA32-40.

189. Wolfer A, Ramaswamy S (2011) MYC and metastasis. Cancer Res 71: 2034-2037.

190. Mook OR, Frederiks WM, Van Noorden CJ (2004) The role of gelatinases in colorectal cancer progression and metastasis. Biochim Biophys Acta 1705: 69-89.

191. Dony C, Kessel M, Gruss P (1985) Post-transcriptional control of myc and p53 expression during differentiation of the embryonal carcinoma cell line F9. Nature 317: 636-639.

192. Sejersen T, Jin P, Rahm M, Ringertz NR (1989) Changes in c-onc expression during embryonal carcinoma cell differentiation. Environ Health Perspect 80: 247-256.

193. Wang CC, Tsai MF, Hong TM, Chang GC, Chen CY, et al. (2005) The transcriptional factor YY1 upregulates the novel invasion suppressor HLJ1 expression and inhibits cancer cell invasion. Oncogene 24: 4081-4093.

194. Chen HW, Yu SL, Chen JJ, Li HN, Lin YC, et al. (2004) Anti-invasive gene expression profile of curcumin in lung adenocarcinoma based on a high throughput microarray analysis. Mol Pharmacol 65: 99-110.

195. Tsai MF, Wang CC, Chang GC, Chen CY, Chen HY, et al. (2006) A new tumor suppressor DnaJ-like heat shock protein, HLJ1, and survival of patients with non-small-cell lung carcinoma. J Natl Cancer Inst 98: 825-838.

196. Sobarzo CM, Lustig L, Ponzio R, Suescun MO, Denduchis B (2009) Effects of di(2-ethylhexyl) phthalate on gap and tight junction protein expression in the testis of prepubertal rats. Microsc Res Tech 72: 868-877.

197. Weider K, Bergmann M, Brehm R (2011) Connexin 43: its regulatory role in testicular junction dynamics and spermatogenesis. Histol Histopathol 26: 1343-1352.

198. Kandouz M, Batist G (2010) Gap junctions and connexins as therapeutic targets in cancer. Expert Opin Ther Targets 14: 681-692.

199. Leithe E, Sirnes S, Omori Y, Rivedal E (2006) Downregulation of gap junctions in cancer cells. Crit Rev Oncog 12: 225-256.

200. Paznekas WA, Karczeski B, Vermeer S, Lowry RB, Delatycki M, et al. (2009) GJA1 mutations, variants, and connexin 43 dysfunction as it relates to the oculodentodigital dysplasia phenotype. Hum Mutat 30: 724-733.

201. Song YN, Zhang H, Zhao JY, Guo XL (2009) Connexin 43, a new therapeutic target for cardiovascular diseases. Pharmazie 64: 291-295.

202. Strale PO, Clarhaut J, Lamiche C, Cronier L, Mesnil M, et al. (2011) Down-regulation of connexin43 expression reveals the involvement of caveolin-1 containing lipid rafts in human U251 glioblastoma cell invasion. Mol Carcinog.

203. Kang KS, Lee YS, Kim HS, Kim SH (2002) DI-(2-ethylhexyl) phthalate-induced cell proliferation is involved in the inhibition of gap junctional intercellular communication and blockage of apoptosis in mouse Sertoli cells. J Toxicol Environ Health A 65: 447-459.

204. Isenberg JS, Kamendulis LM, Smith JH, Ackley DC, Pugh G, Jr., et al. (2000) Effects of Di-2-ethylhexyl phthalate (DEHP) on gap-junctional intercellular communication (GJIC), DNA synthesis, and peroxisomal beta oxidation (PBOX) in rat, mouse, and hamster liver. Toxicol Sci 56: 73-85.

205. Ziegler WH, Liddington RC, Critchley DR (2006) The structure and regulation of vinculin. Trends Cell Biol 16: 453-460.

206. Carisey A, Ballestrem C (2011) Vinculin, an adapter protein in control of cell adhesion signalling. Eur J Cell Biol 90: 157-163.

207. Rodriguez Fernandez JL, Geiger B, Salomon D, Sabanay I, Zoller M, et al. (1992) Suppression of tumorigenicity in transformed cells after transfection with vinculin cDNA. J Cell Biol 119: 427-438.

208. Lifschitz-Mercer B, Czernobilsky B, Feldberg E, Geiger B (1997) Expression of the adherens junction protein vinculin in human basal and squamous cell tumors: relationship to invasiveness and metastatic potential. Hum Pathol 28: 1230-1236.

209. Palma I, Pena RY, Contreras A, Ceballos-Reyes G, Coyote N, et al. (2008) Participation of OCT3/4 and beta-catenin during dysgenetic gonadal malignant transformation. Cancer Lett 263: 204-211.

210. Chang H, Guillou F, Taketo MM, Behringer RR (2009) Overactive beta-catenin signaling causes testicular sertoli cell tumor development in the mouse. Biol Reprod 81: 842-849.

211. Sobarzo CM, Lustig L, Ponzio R, Denduchis B (2006) Effect of di-(2-ethylhexyl) phthalate on N-cadherin and catenin protein expression in rat testis. Reprod Toxicol 22: 77-86.

212. Maranghi F, Lorenzetti S, Tassinari R, Moracci G, Tassinari V, et al. (2010) In utero exposure to di-(2-ethylhexyl) phthalate affects liver morphology and metabolism in post-natal CD-1 mice. Reprod Toxicol 29: 427-432.

213. Bhatia N, Spiegelman VS (2005) Activation of Wnt/beta-catenin/Tcf signaling in mouse skin carcinogenesis. Mol Carcinog 42: 213-221.

214. Yochum GS, Sherrick CM, Macpartlin M, Goodman RH (2010) A beta-catenin/TCF-coordinated chromatin loop at MYC integrates 5' and 3' Wnt responsive enhancers. Proc Natl Acad Sci U S A 107: 145-150.

215. Osanai M, Murata M, Chiba H, Kojima T, Sawada N (2007) Epigenetic silencing of claudin-6 promotes anchorage-independent growth of breast carcinoma cells. Cancer Sci 98: 1557-1562.

216. Wu Q, Liu Y, Ren Y, Xu X, Yu L, et al. (2010) Tight junction protein, claudin-6, downregulates the malignant phenotype of breast carcinoma. Eur J Cancer Prev 19: 186-194.

217. Yafang L, Qiong W, Yue R, Xiaoming X, Lina Y, et al. (2011) Role of Estrogen Receptor-alpha in the Regulation of Claudin-6 Expression in Breast Cancer Cells. J Breast Cancer 14: 20-27.

218. Oka D, Yamashita S, Tomioka T, Nakanishi Y, Kato H, et al. (2009) The presence of aberrant DNA methylation in noncancerous esophageal mucosae in association with smoking history: a target for risk diagnosis and prevention of esophageal cancers. Cancer 115: 3412-3426.

219. Zavala-Zendejas VE, Torres-Martinez AC, Salas-Morales B, Fortoul TI, Montano LF, et al. (2011) Claudin-6, 7, or 9 overexpression in the human gastric adenocarcinoma cell line AGS increases its invasiveness, migration, and proliferation rate. Cancer Invest 29: 1-11.

220. Birks DK, Kleinschmidt-DeMasters BK, Donson AM, Barton VN, McNatt SA, et al. (2010) Claudin 6 is a positive marker for atypical teratoid/rhabdoid tumors. Brain Pathol 20: 140-150.

221. Vare P, Soini Y (2010) Twist is inversely associated with claudins in germ cell tumors of the testis. Apmis 118: 640-647.

222. Turksen K, Troy TC (2002) Permeability barrier dysfunction in transgenic mice overexpressing claudin 6. Development 129: 1775-1784.

223. Hong YH, Hishikawa D, Miyahara H, Nishimura Y, Tsuzuki H, et al. (2005) Up-regulation of the claudin-6 gene in adipogenesis. Biosci Biotechnol Biochem 69: 2117-2121.

224. Turksen K, Troy TC (2001) Claudin-6: a novel tight junction molecule is developmentally regulated in mouse embryonic epithelium. Dev Dyn 222: 292-300.

225. Ruzinova MB, Benezra R (2003) Id proteins in development, cell cycle and cancer. Trends Cell Biol 13: 410-418.

226. Perk J, Iavarone A, Benezra R (2005) Id family of helix-loop-helix proteins in cancer. Nat Rev Cancer 5: 603-614.

227. Sadate-Ngatchou PI, Pouchnik DJ, Griswold MD (2004) Follicle-stimulating hormone induced changes in gene expression of murine testis. Mol Endocrinol 18: 2805-2816.

228. Treinen KA, Dodson WC, Heindel JJ (1990) Inhibition of FSH-stimulated cAMP accumulation and progesterone production by mono(2-ethylhexyl) phthalate in rat granulosa cell cultures. Toxicol Appl Pharmacol 106: 334-340.

229. Bertolino E, Reimund B, Wildt-Perinic D, Clerc RG (1995) A novel homeobox protein which recognizes a TGT core and functionally interferes with a retinoid-responsive motif. J Biol Chem 270: 31178-31188.

230. Wotton D, Lo RS, Lee S, Massague J (1999) A Smad transcriptional corepressor. Cell 97: 29-39.

231. Demange C, Ferrand N, Prunier C, Bourgeade M-F, Atfi A (2009) A model of partnership co-opted by the homeodomain protein TGIF and the Itch/AIP4 ubiquitin ligase for effective execution of TNF-alpha cytotoxicity. Molecular Cell 36: 1073-1158.